DOI: https://doi.org/10.24297/jap.v20i.9215

The Structure of Space and its Impact on Interplanetary Travel and Answers to Fundamental Cosmological Questions

*Natalia Julia Sobolewska[1], *Joanna Paulina Sobolewska[2], *Marek Juliusz Sobolewski[3], *Michał Amadeusz Sobolewski[4], *Dariusz Stanisław Sobolewski[5]

[1,2,3,4,5]Physics department, Theoretical physics, HTS High Technology Solutions, Poland

Abstract

The article presents the far-reaching implications of the theory entitled "Theory of Space" (Sobolewski D. S., Theory of Space, 2016) (Sobolewski D. S., Theory of Space, 2017) (Sobolewski D. S., Theory of Space, 2022 - new unpublished edition) and of the publication "New Generations of Rocket Engines" (Sobolewska, Sobolewska, Sobolewski, Sobolewski, & Sobolewski, 2021). Among others, it presents the shape of curved space in E^4 for selected planets of the solar system and the Sun, taking into account boundary hypersurfaces ${}^{\alpha}\aleph^{\alpha}$ and ${}^{\beta}\aleph^{\beta}$ and gravitational interactions. The existence of space tunnels was analysed and the perspective of new technologies enabling interplanetary travel was outlined. Furthermore, due to the revealed structure of space, cosmological issues including the existence of other Universes and possible effects of their interactions are addressed. The constant Gdańsk was also introduced $G_{Gdańsk}$ which, together with the introduced equation, makes it possible to determine the maximum immersion depth of an astronomical object of mass M.

(All co-authors of this article made the same contribution under the direction of D.S. Sobolewski.)

Keywords: Interstellar Travel, Gravitational interactions, Curvature of the space, Cosmology, Theory of Space, Radius of the universe, Curvature of the hypersurface alpha, Curvature of the hypersurface beta, Universes, Poznań constant, Gdańsk constant

Introduction

The theory entitled "Theory of Space" (Sobolewski D. S., Theory of Space, 2016) (Sobolewski D. S., Theory of Space, 2017) derives fundamental concepts of physics such as the passage of time, matter and energy from the concept of space, which is a four-dimensional differential manifold ${}^{Re}M$ immersed in a four-dimensional Euclidean space.

Matter, according to the cited theory, appears to us in the form of space swirls, of which elementary particles are built, and the velocity of time flow in a given region of space characterizes its properties. Therefore, one may say that the currently applied concept of space-time is nothing else but a far-reaching simplification of description of physical phenomena by reducing properties of four-dimensional space to three-dimensional space and lapse of time, which depends on properties of space, including distances between four-dimensional boundary hypersurfaces ${}^{\beta}\aleph^{\beta}$, ${}^{\alpha}\aleph^{\alpha}$, which is shown in Fig. 1 (Sobolewski D. S., Theory of Space, 2016) (Sobolewski D. S., Theory of Space, 2017).

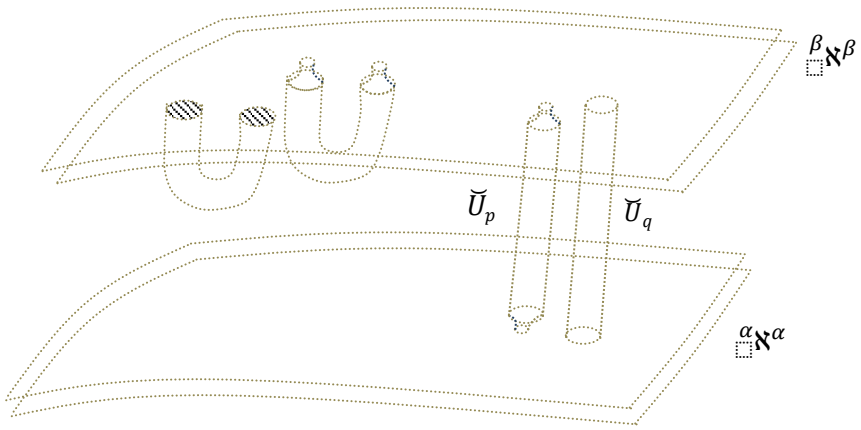

Fig. 1 Area of space $U \subset {}^{Re}M$ bounded by four-dimensional boundary hypersurfaces ${}^{\beta}\aleph^{\beta}$, ${}^{\alpha}\aleph^{\alpha}$ (Sobolewski D. S., Theory of Space, 2017).

In this paper, we will focus on the differentiated properties of boundary hypersurfaces ${}^{\alpha}\aleph^{\alpha}$ and ${}^{\beta}\aleph^{\beta}$ using for this purpose the analysis of their deformations under the influence of matter (space channels of the type $\breve{U}_p$ and $\breve{U}_q$), which is consistent with the revealed deformations revealed in the "Theory of Space" (Sobolewski D. S., Theory of Space, 2016).

We shall also determine the shape of boundary hypersurfaces ${}^{\alpha}\aleph^{\alpha}$ and ${}^{\beta}\aleph^{\beta}$ for a single astronomical object of mass M including black holes.

In addition, we will present the cosmological consequences of the results obtained including the formation of four-dimensional space tunnels and present the emerging possibility of using the gravitational field to orient the space channels of the rocket as mentioned in "New Generations of Rocket Engines" (Sobolewski D. S., Sobolewski, Sobolewski, Sobolewska, & Sobolewska, 2020).

Materials and Methods

The grounds of presented results refer to the theory from the field of theoretical physics entitled: "Theory of space" (Sobolewski D. S., Theory of Space, 2016) (Sobolewski D. S., Theory of Space, 2017) (Sobolewski D. S., Theory of Space, 2022 - new unpublished edition), which gave us, among others, the essence of the gravitational interactions and equations describing the curvature of the space.

Summing up, in this work method of analysis and logical structure have been applied based on notions, models and equations introduced by the "Theory of Space", along with "New Generations of Rocket Engines" (Sobolewska, Sobolewska, Sobolewski, Sobolewski, & Sobolewski, 2021).

Results and Discussion

Shape of the hypersurface ${}^{\alpha}\aleph^{\alpha}$

Using numerical calculations, a solution to the nonlinear differential equation (1) describing the boundary hypersurface ${}^{\alpha}\aleph^{\alpha}$ (Fig. 1) outside the astronomical object presented in the "Theory of Space" (Sobolewski D. S., Theory of Space, 2016) (Sobolewski D. S., Theory of Space, 2017) (Sobolewski D. S., Theory of Space, 2022 - new unpublished edition) for single astronomical objects.

The differential equation (2) describing a boundary hypersurface ${}^{\alpha}\aleph^{\alpha}$ (Fig. 1) inside the astronomical object was introduced and solved numerically.

$$x = \frac{G\,M}{c^2}\left(-Log\left(\frac{GM}{c^2 R}\right) + Log\left(\frac{\sqrt{\chi'(x)^2+1}-1}{\sqrt{\chi'(x)^2+1}}\right) + \frac{1}{\sqrt{\chi'(x)^2+1}-1} - \frac{1}{3}\right) \quad \{\chi'(x): 0 \le \chi'(x) \le \chi'(x_R)\} \quad (1)$$

$$x = \sqrt{3 - \frac{2c^2R(\sqrt{\chi'(x)^2+1}-1)}{GM\sqrt{\chi'(x)^2+1}}\left(\frac{R(2\sqrt{\chi'(x)^2+1}+1)}{3\sqrt{\chi'(x)^2+1}} - \frac{GM}{c^2}\right)} \ \{\chi'(x): \chi'(0) \leq \chi'(x) \leq \chi'(x_R)\} \quad (2)$$

The results are presented as two- and three-dimensional diagrams in the Euclidean space coordinate system E^4 with the origin of the coordinate system located at the center of the astronomical object - Fig. 2, Fig. 3.

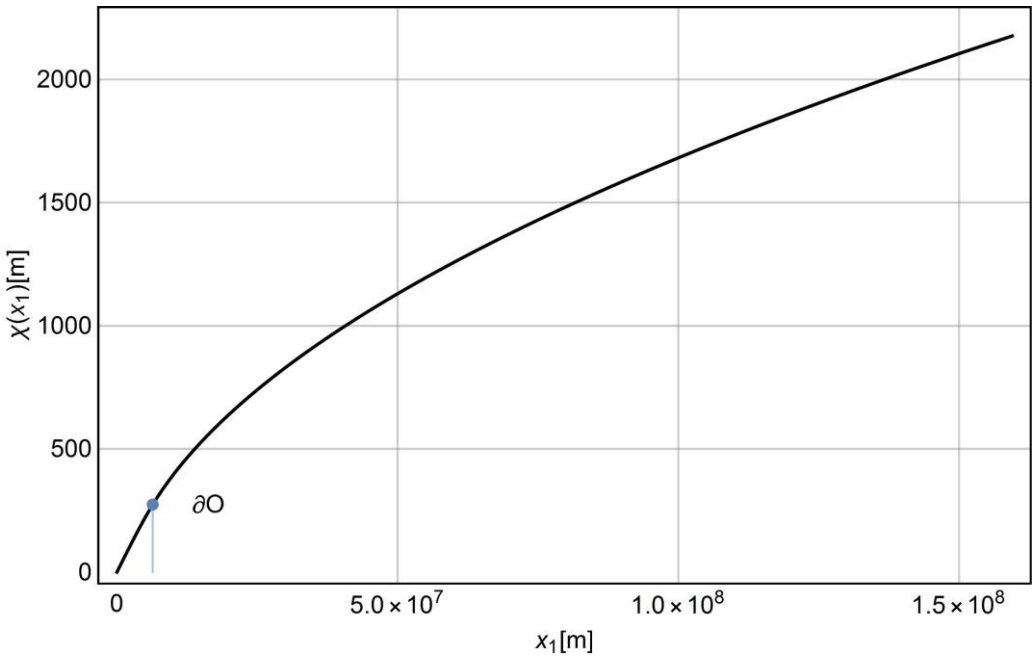

Fig. 2 Shape of the boundary hypersurface ${}^{\alpha}\aleph^{\alpha}$ near the Earth. By ∂O denotes the edge of the Earth.

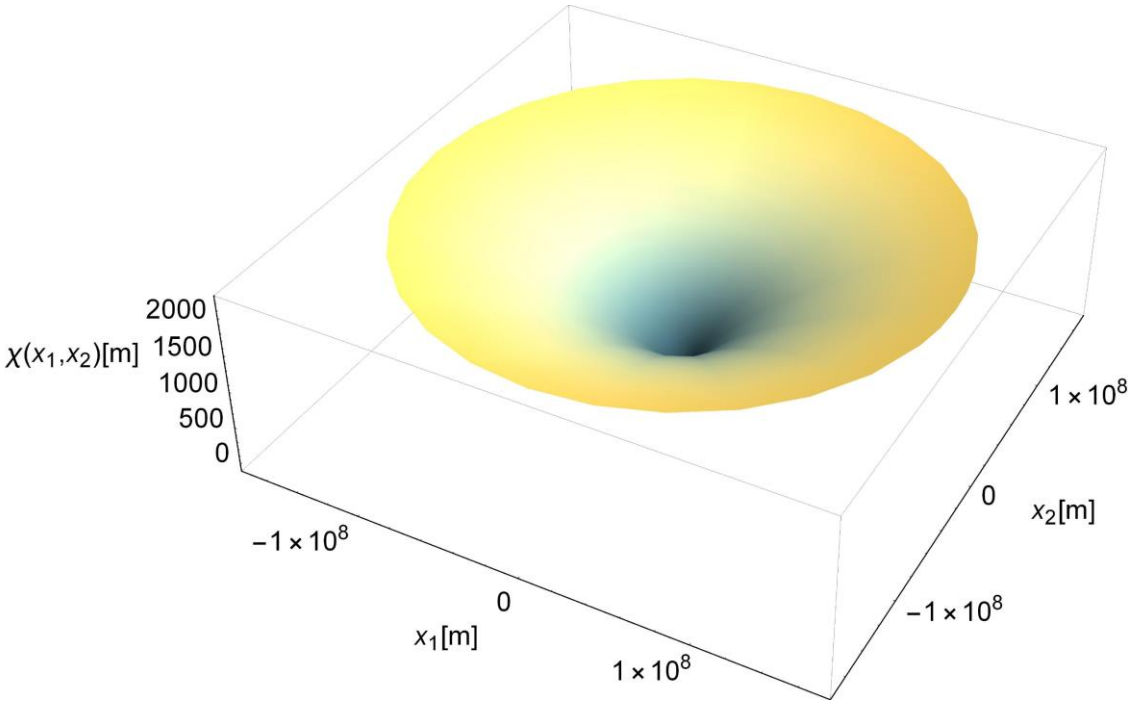

Fig. 3 Shape of the boundary hypersurface ${}^{\alpha}\aleph^{\alpha}$ near the Earth.

Shape of the hypersurface ${}^{\beta}\aleph^{\beta}$

A differential equation describing the boundary hypersurface is introduced ${}^{\beta}\aleph^{\beta}$ (Fig. 1) in the interior of a single astronomical object in the curvilinear coordinate system associated with the hypersurface ${}^{\alpha}\aleph^{\alpha}$which has been solved (4) and presented in the form of a diagram together with the solution disclosed outside the astronomical object (3) in the theory entitled "Theory of Space" (Sobolewski D. S., Theory of Space, 2016) (Sobolewski D. S., Theory of Space, 2017) (Sobolewski D. S., Theory of Space, 2022 - new unpublished edition).

$$ {}^{\beta}\chi(r) = \sqrt{\frac{GM}{ck}} F\left(\frac{1}{2}\cos^{-1}\left(\frac{GM}{ckr^2}\right)|2\right) + C_1 \quad \{r: R \le r\} \tag{3} $$

$$ {}^{\beta}\chi(r) = -\frac{c\,k\,R^3\sqrt{1-\frac{G^2M^2r^2}{c^2k^2R^6}}}{G\,M} + C_2 \quad \{r: 0 \le r \le R\} \tag{4} $$

The diagram of relations ${}^{\beta}\chi(r)$ in the curvilinear system for single astronomical objects, including the Earth - Fig. 4, Fig. 5.

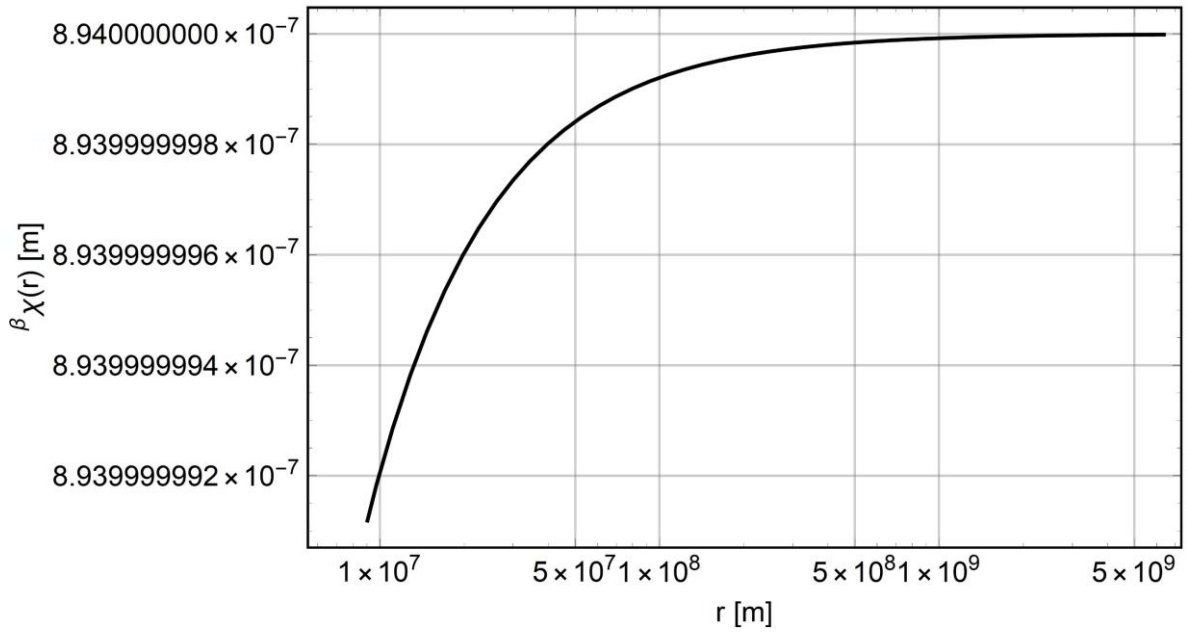

Fig. 4. Dependence diagram ${}^{\beta}\chi(r)$ for $r \geq R_E$ for the Earth.

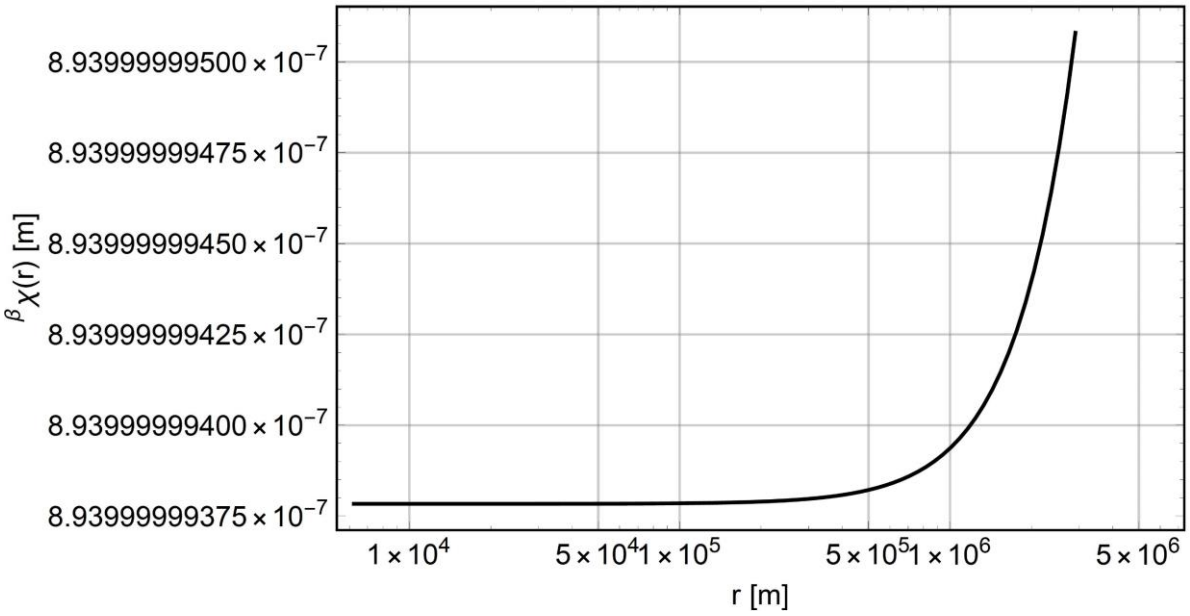

Fig. 5. Dependence diagram ${}^{\beta}\chi(r)$ for $0 \leq r \leq R_E$ for the Earth.

Orientation distribution of space channels in the interior of an astronomical object

It has been shown that for homogeneous astronomical objects, the orientation distribution of spatial channels $\breve{U}_p$ and $\breve{U}_q$ is approximately equal to the average value of their orientation, which means that on the surface of astronomical objects the orientation of space channels is close to the orientation of space channels in areas far from sources of gravity.

This effect was justified by the interactions between spatial channels with different orientations, which lead to a distribution of the mean values of their orientations.

The exceptions are heterogeneous astronomical objects including astronomical objects having a specific structure of the nucleus or its dynamics. In such cases differentiated orientation of space channels may be a source of magnetic field of astronomical object, what follows directly from the theory "Theory of Space". "Theory of Space". (Sobolewski D. S., Theory of Space, 2016) (Sobolewski D. S., Theory of Space, 2017) (Sobolewski D. S., Theory of Space, 2022 - new unpublished edition).

Constant Gdansk $G_{Gdańsk}$

The constant Gdańsk was introduced $G_{Gdańsk}$, and defined as follows:

$$G_{Gdańsk} = \max\{k_{nR_S}: nR_S \in \Omega_O\} \approx 1.4847 \times 10^{-23} \frac{m}{kg} \quad (5)$$

where Ω_O is the set of radii of existing astronomical objects and k_{nR_S} proportionality coefficients between the maximum deformation of the boundary hypersurface ${}^{\alpha}\chi$ for an astronomical object with radius that is a multiple of the radius of the Sun and the mass M of the astronomical object.

Using the introduced Gdańsk constant, the maximum deformation can be determined from the mass of the astronomical object ${}^{\alpha}\chi$, which can be equated with the depth of the space tunnel using the following formula:

$${}^{\alpha}\chi_{max} = G_{Gdańsk} \times M \quad (6)$$

The introduced constant $G_{Gdańsk}$ together with the equation (6) allows to study the existence of wormholes, which was done for the black hole marked TON 618 of mass equal to $M_{T618} = 6.6 \times 10^{10} M_S$, where M_S stands for the mass of the Sun.

Space parameters ${}^{\alpha\beta}\xi, \tau, {}^{\beta}\chi, \frac{\partial\,{}^{\alpha}\chi}{\partial x_i}$ **for selected astronomical objects**

Numerically determined values of space parameters such as:

- Asymmetry vector ${}^{\alpha\beta}\xi(R)$ on the surface of an astronomical object,
- Distance between boundary hypersurfaces on the surface of an astronomical object $\tau(R) = {}^{\beta}\chi(R)$ and at its center $\tau(0) = {}^{\beta}\chi(0)$,
- Maximum inclination of the boundary hypersurface ${}^{\alpha}\aleph$ on the surface of an astronomical object $\frac{\partial\,{}^{\alpha}\chi}{\partial x_i}(x_R)$ and at its center $\frac{\partial\,{}^{\alpha}\chi}{\partial x_i}(0)$.

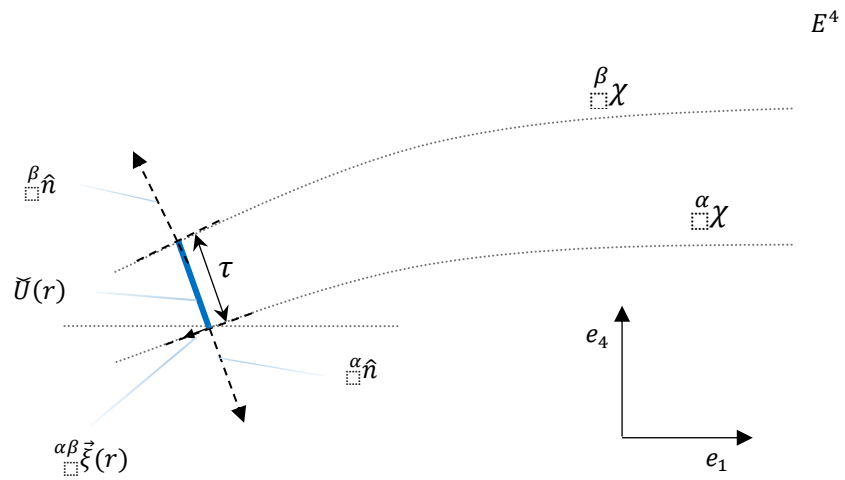

Fig. 6. Interpretation of the asymmetry vector ${}^{\alpha\beta}\vec{\xi}(r)$ and distances between gb-surfaces τ. (Sobolewski D. S., Theory of Space, 2016) (Sobolewski D. S., Theory of Space, 2017) (Sobolewski D. S., Theory of Space, 2022 - new unpublished edition)

Radius of the Universe

A definition of the apparent radius of the Universe has been introduced R_v in relation to the actual radius of the Universe R_W as equal to $R_v = \pi\, R_W$ as shown in figure **Fig. 7**.

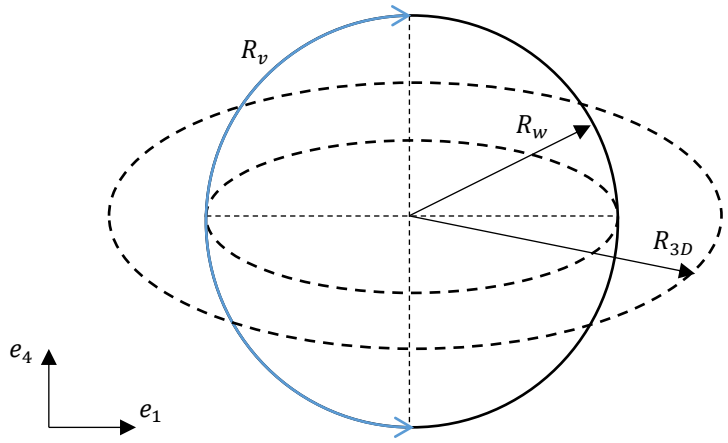

Fig. 7. Universe of radius R_w with the apparent radius marked R_v and the radius of a three-dimensional sphere R_{3D} with a volume equal to the 3D surface of a four-dimensional sphere.

The three-dimensional radius of the universe was also defined R_{3D} as the radius of a three-dimensional sphere whose volume is equal to the area of a four-dimensional sphere of radius R_w.

In summary, the defined radii are respectively:

$R_w = 1.2468 \times 10^{26} m$

$R_{3D} = \sqrt[3]{\frac{3}{2}\pi {R_w}^3} = 2.09 \times 10^{26} m$

$R_v = \pi R_w = 3.92 \times 10^{26} m$

Optimal configuration of the rocket before launch

Theoretical possibilities of optimal configuration of space channel orientation of a rocket before its launch with passengers using energy supplied from the Earth are presented.

Consequently, due to the assumed possibility of their stabilization, a change in the orientation of the space channels of the rocket with its passengers is presented in stages, as shown in the illustrative figure Fig. 8.

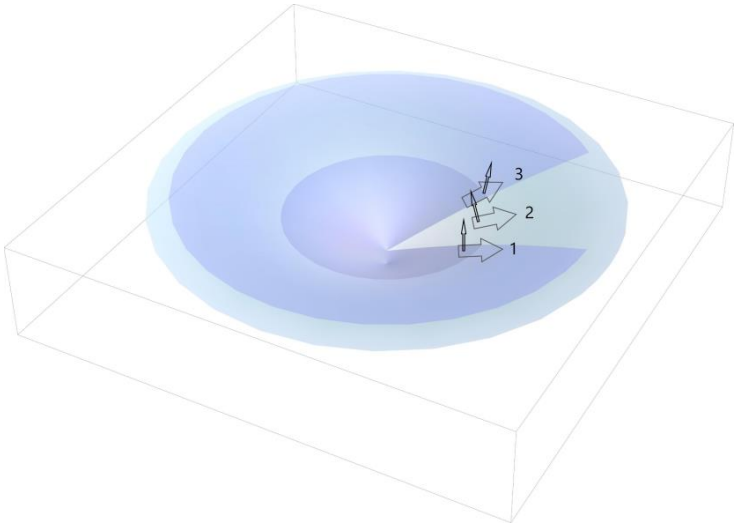

Fig. 8. Overview drawing showing the successive stages of orientation of the rocket's space channels prior to launch.

The illustrative figure Fig. 8 shows the successive stages of orientation of the space channels of the rocket with passengers, where:

1 - Initial state of the rocket before configuration,

2 - State of the rocket after orthogonalization of the space channels to the hypersurface ${}^{\alpha}\aleph^{\alpha}$ - the perceived effect is a downward slope,

3 - Status of the rocket after configuration.

At the same time the passengers would feel in the configuration stage 1 → 2 effect similar to falling down and after the rocket's take-off they would feel the effects of braking, as the gradually released energy from the reoriented space channels would be used to overcome the Earth's gravitational field.

Dark Matter and The Existence of Other Universes

The implications of the "Theory of Space" (Sobolewski D. S., Theory of Space, 2016) (Sobolewski D. S., Theory of Space, 2017) (Sobolewski D. S., Theory of Space, 2022 - new unpublished edition) on cosmological issues are discussed, including the existence of space tunnels by using the introduced relation (6) and Gdańsk constant $G_{Gdańsk}$ to the object TON 618.

It is shown that the space wormhole that forms is several orders of magnitude smaller than the radius of the universe, which would mean that space wormholes do not exist:

$$ {}^{\alpha}\chi_{Smax}^{T618} = k_{R_S} \times M_{T618} \cong 1.948 \times 10^{18} m < R_W \cong 1.2468 \times 10^{26} m \quad (7) $$

It is also shown that it is unlikely that there is a concentric Universe inside ours due to its small dimensions of the order of $10^6\ m$ and the universe outside, if it existed, would have a radius of the order $10^{44} m$.

It was also shown, referring to the essence of gravitational interactions (Sobolewski D. S., Theory of Space, 2016) (Sobolewski D. S., Theory of Space, 2017) (Sobolewski D. S., Theory of Space, 2022 - new unpublished edition)that effects of interactions between universes [1]can be seen in the form of dark matter (reduction of distances between boundary hypersurfaces due to interactions), generation of matter from space (due to the revealed essence of the structure of matter, i.e. tubes connecting boundary hypersurfaces, as shown in Fig. Fig. 1), or gravitational and fluctuation waves (Sobolewski D. S., Sobolewski, Sobolewski, Sobolewska, & Sobolewska, 2020) (Sobolewska, Sobolewska, Sobolewski, Sobolewski, & Sobolewski, 2021).

Structure of the space (Main Text)

The quoted theory entitled. "Theory of Space" (Sobolewski D. S., Theory of Space, 2016) (Sobolewski D. S., Theory of Space, 2017) (Sobolewski D. S., Theory of Space, 2022 - new unpublished edition) reveals a three-layer structure of space ${}^{Re}M$ consisting of a four-dimensional main layer $\widetilde{\aleph}$in which turbulence is created and two four-dimensional boundary layers with elastic properties ${}^{\beta}\aleph^{\beta}$, ${}^{\alpha}\aleph^{\alpha}$, which is shown in Fig. Fig. 9.

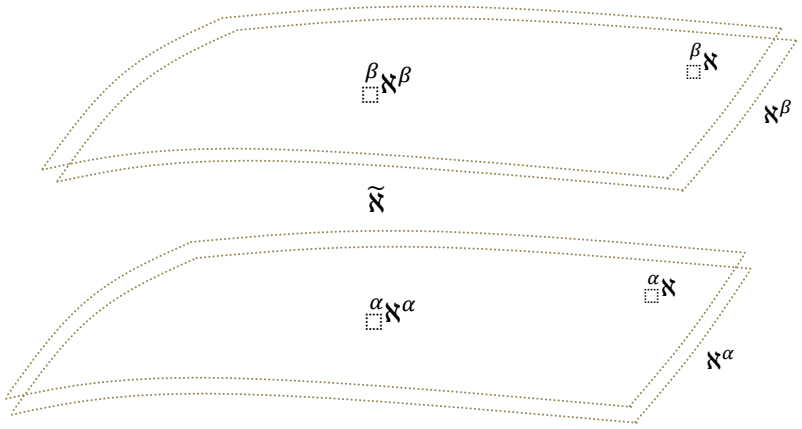

Fig. 9 Structure of the space $U \subset {}^{Re}M$ bounded by four-dimensional boundary hypersurfaces ${}^{\alpha}\aleph$ and $\aleph^{\alpha}$ and ${}^{\beta}\aleph$ and $\aleph^{\beta}$ (Sobolewski D. S., Theory of Space, 2016) (Sobolewski D. S., Theory of Space, 2017) (Sobolewski D. S., Theory of Space, 2022 - new unpublished edition).

Layer $\widetilde{\aleph}$ is separated from layers ${}^{\beta}\aleph^{\beta}$, ${}^{\alpha}\aleph^{\alpha}$ three-dimensional boundary hypersurfaces $\aleph^{\beta}$ and ${}^{\alpha}\aleph$. Whereby the four-dimensional layers ${}^{\beta}\aleph^{\beta}$, ${}^{\alpha}\aleph^{\alpha}$ also have external three-dimensional boundary hypersurfaces ${}^{\beta}\aleph$ and $\aleph^{\alpha}$as shown in figure Fig. 9.

The question arises as to what is the structure of four-dimensional space layers $\widetilde{\aleph}$, ${}^{\beta}\aleph^{\beta}$, ${}^{\alpha}\aleph^{\alpha}$ and their properties?

A question posed in this way puts us in a similar position to that of Melissos of Samos (5th century BC), Plato (427 BC - 347 BC), or Democritus of Abdera (460 BC - 370 BC) and Aristotle (384 BC - 322 BC), which is astonishing.

[1] Universes, that are thin layers of spheres, that have no common part.

Unfortunately, due to the limited scope of this publication, we will only focus on some of the properties of space including its deformation due to the different properties of boundary hypersurfaces ${}^{\beta}\aleph^{\beta}$, ${}^{\alpha}\aleph^{\alpha}$ and their shape for a single astronomical object of mass M, which we will assume to be homogeneous $\rho(r) = const$.

It should be emphasized that the paper is the result of the first stage of the scientific and research work of the HTS High Technology Solutions institute, which aims to develop a complete model of space and elementary particles for the simulation of collisions of elementary particles and for the analysis of interactions of all known types.

Shape of the hypersurface ${}^{\alpha}\aleph^{\alpha}$

In order to determine the shape of a boundary hypersurface ${}^{\alpha}\aleph^{\alpha}$ of a homogeneous astronomical object of mass M and of radius R we will use equations derived in the theory "Theory of Space". "Theory of Space". (Sobolewski D. S., Theory of Space, 2016) (Sobolewski D. S., Theory of Space, 2017) (Sobolewski D. S., Theory of Space, 2022 - new unpublished edition) for a body falling freely from infinity with unit mass, for which:

$$E_M^G(r) + E_k(r) = 0 \quad (8)$$

where $E_M^G(r)$ - potential energy of gravitation at a distance r from the center of an astronomical object of mass M, $E_k(r)$ - kinetic energy of a freely falling body of unit mass from infinity at a distance r from the center of the astronomical object.

The equation (8) leads to equations (Sobolewski D. S., Theory of Space, 2016) (Sobolewski D. S., Theory of Space, 2017) (Sobolewski D. S., Theory of Space, 2022 - new unpublished edition):

$$-G\frac{M}{r} + c^2(1 - cos\,\Theta_v) = 0 \ \{r: r \geq R\} \quad (9)$$

$$-\frac{3}{2}G\frac{M}{R} + \frac{1}{2}G\frac{M}{R^3}r^2 + c^2(1 - cos\,\Theta_v) = 0 \ \{r: 0 \leq r \leq R\} \quad (10)$$

where $c^2(1 - cos\,\Theta_v)$ is the kinetic energy of a body of unit mass falling freely from a distance r from an astronomical object, from which the relation $x\left(\frac{d^{\alpha}\chi}{dx}(x)\right)$:

$$x = \frac{G\,M}{c^2}\left(\frac{1}{-1+\sqrt{1+\left(\frac{d^{\alpha}\chi}{dx}(x)\right)^2}} - \frac{1}{3} + \mathrm{Log}\left[\frac{-1+\sqrt{1+\left(\frac{d^{\alpha}\chi}{dx}(x)\right)^2}}{\sqrt{1+\left(\frac{d^{\alpha}\chi}{dx}(x)\right)^2}}\right] - \mathrm{Log}\left[\frac{G\,M}{c^2\,R}\right]\right) \quad \left\{\frac{d^{\alpha}\chi}{dx}(x): 0 \leq \frac{d^{\alpha}\chi}{dx}(x) \leq \frac{d^{\alpha}\chi}{dx}(x_R)\right\} \quad (11)$$

$$x = \sqrt{3 - \frac{2c^2R}{G\,M}\frac{-1+\sqrt{1+\left(\frac{d^{\alpha}\chi'}{dx}(x)\right)^2}}{\sqrt{1+\left(\frac{d^{\alpha}\chi'}{dx}(x)\right)^2}}}\left(\frac{1}{3}R\frac{1+2\sqrt{1+\left(\frac{d^{\alpha}\chi'}{dx}(x)\right)^2}}{\sqrt{1+\left(\frac{d^{\alpha}\chi'}{dx}(x)\right)^2}} - \frac{G\,M}{c^2}\right) \quad \left\{\frac{d^{\alpha}\chi'}{dx}(x): \frac{d^{\alpha}\chi'}{dx}(0) \leq \frac{d^{\alpha}\chi'}{dx}(x) \leq \frac{d^{\alpha}\chi'}{dx}(x_R)\right\} \quad (12)$$

For Earth for $4.567335711901286 * 10^{-5} \geq \frac{d^{\alpha}\chi'}{dx}(x) \geq 3.729214091953053 * 10^{-5} \geq \frac{d^{\alpha}\chi}{dx}(x) \geq 10^{-7}$:

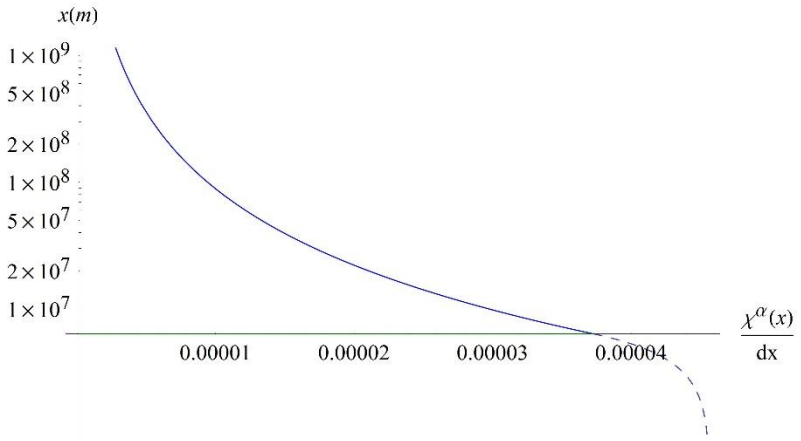

Fig. 10 Dependence diagram $x\left(\frac{d^{\alpha}\chi}{dx}(x)\right)$ for the Earth. (Sobolewski D. S., Theory of Space, 2022 - new unpublished edition)

and for the Sun $2.5233918661764134 * 10^{-3} \geq \frac{d^{\alpha}\chi'}{dx}(x) \geq 2.060339191250505 * 10^{-3} \geq \frac{d^{\alpha}\chi}{dx}(x) \leq 10^{-5}$:

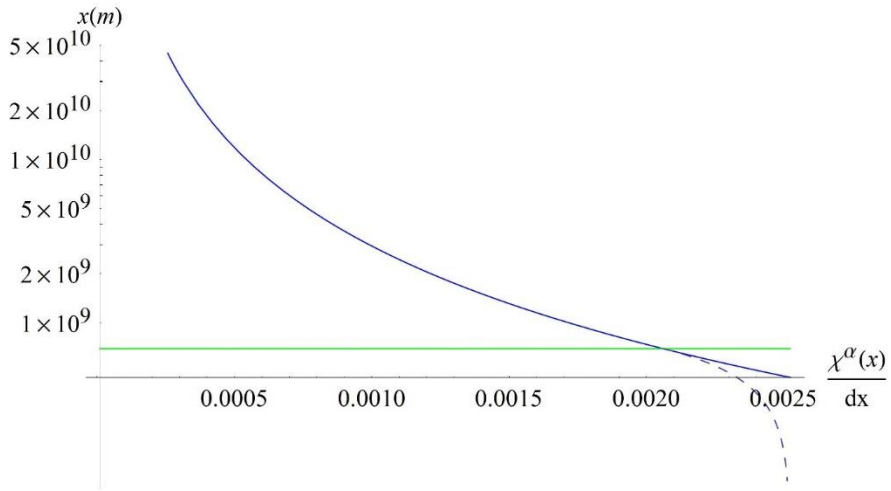

Fig. 11 Dependence diagram $x\left(\frac{d^{\alpha}\chi}{dx}(x)\right)$ for the Sun. (Sobolewski D. S., Theory of Space, 2022 - new unpublished edition)

Let us pay attention to the small angle of inclination of the boundary hypersurface ${}^{\alpha}\aleph^{\alpha}$which for the Sun equals maximally $\max\frac{d^{\alpha}\chi}{dx}(0) \approx arctg(2.5233918661764134 \times 10^{-3}) \approx 2.5233865 \times 10^{-3} rad \approx 0.1446°$, therefore scaled diagrams of astronomical objects should be interpreted taking into account proper proportions.

First degree nonlinear differential equations (11) and (12) will be solved numerically with scripts that allow us to repeat the results obtained or to increase their accuracy[2].

In summary, we are looking for the solution of the following equations[3]:

$$x = \frac{G\,M}{c^2}\left(-Log\left(\frac{GM}{c^2 R}\right) + Log\left(\frac{\sqrt{\chi'(x)^2+1}-1}{\sqrt{\chi'(x)^2+1}}\right) + \frac{1}{\sqrt{\chi'(x)^2+1}-1} - \frac{1}{3}\right) \quad \{\chi'(x): 0 \leq \chi'(x) \leq \chi'(x_R)\} \quad (13)$$

[2] The scripts will be available at www.theoryofspace.info.

[3] To simplify the equations, the derivative $\frac{\partial^{\alpha}\chi}{\partial x_i}$, where $i \in \{1,2,3\}$, will also be written in the short form ${}^{\alpha}\chi'$ or χ' and $\frac{d^{\alpha}\chi}{dx}$, which should not lead to confusion.

$$x = \sqrt{3 - \frac{2c^2R(\sqrt{\chi'(x)^2+1}-1)}{GM\sqrt{\chi'(x)^2+1}}\left(\frac{R(2\sqrt{\chi'(x)^2+1}+1)}{3\sqrt{\chi'(x)^2+1}} - \frac{GM}{c^2}\right)} \; \{\chi'(x): \chi'(0) \leq \chi'(x) \leq \chi'(x_R)\} \quad (14)$$

We will assume that the origin of the coordinate system in E^4 coincides with the center of gravity of an astronomical object, which we assume to be homogeneous $\rho(r) = const\ \{r: r < R\}$.

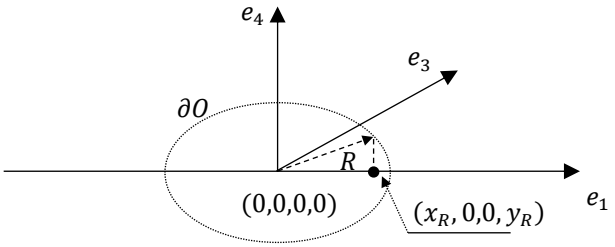

Fig. 12 Local coordinate system for an astronomical object O having mass M and radius R.

We will take as initial condition: ${}^{\alpha}\chi(0) = 0$.

The points of the graph $(x, y'(x))$ are determined by the equation (14) within ${}^{\alpha}\chi'(x)$: ${}^{\alpha}\chi'(0) \geq {}^{\alpha}\chi'(x) \geq {}^{\alpha}\chi'(x_R)$, where $\frac{\partial\, {}^{\alpha}\chi}{\partial x_1}(0)$:

$$\frac{\partial\, {}^{\alpha}\chi}{\partial x_1}(0) = \sqrt{\frac{4R^2c^4}{(2Rc^2 - 3G\,M)^2} - 1} \quad (15)$$

a, $\frac{\partial\, {}^{\alpha}\chi}{\partial x_1}(x_R)$:

$$\frac{\partial\, {}^{\alpha}\chi}{\partial x_1}(x_R) = \sqrt{\frac{c^4R^2}{(c^2R - G\,M)^2} - 1} \quad (16)$$

and by means of the equation (13) within $\{y'[x]: Ymin \leq y[x] \leq y[x_R]\}$, where $Ymin$ is the assumed parameter, although the reader may increase the solution interval to larger areas.

Equation (15) allows to determine the maximum inclination of the boundary hypersurface for an astronomical object, as shown in Fig. Fig. 13 in units of mass of the Sun and its radius[4].

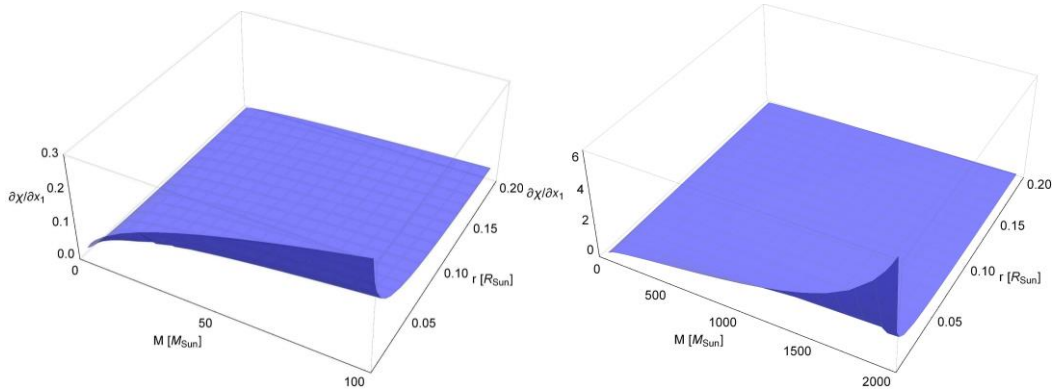

[4] See addenda where values are given $\frac{\partial\, {}^{\alpha}\chi}{\partial x_i}(0)$ and $\frac{\partial\, {}^{\alpha}\chi}{\partial x_i}(x_R)$, where $i \in \{1,2,3\}$ for each of the astronomical objects analysed.

Fig. 13 Derivative $\frac{\partial\,{}^{\alpha}\chi}{\partial x_1}(R,M) = \frac{\partial\,{}^{\alpha}\chi}{\partial x_2}(R,M) = \frac{\partial\,{}^{\alpha}\chi}{\partial x_3}(R,M)$ on the surface of an astronomical object in units of the mass of the Sun and its radius.

On the diagrams we will mark the coordinate x_R determined from equation (14) by substituting for ${}^{\alpha}\chi'[x]$ the right-hand side of the equation (16), for the Sun we have:

$$x_{R_S} = 6.956980311133373 * 10^8 m < R_S \tag{17}$$

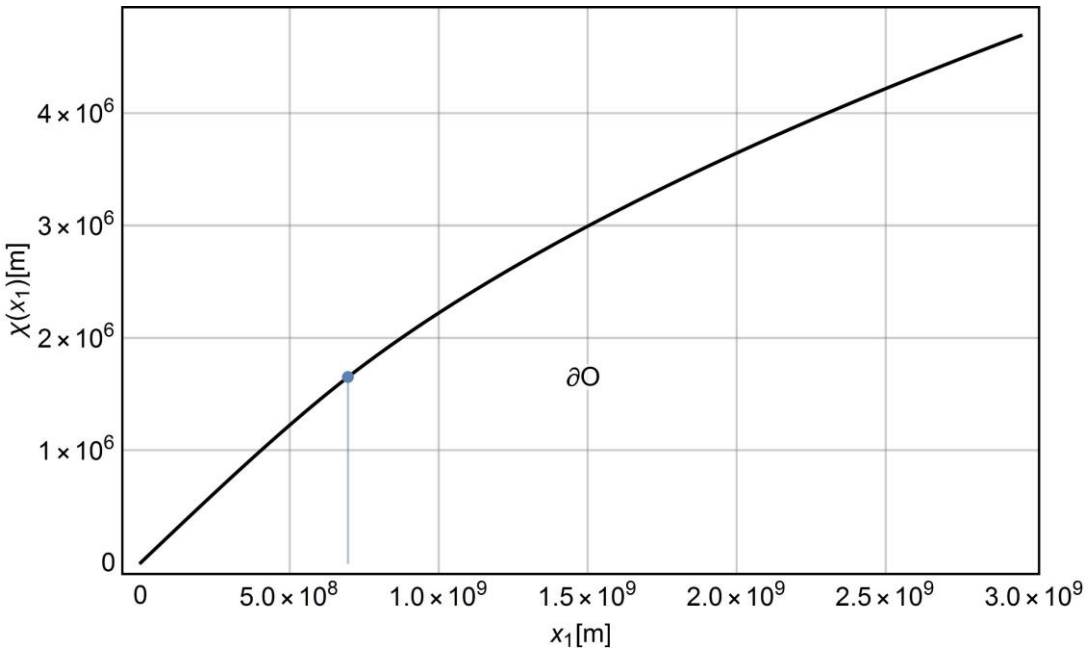

Fig. 14 Deformation of the boundary hypersurface ${}^{\alpha}\chi(x_1)$ near the Sun. The blue line indicates the coordinate x_R of the Sun's edge ∂O.

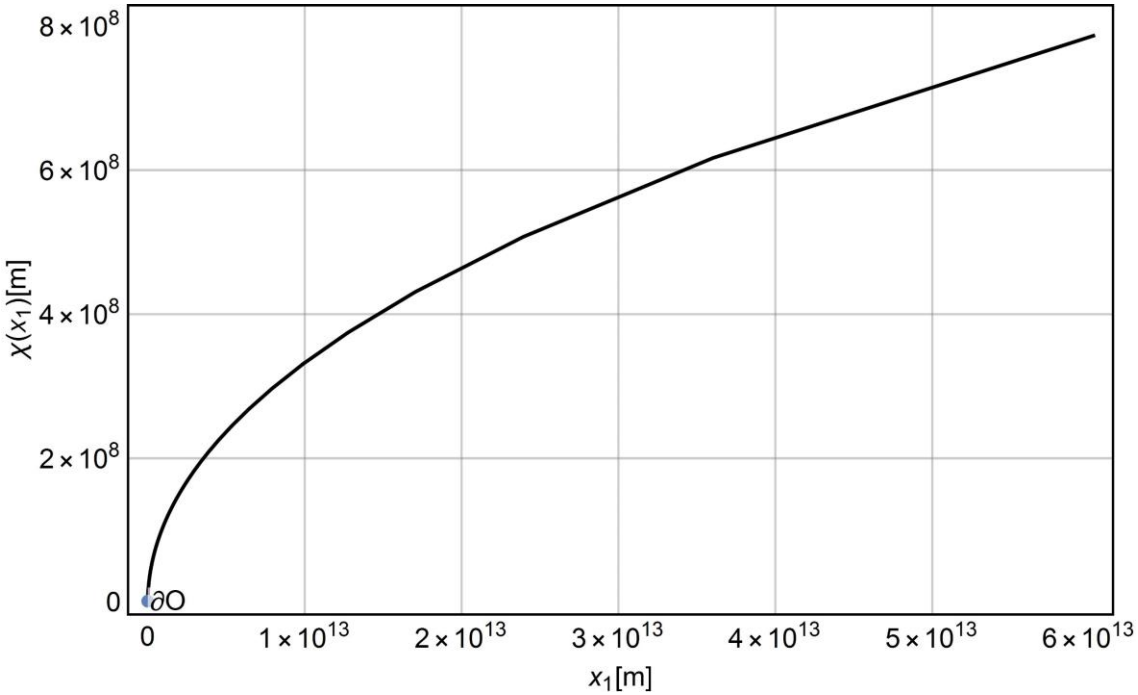

Fig. 15 Deformation of the boundary hypersurface ${}^{\alpha}\chi(x_1)$ for the Sun. The blue line indicates the coordinate x_R of the Sun's edge ∂O.

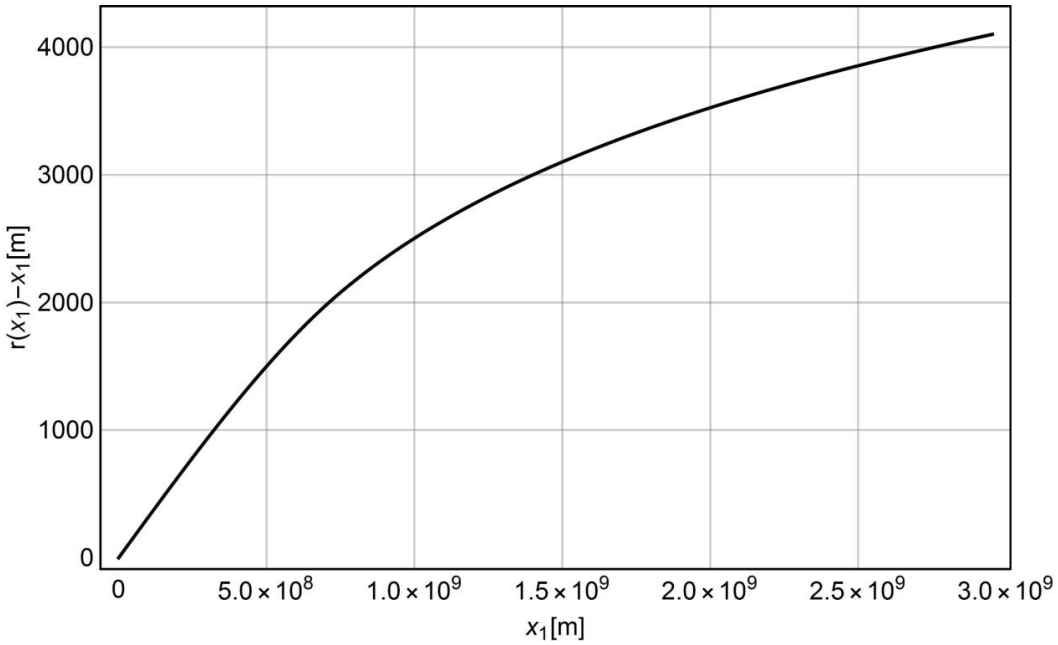

Fig. 16 Dependence diagram $r(x_1) - x_1$ for the Sun.

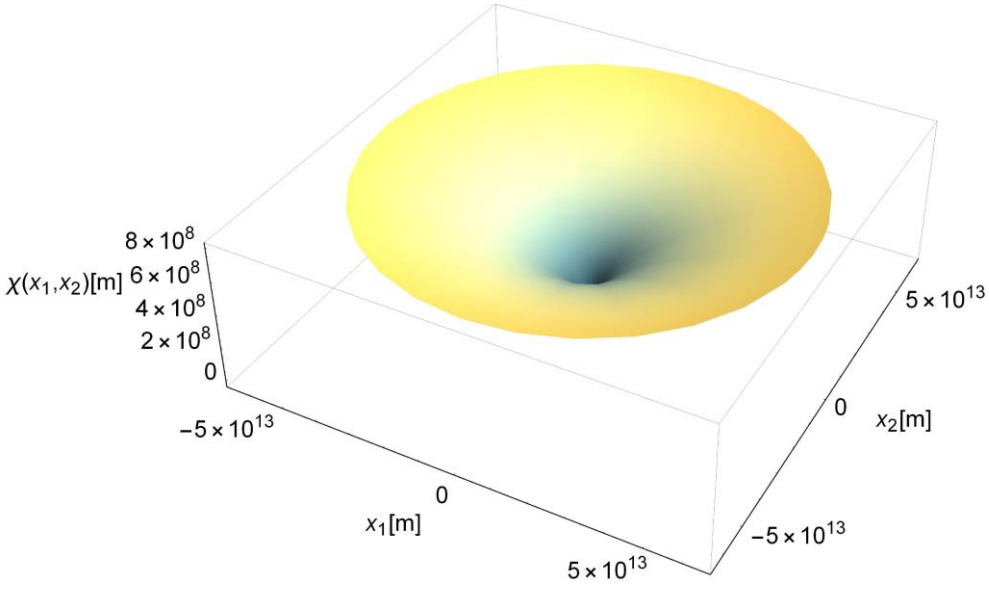

Fig. 17 Deformation of the boundary hypersurface ${}^{\alpha}\chi(x_1, x_2)$ for the Sun.

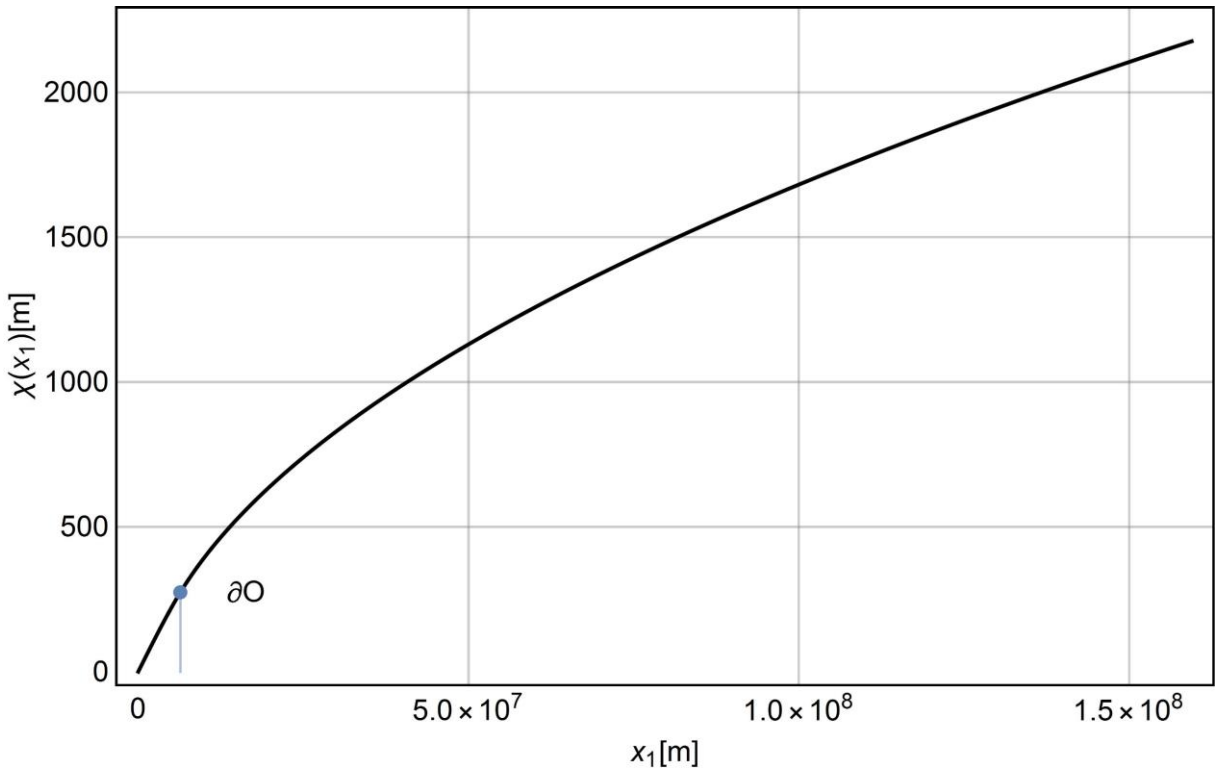

Fig. 18 Deformation of the boundary hypersurface ${}^{\alpha}\chi(x_1)$ near the Earth. The blue line indicates the coordinate x_R of the Earth's edge ∂O.

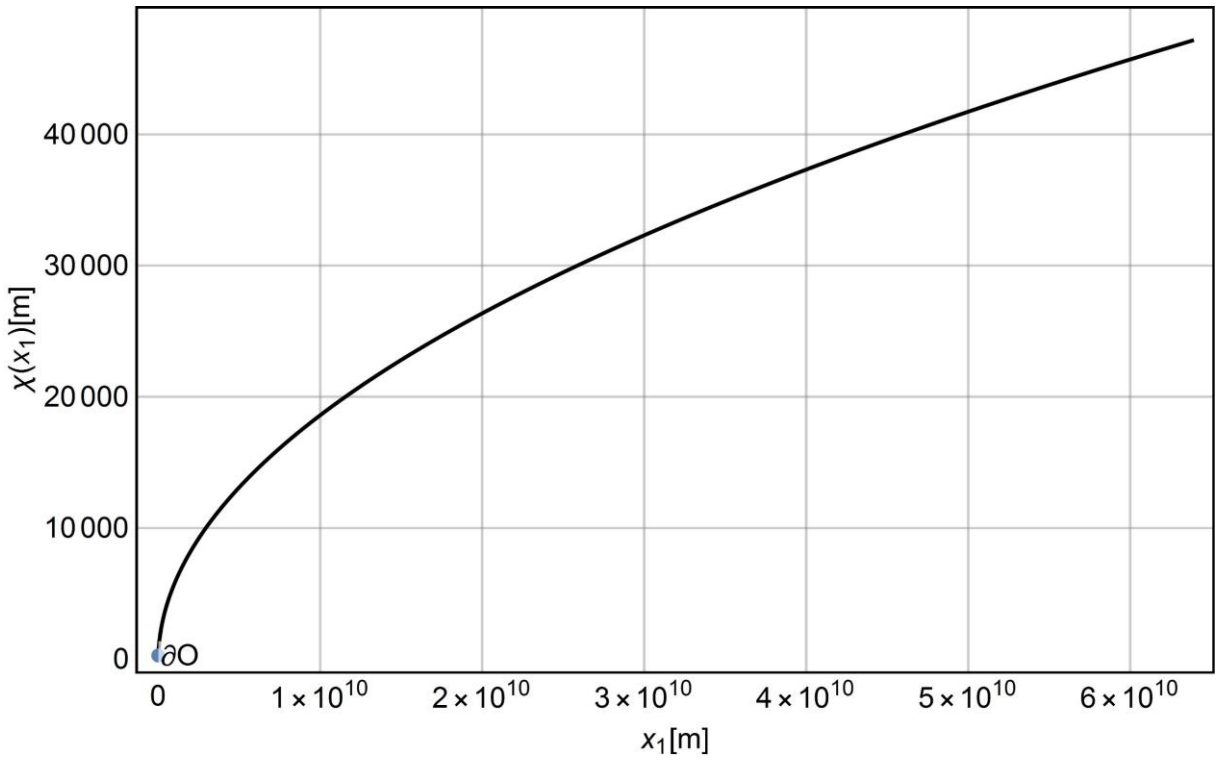

Fig. 19 Deformation of the boundary hypersurface ${}^{\alpha}\chi(x_1)$ for the Earth. The blue line indicates the coordinate x_R of the Earth's edge ∂O.

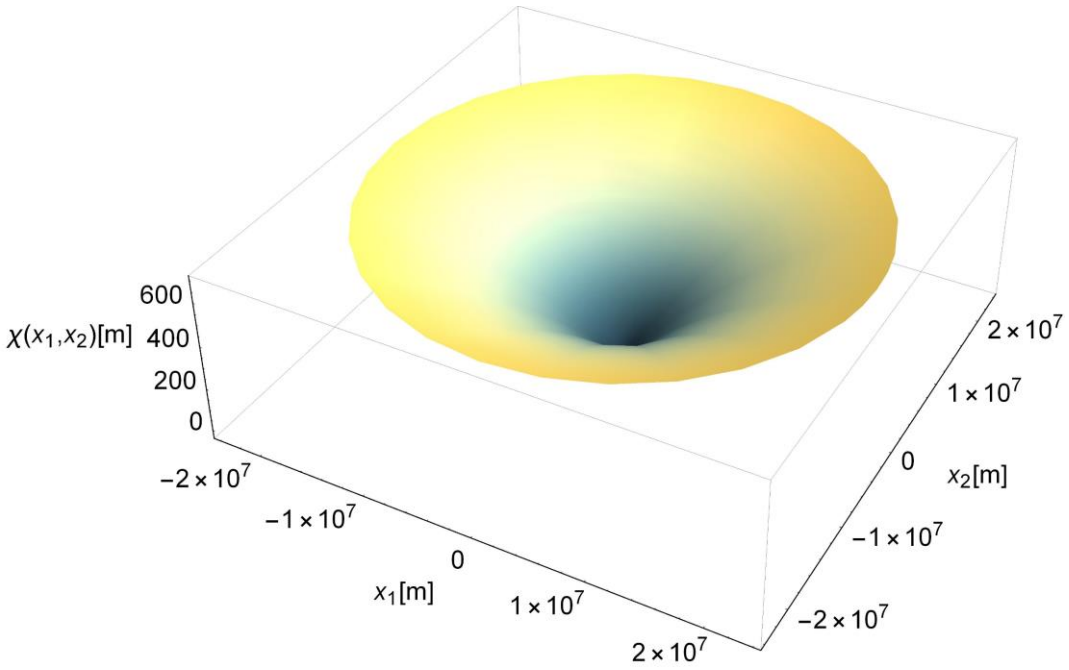

Fig. 20 Deformation of the boundary hypersurface ${}^{\alpha}\chi(x_1, x_2)$ for the Earth.

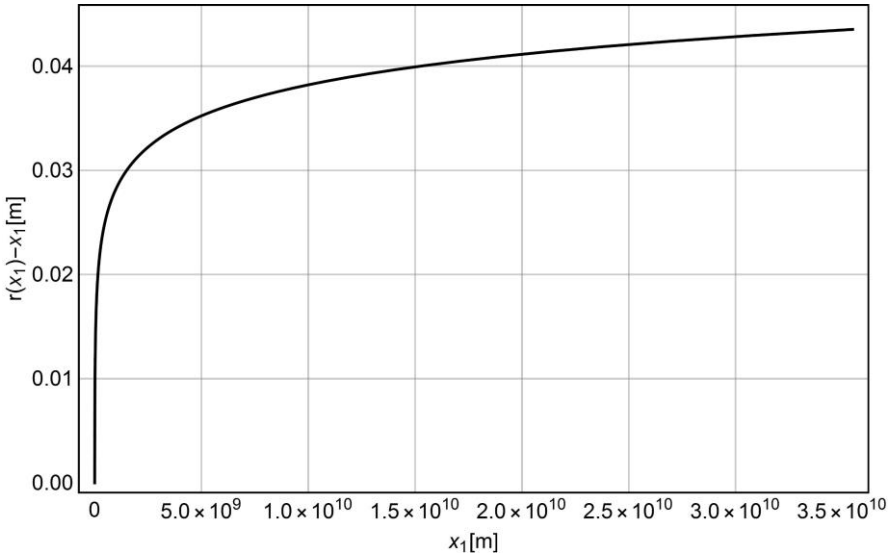

Fig. 21 Dependence diagram $r(x_1) - x_1$ for the Earth.

In the supplements the reader will find diagrams of dependencies ${}^{\alpha}\chi(x_1)$, ${}^{\alpha}\chi(x_1, x_2)$ and $r(x_1) - x_1$ for selected astronomical objects of the solar system.

Let us pay attention to the shape of boundary hypersurface ${}^{\alpha}\aleph^{\alpha}$ inside the astronomical object determined from Eq. (10)which makes no physical sense, which means that equation (10) is wrong. We will return to this topic after determining the shape of the hypersurface ${}^{\beta}\aleph^{\beta}$ and in subsequent publications.

Shape of the hypersurface ${}^{\beta}\aleph^{\beta}$

The theory cited by us entitled. "Theory of Space" introduces the concept of asymmetry vector ${}^{\alpha\beta}\vec{\xi}(r)$ of boundary hypersurfaces ${}^{\alpha}\aleph^{\alpha}$, ${}^{\beta}\aleph^{\beta}$which are not parallel in the vicinity of gravity sources. (Sobolewski D. S., Theory of Space, 2016) (Sobolewski D. S., Theory of Space, 2017) (Sobolewski D. S., Theory of Space, 2022 - new unpublished edition)

The vector ${}^{\alpha\beta}\vec{\xi}(r)$ is the projection of the unit vector ${}^{\beta}\hat{n}$ orthogonal to ${}^{\boldsymbol{\beta}}\boldsymbol{\aleph}^{\boldsymbol{\beta}}$ at a distance r from the gravity source onto the tangential beam $T\,{}^{\boldsymbol{\alpha}}\boldsymbol{\aleph}_{\boldsymbol{r}}^{\boldsymbol{\alpha}}$as shown in figure Fig. 22. (Sobolewski D. S., Theory of Space, 2016) (Sobolewski D. S., Theory of Space, 2017) (Sobolewski D. S., Theory of Space, 2022 - new unpublished edition)

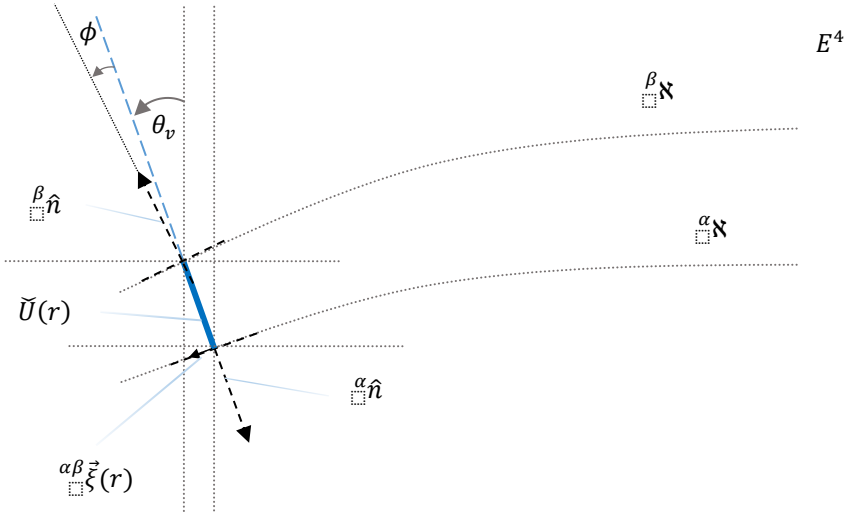

Fig. 22. Interpretation of asymmetry vector ${}^{\alpha\beta}\vec{\xi}(r)$. (Sobolewski D. S., Theory of Space, 2016) (Sobolewski D. S., Theory of Space, 2017) (Sobolewski D. S., Theory of Space, 2022 - new unpublished edition)

Further, the space theory we have cited introduces a geometric object in the form of a scalar - a constant $k_{Poznań}$, which relates the rate of change of $\frac{d\Theta_v}{dt}$ of the inclination angle Θ_v of the orientation of the space channel $\breve{U}(r)$ with the asymmetry vector ${}^{\alpha\beta}\xi_1(r)$. (Sobolewski D. S., Theory of Space, 2016) (Sobolewski D. S., Theory of Space, 2017) (Sobolewski D. S., Theory of Space, 2022 - new unpublished edition)

$$\frac{d\Theta_v}{dt}(r) = k_{Poznań}\,{}^{\alpha\beta}\xi_1(r) = -k_P\left\|{}^{\beta}\hat{n}\right\|\,\sin\phi(r) \qquad (18)$$

Finally, the following equations are obtained (Sobolewski D. S., Theory of Space, 2016) (Sobolewski D. S., Theory of Space, 2017) (Sobolewski D. S., Theory of Space, 2022 - new unpublished edition):

$$\frac{d\,{}^{\beta}\chi(r)}{dr} = \frac{1}{\sqrt{\frac{c^2\left\|{}^{\beta}\hat{n}\right\|^2 {k_P}^2}{G^2\,M^2}r^4 - 1}} \quad \{r: R \le r\} \qquad (19)$$

$$\frac{d\,{}^{\beta}\chi'(r)}{dr} = \frac{G\,M\,r}{\sqrt{-G^2M^2r^2 + c^2\left\|{}^{\beta}\hat{n}\right\|^2 {k_P}^2 R^6}} \quad \{r: 0 \le r \le R\} \qquad (20)$$

, where:

$k_P \approx 1.676691598386682\;10^{14}\;\frac{rad}{m\,s}$

$C_1 = 3.272020135300692\;10^{28}\;m$

$A_\gamma = \frac{c}{G}$

M, R - Mass and radius of an astronomical object,

r - the distance from the center of gravity of a gravity source measured along the geodesic,

$\left\|{}^{\beta}\hat{n}\right\| = 1m$ - the length of the unit vector.

Whereby the boundary condition is required to be satisfied ${}^{\beta}\chi'(R) = {}^{\beta}\chi(R)$. (Sobolewski D. S., Theory of Space, 2016) (Sobolewski D. S., Theory of Space, 2017) (Sobolewski D. S., Theory of Space, 2022 - new unpublished edition)

The determined maximum distance between boundary hypersurfaces away from gravitational field sources is $\tau_{max} \approx 8.94\ 10^{-7}m + 1.355\ 10^{-20}\ m$. The distance between boundary hypersurfaces on the Earth's surface is $\tau_{Earth} \approx 8.94\ 10^{-7}m$, which means that the Earth decreases the distance between boundary hypersurfaces by $\Delta\tau \approx 1.35525271560688 \times 10^{-20}\ m$. (Sobolewski D. S., Theory of Space, 2022 - new unpublished edition)

To sum up, find numerically the solution of equation (19) and then move from a curvilinear coordinate system to a coordinate system in E^4 with the origin coinciding with the center of gravity of the astronomical[5] object.

Let us note that the relation determined by us numerically $r(x_1)$ for a given astronomical object allows us to analyse deformations of boundary hypersurfaces in Cartesian coordinates with the origin located at its center of gravity.

To sum up, we will solve all equations describing the hypersurface ${}^{\beta}\chi(r)$ in the curvilinear coordinate system defined by the graph ${}^{\alpha}\chi(r)$in which $cos\,\Theta_v = 1$. It should be emphasized that the solution of equation (21) for $r \geq R$ is presented in the theory entitled. "Theory of Space", which we cite courtesy of the author to have a set of equations (Sobolewski D. S., Theory of Space, 2016) (Sobolewski D. S., Theory of Space, 2017) (Sobolewski D. S., Theory of Space, 2022 - new unpublished edition):

$$k_P \left\| {}^{\beta}\hat{n} \right\| \sin\phi(r) = \frac{G}{c}\frac{M}{r^2} \quad \{r: R \leq r\} \qquad (21)$$

$$k_P \left\| {}^{\beta}\hat{n} \right\| \sin\phi(r) = \frac{G}{c}\frac{M}{R^3} r \quad \{r: 0 \leq r \leq R\} \qquad (22)$$

Determining r from the equations (21) and (22) and calculating respectively $\frac{dr}{d\phi}$ we have:

$$\frac{dr}{d\phi} = -\frac{\sqrt{G}\sqrt{M}\cos(\phi)\csc^{\frac{3}{2}}(\phi)}{2\sqrt{c}\sqrt{k}} \quad \{r: R \leq r\} \qquad (23)$$

$$\frac{dr}{d\phi} = \frac{ckR^3\cos(\phi)}{GM} \quad \{r: 0 \leq r \leq R\} \qquad (24)$$

Determining dr from the equations (23) and (24) and substituting into the equations resulting from the geometric interpretation of the derivative:

$$\frac{d\,{}^{\beta}\chi}{dr} = \tan(\phi) \qquad (25)$$

, we obtain:

$$d\,{}^{\beta}\chi = -\tan(\phi)\frac{\sqrt{G}\sqrt{M}\cos(\phi)\csc^{\frac{3}{2}}(\phi)}{2\sqrt{c}\sqrt{k}} d\phi \quad \{r: R \leq r\} \qquad (26)$$

$$d\,{}^{\beta}\chi = \tan(\phi)\frac{ckR^3\cos(\phi)}{G\,M} d\phi \quad \{r: 0 \leq r \leq R\} \qquad (27)$$

By integrating the two-sided equations (26), (27) we obtain:

$${}^{\beta}\chi = -\int \frac{\sqrt{G}\sqrt{M}\sqrt{\csc(\phi)}}{2\sqrt{c}\sqrt{k}} d\phi = \frac{\sqrt{G}\sqrt{M}\sqrt{\sin(\phi)}\sqrt{\csc(\phi)}F\left(\frac{1}{4}(\pi - 2\phi)|2\right)}{\sqrt{c}\sqrt{k}} + C_1 \quad \{r: R \leq r\} \qquad (28)$$

$${}^{\beta}\chi = \int \tan(\phi)\frac{ckR^3\cos(\phi)}{G\,M} d\phi = -\frac{ckR^3\cos(\phi)}{GM} + C_2 \quad \{r: 0 \leq r \leq R\} \qquad (29)$$

[5] In addition, we assume that the astronomical object is homogeneous.

Determining from equations (21) and (22) ϕ we obtain:

$$\phi = \sin^{-1}\left(\frac{G\,M}{c\,k_P\,r^2}\right) \quad \{r: R \le r\} \qquad (30)$$

$$\phi = \sin^{-1}\left(\frac{G\,M\,r}{c\,k_P\,R^3}\right) \quad \{r: 0 \le r \le R\} \qquad (31)$$

By substituting into the equations (28) and (29) for ϕ the right-hand sides of the equations (30) and (31) we obtain:

$${}^{\beta}\chi(r) = \sqrt{\frac{GM}{ck}}F\left(\frac{1}{2}\cos^{-1}\left(\frac{GM}{ckr^2}\right)|2\right) + C_1 \quad \{r: R \le r\} \qquad (32)$$

$${}^{\beta}\chi(r) = -\frac{c\,k\,R^3\sqrt{1-\frac{G^2M^2r^2}{c^2k^2R^6}}}{G\,M} + C_2 \quad \{r: 0 \le r \le R\} \qquad (33)$$

Constants C_1 and C_2 can be determined using the fact that on the Earth the distance τ_{Earth} between boundary hypersurfaces ${}^{\beta}\aleph^{\beta}$ and ${}^{\alpha}\aleph^{\alpha}$ is $\tau_{Earth} \approx 8.94\,10^{-7}m$ (Sobolewski D. S., Theory of Space, 2016) (Sobolewski D. S., Theory of Space, 2017) (Sobolewski D. S., Theory of Space, 2022 - new unpublished edition), which leads to the following equations:

$${}^{\beta}\chi(R_E) = \tau_{Earth} = \sqrt{\frac{G\,M_E}{c\,k_P}}F\left(\frac{1}{2}\cos^{-1}\left(\frac{G\,M_E}{c\,k_P\,{R_E}^2}\right)|2\right) + C_1 \quad \{r: R \le r\} \qquad (34)$$

$${}^{\beta}\chi(R_E) = \tau_{Earth} = -\frac{c\,k_P\sqrt{1-\frac{G^2M^2}{c^2{k_P}^2{R_E}^4}}{R_E}^3}{G\,M} + C_2 \quad \{r: 0 \le r \le R\} \qquad (35)$$

, where R_E and M_E denote the Earth's polar radius and its mass respectively.

Finally, from the equations (34) and (35) we obtain the values of constants C_1 and C_2, which are equal to:

$$C_1 = \tau_{Earth} - \sqrt{\frac{G\,M_E}{c\,k_P}}F\left(\frac{1}{2}\cos^{-1}\left(\frac{G\,M_E}{c\,k_P\,{R_E}^2}\right)\middle|2\right) \approx -1.1585288788904077 \times 10^{-4}\,m \quad \{r: R \le r\} \qquad (36)$$

$$C_2 = \tau_{Earth} + \frac{ck\sqrt{1-\frac{G^2{M_E}^2}{c^2k^2{R_E}^4}}{R_E}^3}{G\,M_E} \approx 3.272020135300692 \times 10^{28}\,m \quad \{r: 0 \le r \le R\} \qquad (37)$$

Using the equations (32) and (33) we will draw for the Earth the diagram of the relationship ${}^{\beta}\chi(r)$ in a curvilinear system and for other astronomical objects of the solar system the reader will find such diagrams in the supplements.

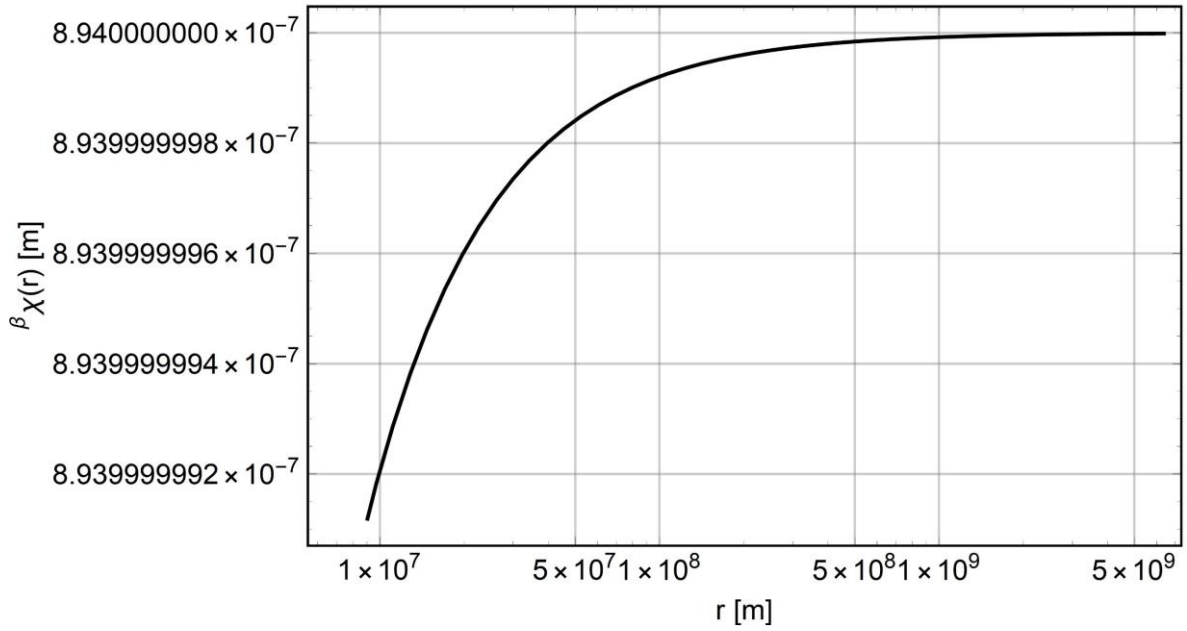

Fig. 23. Dependence diagram ${}^{\beta}\chi(r)$ for $r \geq R_E$ for the Earth.

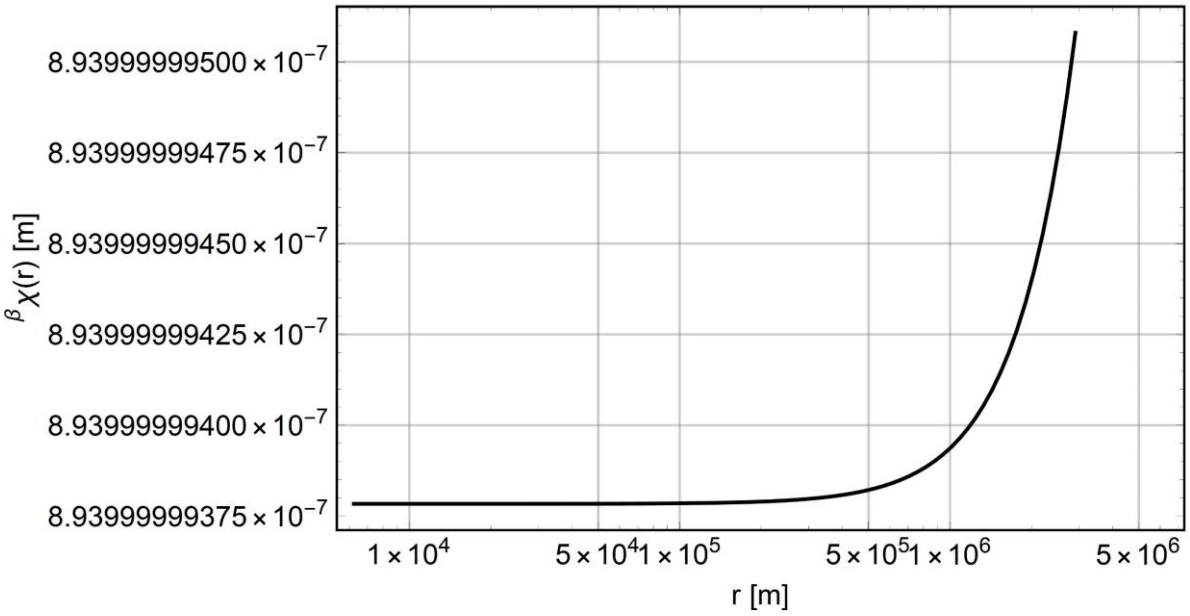

Fig. 24. Dependence diagram ${}^{\beta}\chi(r)$ for $0 \leq r \leq R_E$ for the Earth.

Using the relation $r(x_1)$ determined numerically (the determined relation was used to draw $r(x_1) - x_1$ eq. Fig. 16) for each of the described astronomical objects, it is possible to change the curvilinear system for ${}^{\beta}\chi(r)$ to the Cartesian one, in which the origin of the coordinate system is located at the geometrical center of the astronomical object, coinciding with its center of gravity, as we have assumed that the astronomical objects analysed by us are homogeneous.

Therefore, using the relation $r(x_1)$ for a given astronomical object and the parametric equations:

$$ {}^{\beta}\chi(X^1) = \left(X^1(x^1), X^4(x^1)\right) \tag{38}$$

$$ X^1(x^1) = r^{-1}(r) - \tau(r)\frac{d\,{}^{\alpha}\chi\left(r^{-1}(r)\right)}{dx^1}\frac{1}{\sqrt{1+\left(\frac{d\,{}^{\alpha}\chi\left(r^{-1}(r)\right)}{dx^1}\right)^2}} \tag{39}$$

$$X^4(x^1) = {}^{\alpha}\chi(r^{-1}(r)) + \tau(r)\frac{1}{\sqrt{1+\left(\frac{d\,{}^{\alpha}\chi(r^{-1}(r))}{dx^1}\right)^2}} \quad (40)$$

where $x^1 = r^{-1}(r)$.

In this publication we will not present diagrams of the relations ${}^{\beta}\chi(x_1)$ but the inquisitive reader can do it himself using the equations presented and the scripts: www.theoryofspace.info[7].

Orientation distribution of space channels in the interior of an astronomical object

The determined shape of boundary hypersurface ${}^{\alpha}\aleph^{\alpha}$ in the interior of astronomical objects leads to interesting conclusions. Well, it turns out that the derivative of function j ${}^{\alpha}\chi$ in the point $x = 0$ is discontinuous, what follows directly from equation (12) and the graph of the function presented in Fig. 14 and which has no physical interpretation.

Moreover, taking into account a neutral orientation of the space channels with respect to the boundary hypersurface ${}^{\alpha}\aleph^{\alpha}$, i.e. orthogonal to it and thus not leading to its deformation[6], we will come to the conclusion that in the interior of the astronomical object there are interactions also between space channels.

This is due to the fact that spatial channels inclined with respect to each other should be treated as moving with respect to each other with different velocities, which results from the relation $E(v)$ revealed in the theory entitled "Theory of Space". "Theory of Space" (Sobolewski D. S., Theory of Space, 2016) (Sobolewski D. S., Theory of Space, 2017) (Sobolewski D. S., Theory of Space, 2022 - new unpublished edition):

$$\mathrm{E(v)} = \mathrm{m_0c^2} + \mathrm{E_{\Delta J}} + \mathrm{E_S} \quad (41)$$

where $\mathrm{E_{\Delta J}}$ is the energy needed to change the orientation of vertical disturbances of space:

$$\mathrm{E_{\Delta J}} = \mathrm{m_0c^2(1-\cos(\Theta_v))} \quad (42)$$

while $\mathrm{E_S}$ is the deformation energy of elastic boundary layers:

$$\mathrm{E_S} = \mathrm{m_0c^2(\cos^{-1}\Theta_v + \cos\,(\Theta_v) - 2)} \quad (43)$$

where in accordance with "Theory of Space" (Sobolewski D. S., Theory of Space, 2016) (Sobolewski D. S., Theory of Space, 2017) (Sobolewski D. S., Theory of Space, 2022 - new unpublished edition), $\cos(\Theta_v)$ is equal to:

$$\cos\,(\Theta_v) = \sqrt{1-\frac{v^2}{c^2}} \quad (44)$$

Whereby the angle Θ_v for a space channel falling freely from infinity is indicated in Fig. Fig. 22.

The varying orientation of the spatial channels can be clearly seen in the illustrative drawings Fig. 25 and Fig. 26 especially in the area of the astronomical object nucleus.

[6] Energy $E_S = 0$ and the angle Θ'_v determined in a tangential beam $T\,{}^{\alpha}\aleph^{\alpha}{}_x$ at the point x to the boundary hypersurface ${}^{\alpha}\aleph^{\alpha}$ is equal to zero.

[7] The offered scripts were used in this publication.

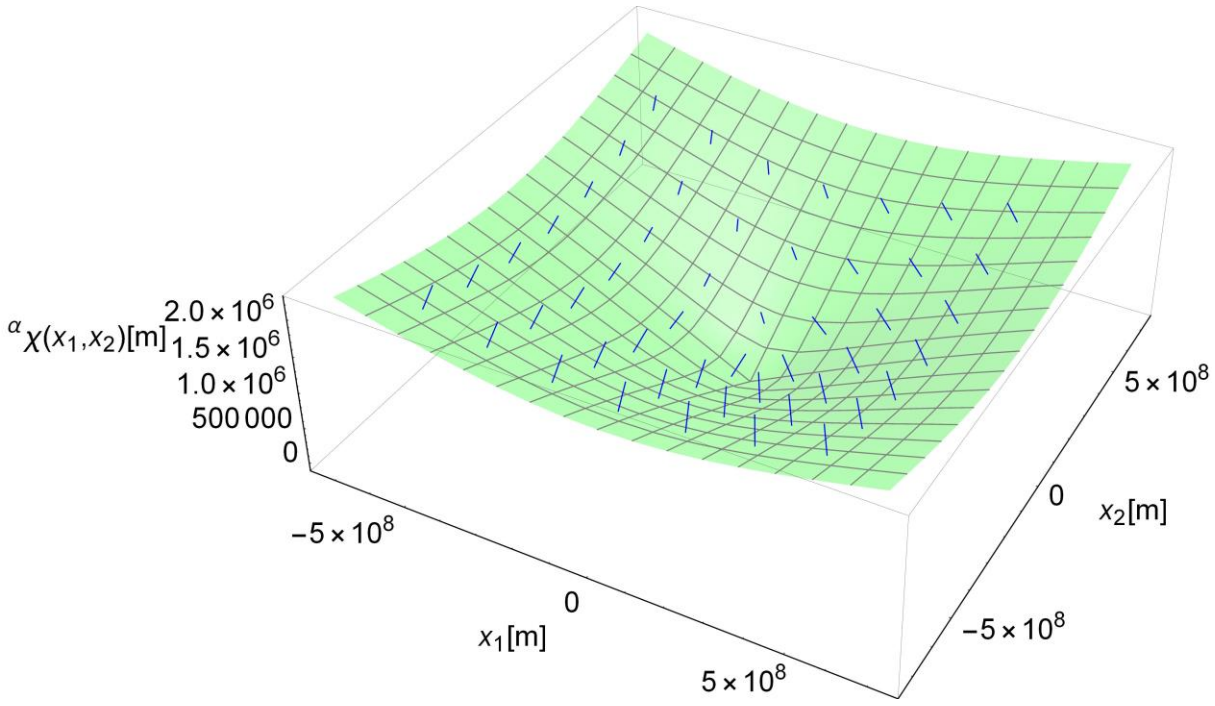

Fig. 25 Overview drawing of the distribution of spatial channel orientations in the Sun's interior and immediate surroundings.

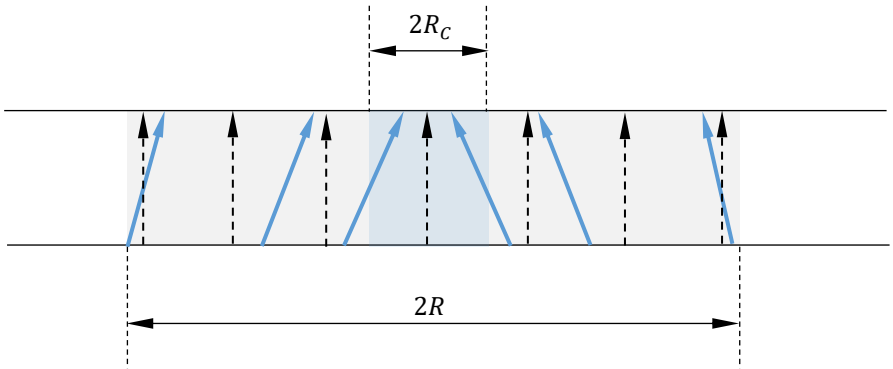

Fig. 26 Illustrative drawing of the distribution of orientation of space channels in the interior of an astronomical object with radius R and radius of the nucleus R_C.

In summary, the different properties of boundary hypersurfaces $^{\alpha}\aleph^{\alpha}$ and $^{\beta}\aleph^{\beta}$ together with the stresses introduced by the space channels connecting these hypersurfaces lead to their deformation and space curvature.

On the other hand, the interaction of space channels in the interior of the astronomical object leads to the normalisation of the distribution of their orientation, which, due to the symmetry of the astronomical object and gravitational field, should be close to the average value of their orientation, i.e. to the orientation of channels orthogonal to the hypersurface $^{\alpha}\aleph^{\alpha}$ at a large distance from the astronomical object, which is marked with dashed arrows in the figure Fig. 26.

Let us note that a different distribution of the orientation of the space channels is possible if the nucleus of the astronomical object rotates relative to the astronomical object or is anisotropic. Let us add that a different distribution of the orientation of the space channels in the interior of the astronomical object would lead to the formation of a magnetic field around the astronomical[7] object.

Optimum configuration of the rocket before launch

It follows directly from the previous section that the orientation of the space channels of an astronomical object including a rocket is approximately the same as the orientation of the space channels in a region of space at a great distance from the astronomical object.

Thus, the energy required for a rocket to leave the gravitational field of an astronomical object is not needed to change the orientation of its space channels, but to perform work against the gravitational forces which are a consequence of the decreasing distance between boundary hypersurfaces and the effect of pulling the space channels into regions of space with smaller distance between boundary hypersurfaces, as shown in Fig.

Fig. **27**.

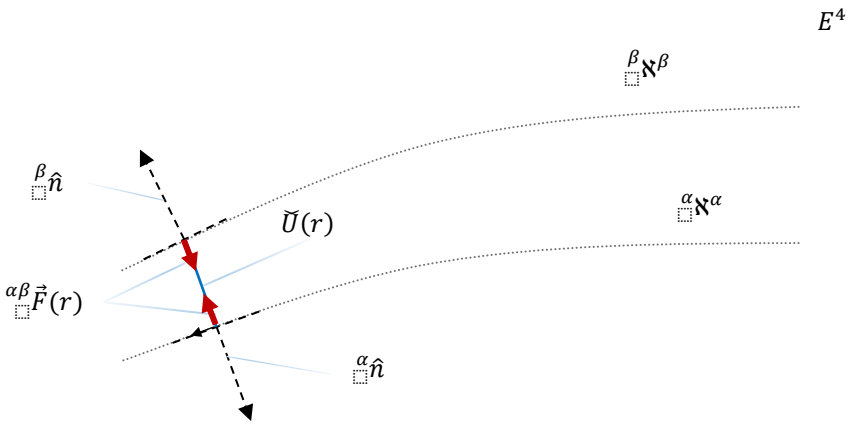

Fig. 27. The effect of pulling down space channels
$\breve{U}(r)$ into space areas with smaller distance between boundary hypersurfaces
${}^{\alpha}\aleph^{\alpha}$ and ${}^{\beta}\aleph^{\beta}$.

Recall that at the Earth's surface the distance between boundary hypersurfaces is reduced by $\Delta\tau \approx 1.35525271560688 \times 10^{-20}\, m$ and in its interior by another $\Delta\tau_2 \approx 6.21644552561128 \times 10^{-16}\, m$ which can be found in the additions.

In the article titled. "New Generations of Rocket Engines" (Sobolewski D. S., Sobolewski, Sobolewski, Sobolewska, & Sobolewska, 2020) (Sobolewska, Sobolewska, Sobolewski, Sobolewski, & Sobolewski, 2021) we touched, among other things, on the use of the Earth's gravitational field to orient the space channels of a rocket before launch.

We mentioned such possibilities when considering the stabilisation of the orientation of spatial channels. Consequently, given the possibility of their stabilisation, one can imagine changing their orientation to be orthogonal to the boundary hypersurface ${}^{\alpha}\aleph^{\alpha}$as shown in the illustrative figure Fig. 25 and then rotate them stabilising their orientation before the rocket launch.

With the reorientation of the rocket's space channels along with the passengers, the travellers themselves would experience a similar effect to falling downwards, so that eventually, after stabilisation of the space channels and their rotation[8], the optimal configuration of the rocket would be achieved before launch.

The illustrative figure Fig. 28 shows the successive stages of orientation of the space channels of the rocket with passengers, where:

[8] During the rotation of the space channels, cosmonauts would theoretically not observe any side effects, although this would be an energy-intensive operation. It should be stressed that we are considering technical possibilities on purely theoretical grounds.

1 - Initial state of the rocket before configuration,

2 - State of the rocket after orthogonalization of the space channels to the hypersurface $^{\alpha}א^{\alpha}$ - the perceived effect is a downward slope,

3 - Status of the rocket after configuration.

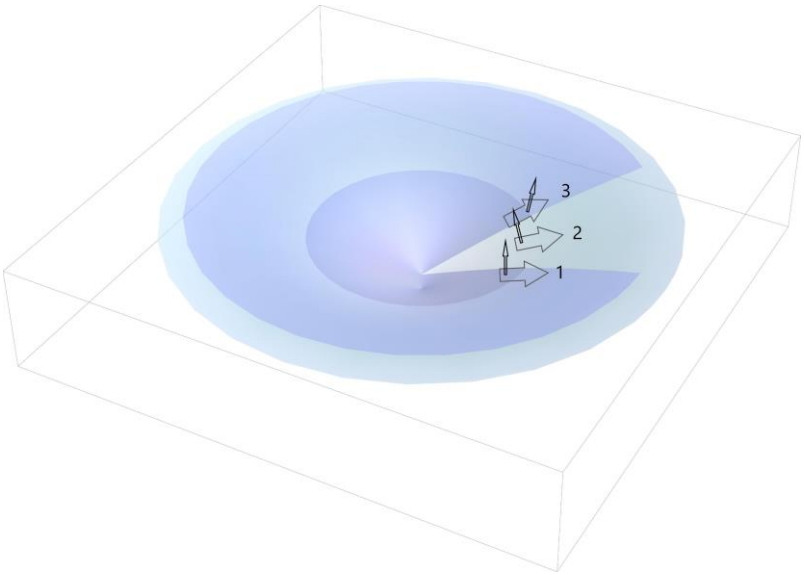

Fig. 28. *Overview drawing showing the successive stages of orientation of the rocket's space channels prior to launch.*

After take-off, the ship's passengers would feel the effects of braking, as the gradually released energy from the reoriented space channels would be used to overcome the Earth's gravitational field. However, the gradual release of energy $E_{\Delta J}$ would also require the use of technology to stabilise the orientation of the space channels (Sobolewski D. S., Sobolewski, Sobolewski, Sobolewska, & Sobolewska, 2020) (Sobolewska, Sobolewska, Sobolewski, Sobolewski, & Sobolewski, 2021).

Dark Matter and The Existence of Other Universes

The universe as we know it is a thin layer of a sphere of radius R_w immersed in E^4. Preliminary estimates suggest[9] that the thickness of the layer is greater than or equal to $0.894\ \mu m$ on the surface of the Earth plus the distance determined in the present project $1.355 \times 10^{-20}\ m$ in areas of space away from the sources of the gravitational field.

The question then arises as to whether other universes exist and whether we will ever be able to find evidence of this?

Well, in the event that universes interact with each other, the effects of their interactions should be observed, which can be predicted using the structure of space revealed in the theory entitled "Theory of Space" revealed in the structure of space (Sobolewski D. S., Theory of Space, 2016) (Sobolewski D. S., Theory of Space, 2017) (Sobolewski D. S., Theory of Space, 2022 - new unpublished edition).

The effect of interacting universes may be to change the distance between boundary hypersurfaces in areas of interaction, which would be observed as so-called dark matter.

Moreover, the interactions could result in the creation of gravitational and fluctuation waves (Sobolewska, Sobolewska, Sobolewski, Sobolewski, & Sobolewski, 2021) (Sobolewski D. S., Sobolewski, Sobolewski, Sobolewska, & Sobolewska, 2020) or even creation of turbulences interpreted as matter generated directly from

[9] See the theory entitled. "Theory of Space" (Sobolewski D. S., Theory of Space, 2016), (Sobolewski D. S., Theory of Space, 2017), (Sobolewski D. S., Theory of Space, 2022 - new unpublished edition).

space, which, taking into account the energy of interactions, would not lead to violation of fundamental principles of physics.

In order to determine whether there are other universes located concentrically with ours, e.g. inside or outside it, one should determine the maximum strain of the boundary hypersurface ${}^{\alpha}\aleph^{\alpha}$which will determine the minimum distance to the universe located inside ours at which no transitions between universes[10] are formed.

The minimum distance between the world located inside our universe, determined in this way, will also apply to the world located concentrically outside our universe, because it can be assumed that its structure will be similar and therefore there will be astronomical objects deforming space inwards, i.e. towards our universe.

It can also be assumed that the deformation of space caused by massive black holes is radially oriented, since we know of no physical reason for them to form along the chords of the universe, which approximates to a thin sphere of radius $R_w \approx 4040{,}33\ \mathrm{Mpc}$[11].

In summary, we are looking for the maximum deformation ${}^{\alpha}\chi_{max}$ in the coordinate system associated with an astronomical object whose origin coincides with its geometric center and center of gravity.

Directly from equations (15) and (16) we obtain:

$$2Rc^2 - 3G\,M > 0 \quad (45)$$

$$c^2R - G\,M > 0 \quad (46)$$

and after transformations respectively[12]:

$$\frac{M}{R} < \frac{2c^2}{3G} \quad (47)$$

$$\frac{M}{R} < \frac{c^2}{G} \cong 1.34659 * 10^{27}\ [\frac{kg}{m}] \quad (48)$$

Directly from the inequality (48) follows that the quotient of the mass by the radius of an astronomical object must be smaller than $\frac{c^2}{G}$ in order to apply formulas for ${}^{\alpha}\chi_{max}$ including numerical calculations based on them.

For example, astronomical objects with a radius of the Sun R_S may have mass at most M_{Smax}, so that the formulae for ${}^{\alpha}\chi_{max}$:

$$M_{Smax} < 1.34659 * 10^{27} * R_S = 9.36823 * 10^{35} kg \cong 0.4711443\ 10^6\ M_S \quad (49)$$

To sum up, we have a serious problem since we cannot determine the maximum deformation ${}^{\alpha}\chi_{max}$ for astronomical objects of radius of the Sun R_S and mass greater than or equal to M_{Smax}.

However, when analysing the relation ${}^{\alpha}\chi_{Smax}(M)$determined using numerical calculations, for a fixed radius of an astronomical object equal to the radius of the Sun R_S we come to the conclusion that it is a linear relationship, as shown in Fig. Fig. 29.

[10] We assume that such transitions between universes do not exist, because they would affect their instability including annihilation or absorption by a co-centric universe.

[11] See the addenda where we explain the interpretation of the radius of the Universe.

[12] Note that using Eq. $c^2R - G\,M = 0$ the Schwarzchild radius can be determined r_{schw} which means that the equations used by us to describe the deformation of a hypersurface ${}^{\alpha}\aleph^{\alpha}$ are applicable to astronomical objects of radius greater than r_{schw}.

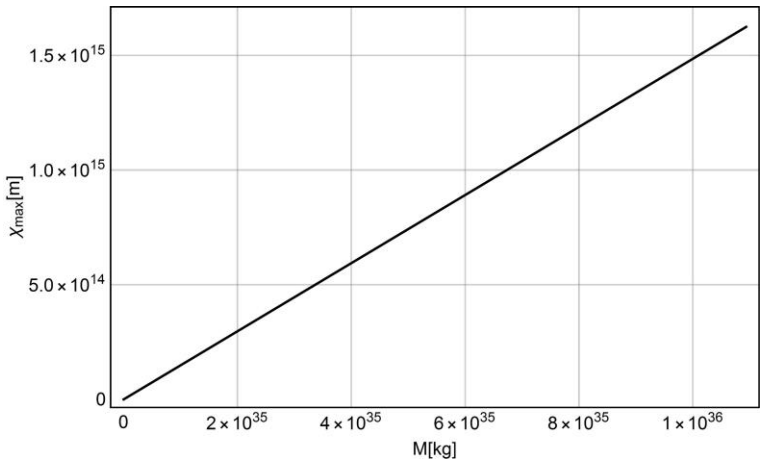

Fig. 29 Relationship ${}^{\alpha}\chi_{max}(M)$ for a fixed radius of an astronomical object equal to the radius of the Sun R_S. The proportionality coefficient is $1.4845 \times 10^{-23}\ \frac{m}{kg}$.

The proportionality factor between the mass of an astronomical object of radius equal to that of the Sun and the maximum deformation of the hypersurface ${}^{\alpha}\chi_{max}$ we shall denote as a constant k_{R_S}. Thus, we have:

$$ {}^{\alpha}\chi_{Smax} = k_{R_S} \times M \quad (50)$$

where $k_{R_S} = 1.4845 * 10^{-22}\ \frac{m}{kg}$

It turns out that the numerically determined relation ${}^{\alpha}\chi_{max}(M)$ for the largest known star UY Scuti, whose radius $R_{UY} \approx 1700\ M_S$ is many times greater than that of the Sun, is also proportional, as shown in Fig. 30.

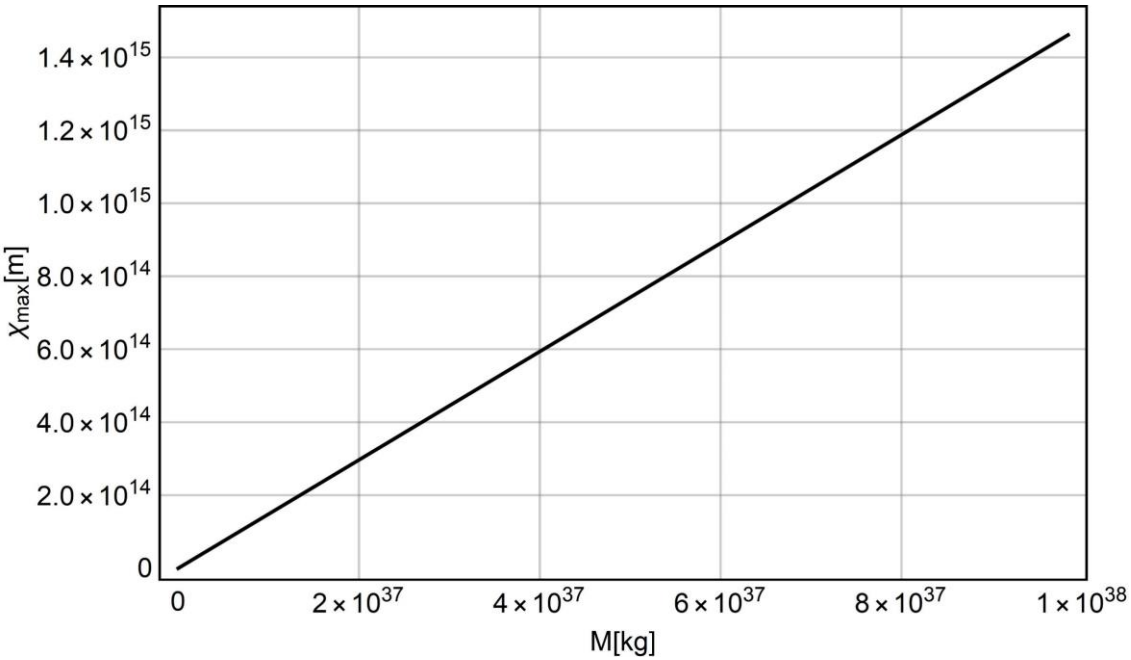

Fig. 30 Relationship ${}^{\alpha}\chi_{max}(M)$ for a fixed radius of an astronomical object equal to the radius UY Scuti of $R = 1700 \times R_S$. The proportionality coefficient is $k_{1700\,R_S} \approx 1.4847 \times 10^{-23}\ \frac{m}{kg}$.

The constant of proportionality for astronomical objects of radius equal to the radius UY Scuti is: $k_{1700\,R_S} \approx 1.4847 \times 10^{-23}\ \frac{m}{kg}$.

In general, it should be assumed that for astronomical objects of different radii we have different proportionality coefficients between their mass and the maximum deformation of the boundary hypersurface ${}^{\alpha}\aleph^{\alpha}$, therefore we will introduce a constant $G_{Gdańsk}$ which we shall call the Gdańsk constant defined as follows:

$$G_{Gdańsk} = \max\{k_{nR_S}: nR_S \in \Omega_O\} \approx 1.4847 \times 10^{-23}\ \frac{m}{kg} \quad (51)$$

where Ω_O is the set of radii of existing astronomical objects.

In summary, using the introduced Gdańsk constant, it is possible to determine the maximum deformation ${}^{\alpha}\chi$ or, in other words, the depth of the space tunnel using the formula:

$${}^{\alpha}\chi_{max} = G_{Gdańsk} \times M \quad (52)$$

Using the equation (52) we can overcome the maximum mass limit $M_{Smax} \approx 0.4711443\ 10^6\ M_S$ by extrapolating the relation (52).

Let us check what is the maximum deformation of the hypersurface ${}^{\alpha}\chi$ by substituting into the formula (52) the most massive astronomical object which is a black hole marked as TON 618 of mass $M_{T618} = 6.6 \times 10^{10} M_S$ mass of the Sun, which is four orders of magnitude greater than M_{Smax}:

$${}^{\alpha}\chi_{Smax}^{T618} = k_{R_S} \times M_{T618} \cong 1.948 \times 10^{18} m < R_W \cong 1.2468 \times 10^{26} m \quad (53)$$

Therefore, the formation of a wormhole is possible in the case ${}^{\alpha}\chi_{max} = 2R_W$ for a single black hole or for two black holes whose sum of the deformations of the hypersurfaces ${}^{\alpha}\chi$ is equal to $2R_W$.

To sum up, if there is a universe concentric with ours located in its interior[13], its radius should be of the order of $10^8 m$ so that the universes are stable and in the case of an external universe, its radius should be of the order $10^{44} m$.

The authors of this paper are convinced that there are no concentric universes, but they agree that there are other universes located in E^4, which can interact with each other.

SUPPLEMENTS

MERCURY

$Asymmetry\ vector\ on\ the\ surface$: ${}^{\alpha\beta}\xi(R) = -7.364065806231202 \times 10^{-23} m$

$Distance\ between\ boundary\ hipersurfaces$: ${}^{\beta}\chi(R) = 8.939999999101694 \times 10^{-7} m$

$Distance\ between\ boundary\ hipersurfaces$: ${}^{\beta}\chi(0) = 8.939999999101694 \times 10^{-7}$m

$Distance\ decrease\ between\ boundary\ hipersurfaces$: ${}^{\beta}\chi(R) - {}^{\beta}\chi(0) = 8.983055673731132 \times 10^{-17} m$

$Maximum\ hypersurface\ inclination\ {}^{\alpha}\chi$: $\forall_{i\in\{1,2,3\}} \frac{\partial\ {}^{\alpha}\chi}{\partial x_i}(0) = 1.7362174147005997 \times 10^{-5}\ rad$

$Maximum\ inclination\ of\ hypersurface\ {}^{\alpha}\chi\ on\ the\ surface\ of\ the\ astronomical\ object$: $\forall_{i\in\{1,2,3\}} \frac{\partial\ {}^{\alpha}\chi}{\partial x_i}(x_R)$
$= 1.4176166270661784 \times 10^{-5}\ rad$

[13] It is difficult to imagine a universe with a radius equal to that of the Sun.

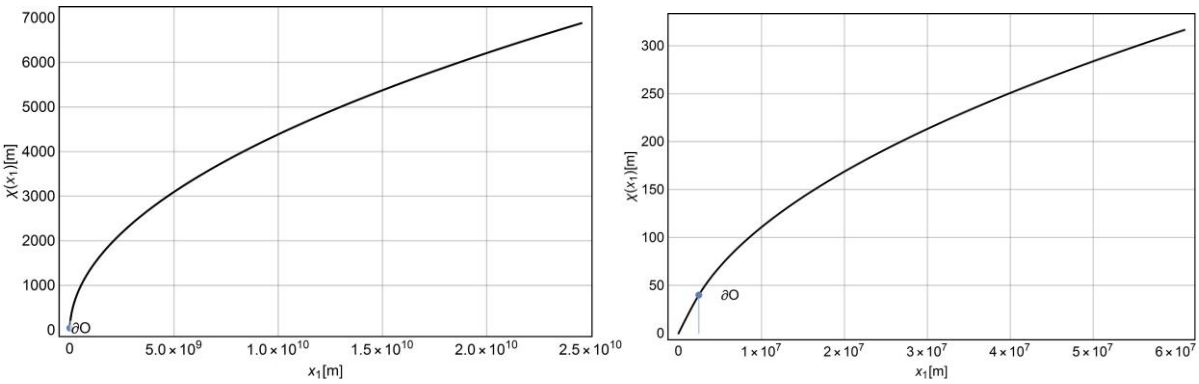

Fig. 31 Deformation of the boundary hypersurface ${}^{\alpha}\chi(x_1)$ for Mercury.

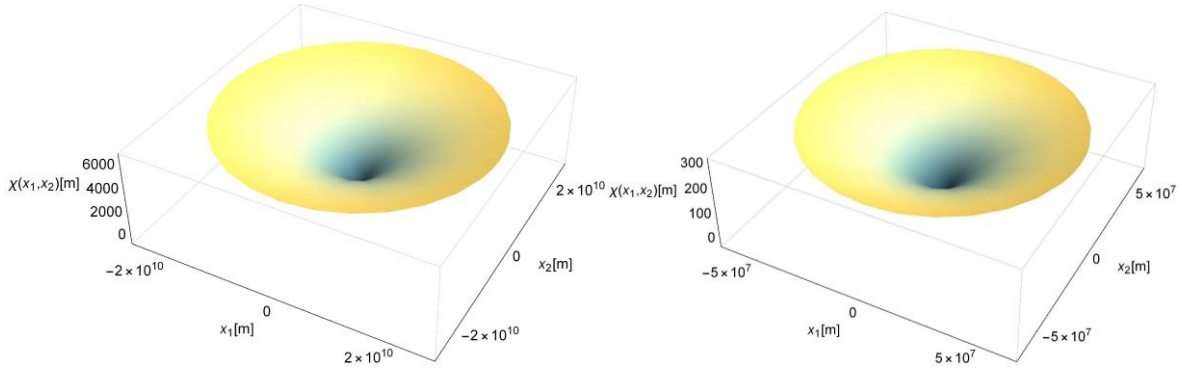

Fig. 32 Deformation of the boundary hypersurface ${}^{\alpha}\chi(x_1, x_2)$ for Mercury.

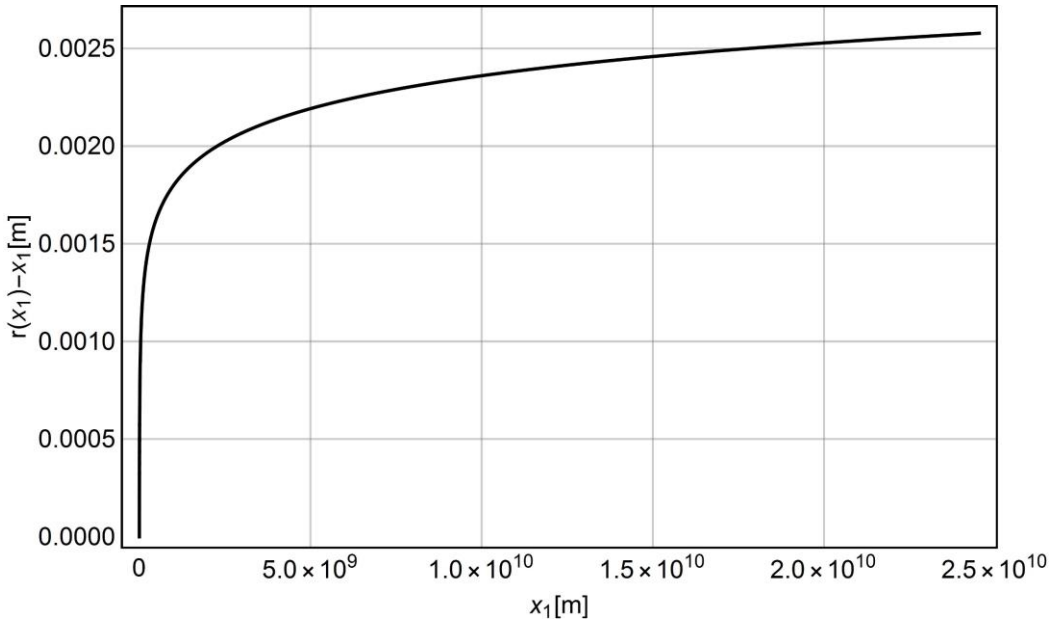

Fig. 33 Dependence diagram $r(x_1) - x_1$ for Mercury.

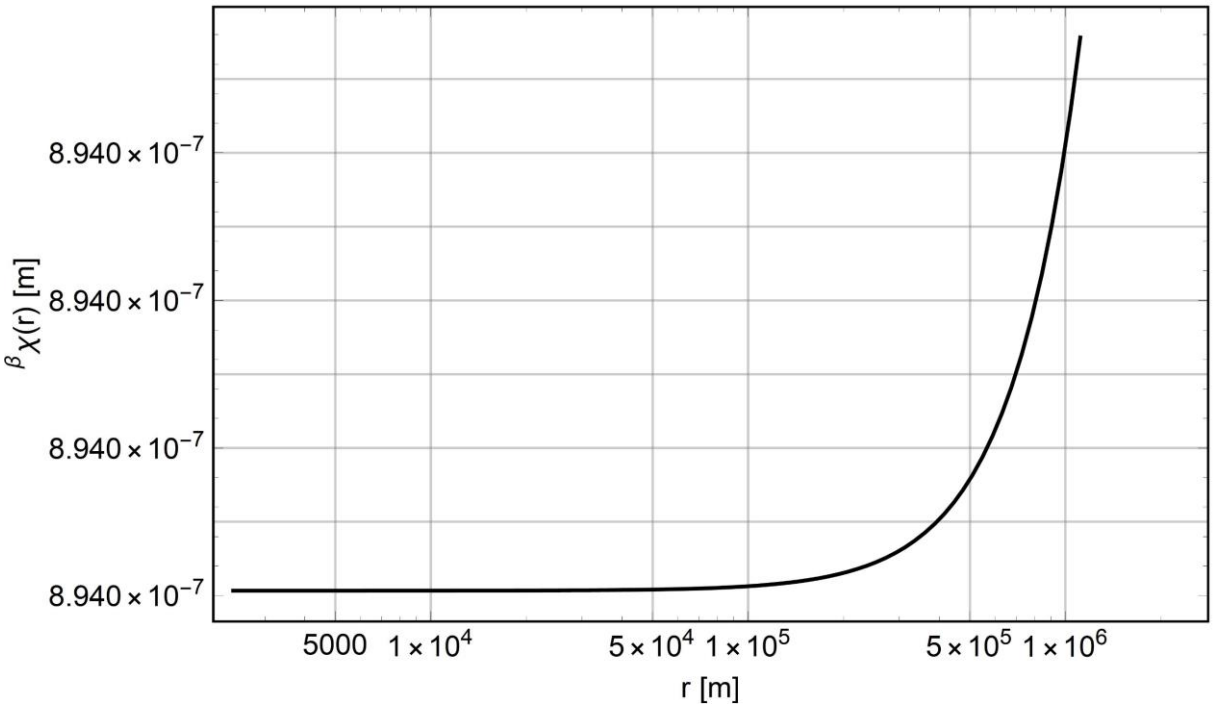

Fig. 34. Dependence diagram ${}^{\beta}\chi(r)$ for $0 \leq r \leq R_E$ for Mercury.

VENUS

$Surface\ asymmetry\ vector$: ${}^{\alpha\beta}\xi(\mathrm{R}) = -1.764509678202776\ 10^{-22} m$

$Distance\ between\ boundary\ hipersurfaces$: ${}^{\beta}\chi(\mathrm{R}) = 8.93999999466077\ 10^{-7} m$

$Distance\ between\ boundary\ hipersurfaces$: ${}^{\beta}\chi(0) = 8.93999999466077\ 10^{-7} m$

$Distance\ decrease\ between\ boundary\ hipersurfaces$: ${}^{\beta}\chi(\mathrm{R}) - {}^{\beta}\chi(0) = 5.33922983527378 \times 10^{-16}$ m

$Maximum\ hypersurface\ inclination\ {}^{\alpha}\chi$: $\forall_{i\in\{1,2,3\}} \frac{\partial\, {}^{\alpha}\chi}{\partial x_i}(0) = 4.232833458981465 \times 10^{-5}\ rad$

$Maximum\ inclination\ of\ hypersurface\ {}^{\alpha}\chi\ on\ the\ surface\ of\ the\ astronomical\ object$: $\forall_{i\in\{1,2,3\}} \frac{\partial\, {}^{\alpha}\chi}{\partial x_i}(x_R) = 3.456093939816062 \times 10^{-5}\ rad$

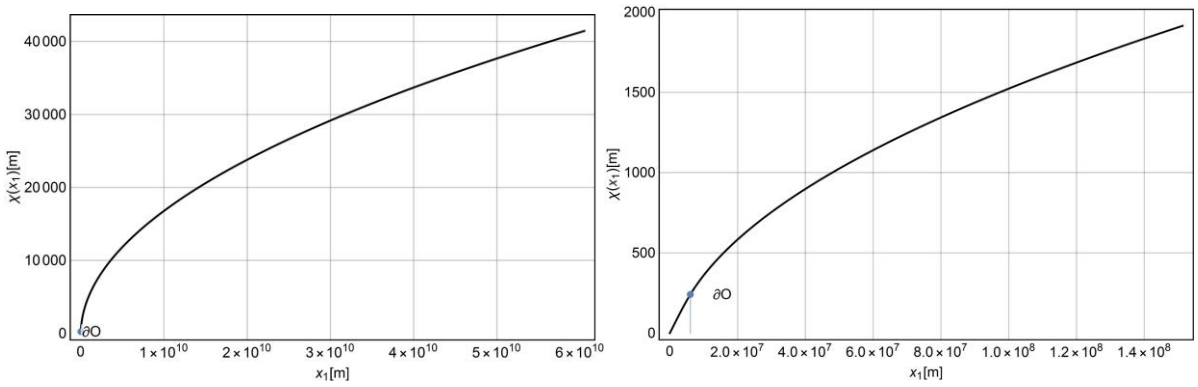

Fig. 35 Deformation of the boundary hypersurface ${}^{\alpha}\chi(x_1)$ for Venus.

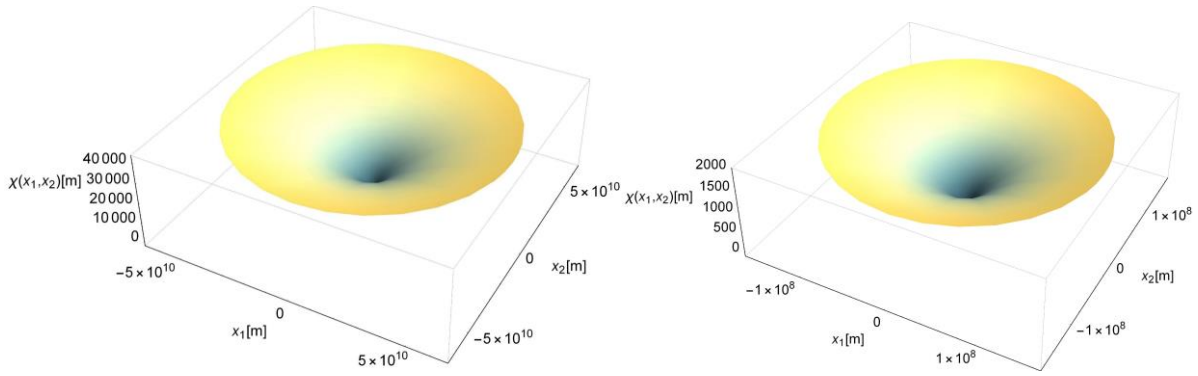

Fig. 36 Deformation of the boundary hypersurface ${}^{\alpha}\chi(x_1, x_2)$ for Venus.

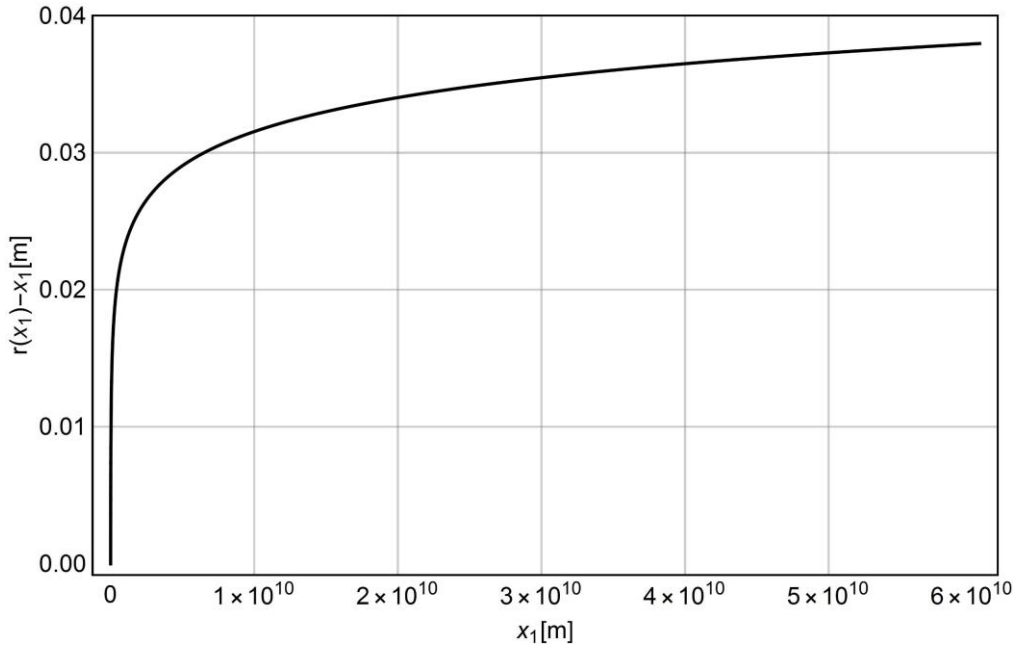

Fig. 37 Dependence diagram $r(x_1) - x_1$ for Venus.

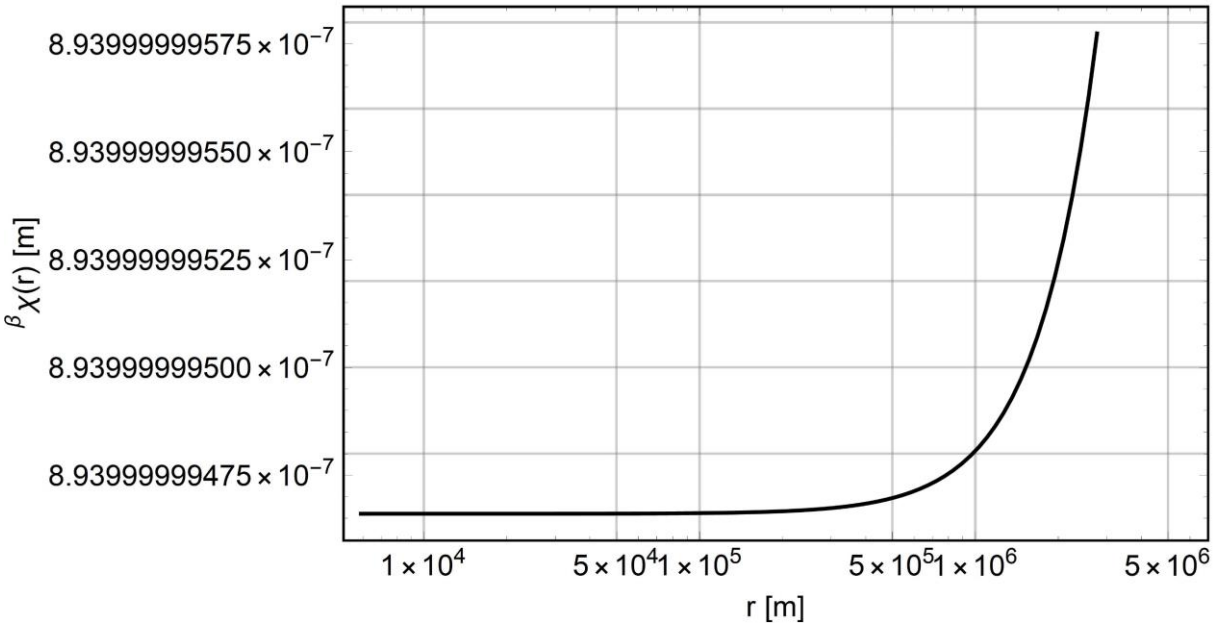

Fig. 38. Dependence diagram ${}^{\beta}\chi(r)$ for $0 \leq r \leq R_E$ for Venus.

EARTH

$Asymmetry\ vector\ on\ the\ surface$: ${}^{\alpha\beta}\xi(\mathrm{R}) = -1.949297295327879 \times 10^{-22}$ m

$Distance\ between\ boundary\ hipersurfaces$: ${}^{\beta}\chi(\mathrm{R}) = 8.939999999999952 \times 10^{-7}$ m

$Distance\ between\ boundary\ hipersurfaces$: ${}^{\beta}\chi(0) = 8.939999999999952 \times 10^{-7}$ m

$Distance\ decrease\ between\ boundary\ hipersurfaces$: ${}^{\beta}\chi(\mathrm{R}) - {}^{\beta}\chi(0) = 6.21644552561128 \times 10^{-16}\ m$

$Maximum\ hypersurface\ inclination\ {}^{\alpha}\chi$: $\forall_{i\in\{1,2,3\}} \frac{\partial\, {}^{\alpha}\chi}{\partial x_i}(0) = 4.567335711901286 \times 10^{-5}\ rad$

$Maximum\ inclination\ of\ hypersurface\ {}^{\alpha}\chi\ on\ the\ surface\ of\ the\ astronomical\ object$: $\forall_{i\in\{1,2,3\}} \frac{\partial\, {}^{\alpha}\chi}{\partial x_i}(x_R) = 3.729214091953053 \times 10^{-5}\ rad$

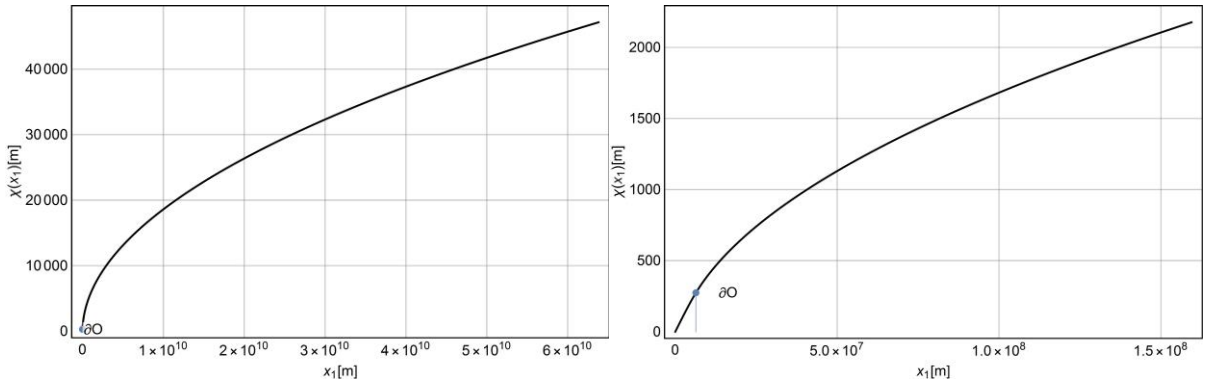

Fig. 39 Deformation of the boundary hypersurface ${}^{\alpha}\chi(x_1)$ for Earth.

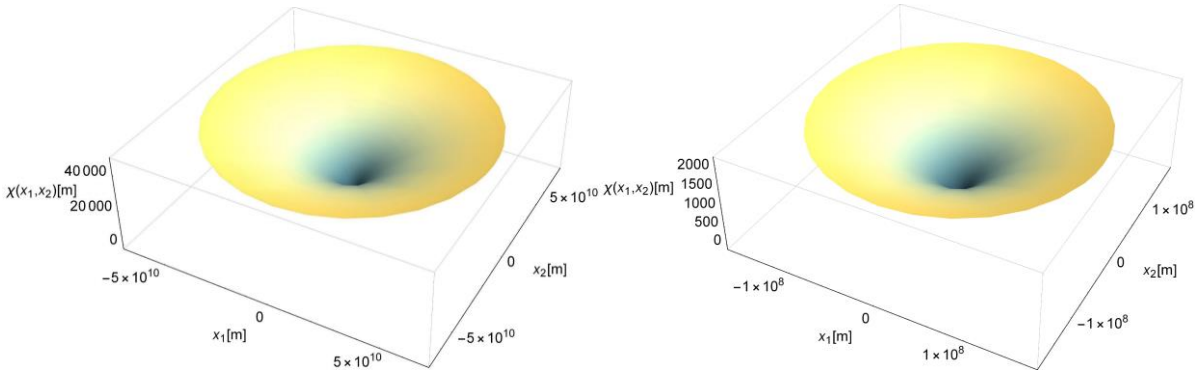

Fig. 40 Deformation of the boundary hypersurface ${}^{\alpha}\chi(x_1, x_2)$ for Earth.

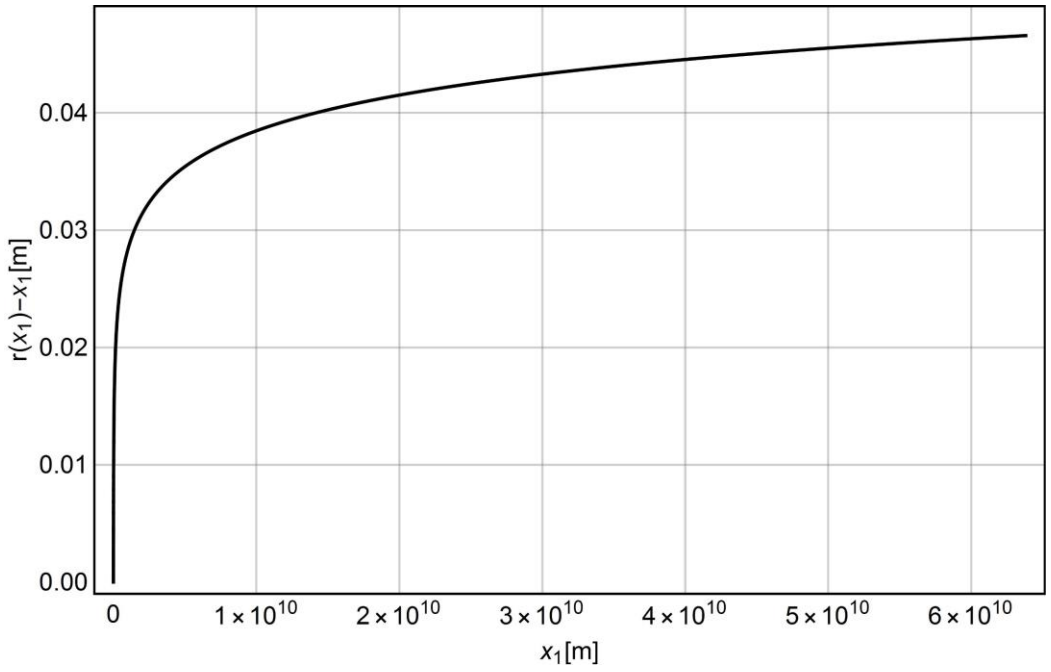

Fig. 41 Dependence diagram $r(x_1) - x_1$ for Earth.

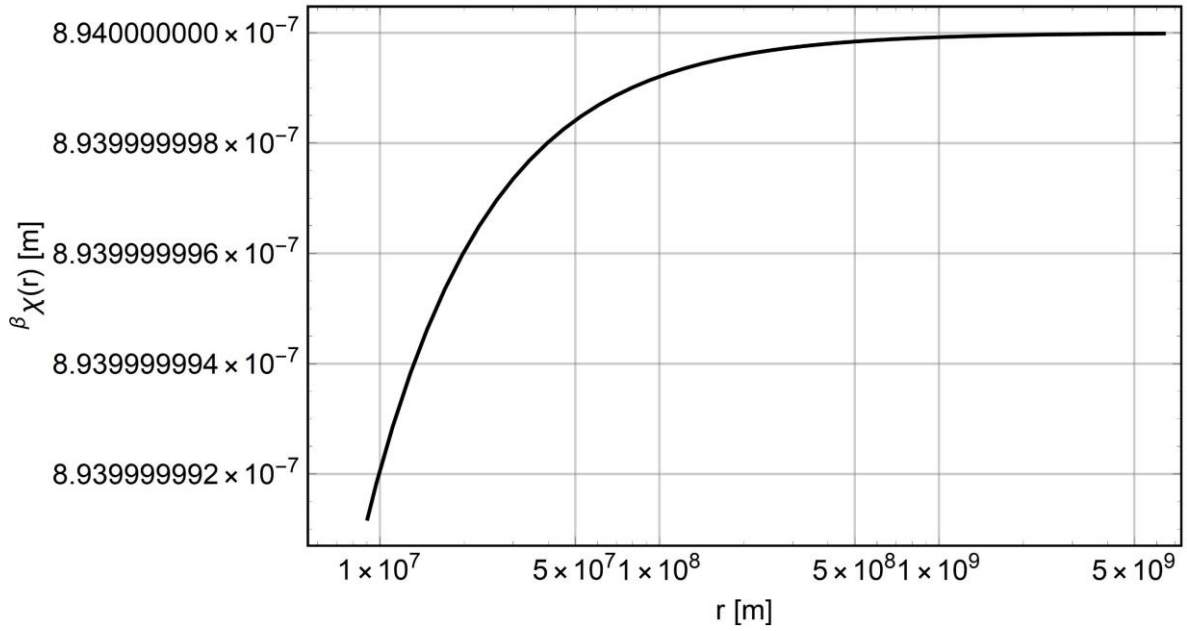

Fig. 42. Dependence diagram ${}^{\beta}\chi(r)$ for $r \geq R_E$ for the Earth.

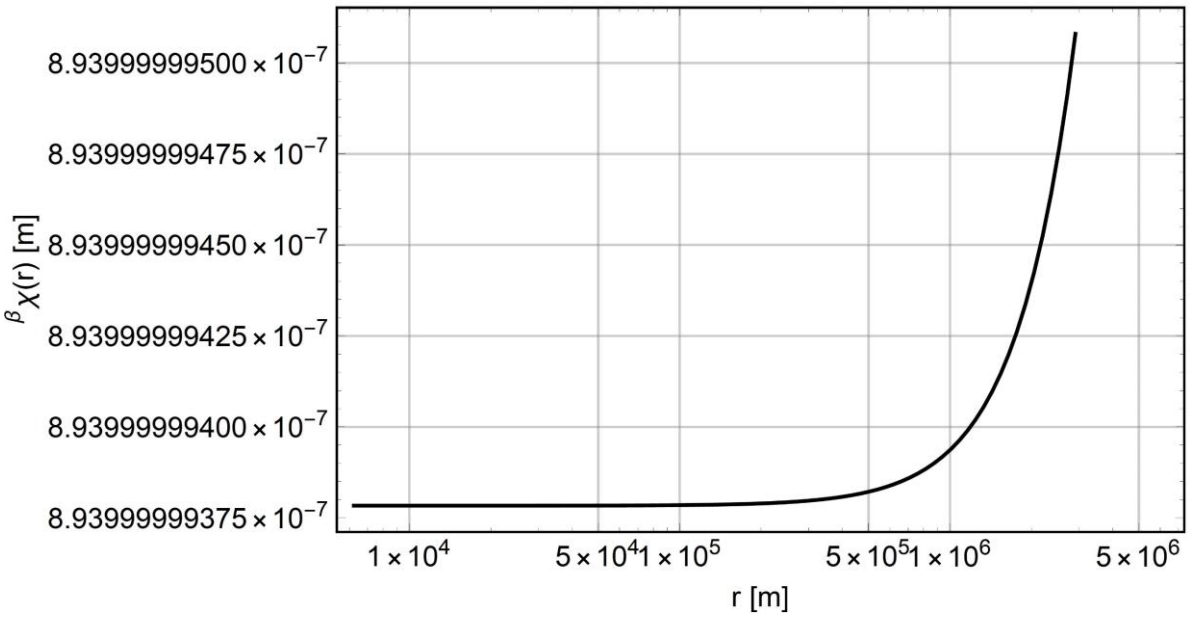

Fig. 43. Dependence diagram ${}^{\beta}\chi(r)$ for $0 \leq r \leq R_E$ for the Earth.

MARS

$Asymmetry\ vector\ on\ the\ surface$: ${}^{\alpha\beta}\xi(\mathrm{R}) = -7.416506184044738 \times 10^{-23}\mathrm{m}$

$Distance\ between\ boundary\ hipersurfaces$: ${}^{\beta}\chi(\mathrm{R}) = 8.939999998743087 \times 10^{-7}\ \mathrm{m}$

$Distance\ between\ boundary\ hipersurfaces$: ${}^{\beta}\chi(0) = 8.939999998743087 \times 10^{-7}\mathrm{m}$

$Distance\ decrease\ between\ boundary\ hipersurfaces$: ${}^{\beta}\chi(\mathrm{R}) - {}^{\beta}\chi(0) = 1.256912385540981 \times 10^{-16}\ m$

$Maximum\ hypersurface\ inclination\ {}^{\alpha}\chi$: $\forall_{i\in\{1,2,3\}} \frac{\partial\, {}^{\alpha}\chi}{\partial x_i}(0) = 2.0537335872748542 \times 10^{-5}\ rad$

$$Maximum\ inclination\ of\ hypersurface\ {}^{\alpha}\chi\ on\ the\ surface\ of\ the\ astronomical\ object\colon \forall_{i\in\{1,2,3\}}\frac{\partial\,{}^{\alpha}\chi}{\partial x_i}(x_R) = 1.6768673349220643\times 10^{-5}\ rad$$

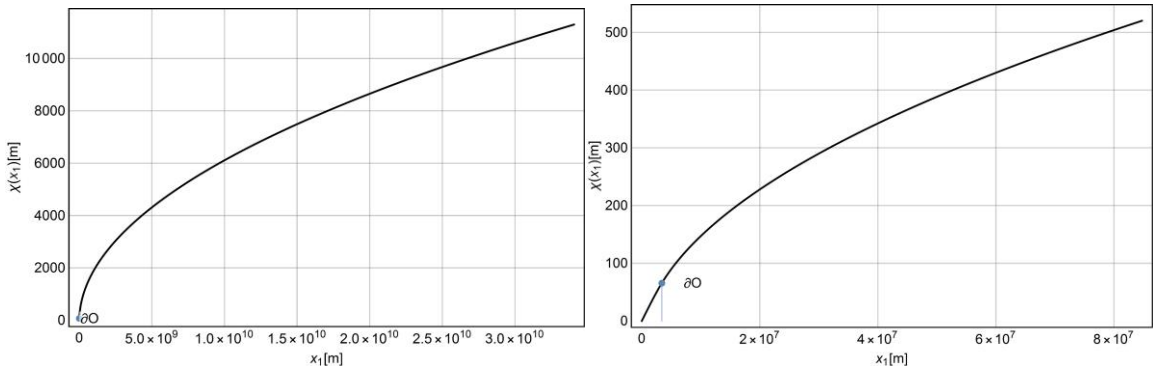

Fig. 44 Deformation of the boundary hypersurface ${}^{\alpha}\chi(x_1)$ for Mars.

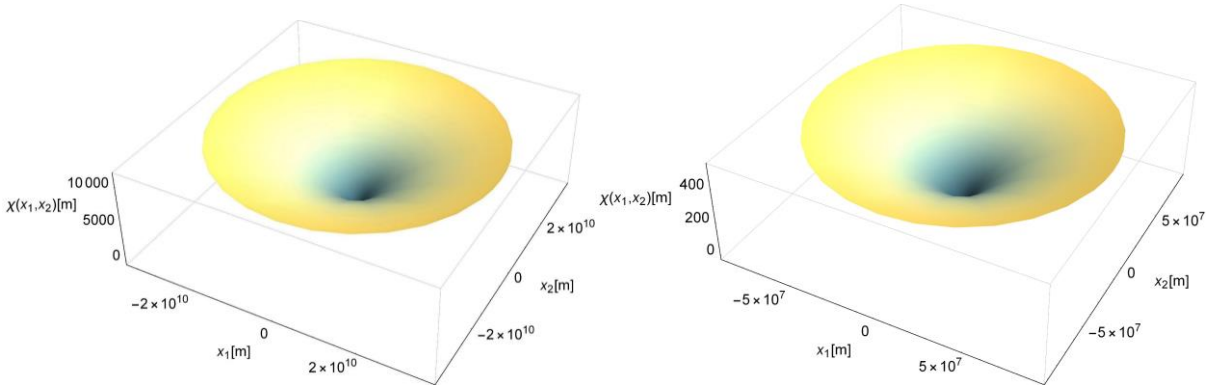

Fig. 45 Deformation of the boundary hypersurface ${}^{\alpha}\chi(x_1, x_2)$ for Mars.

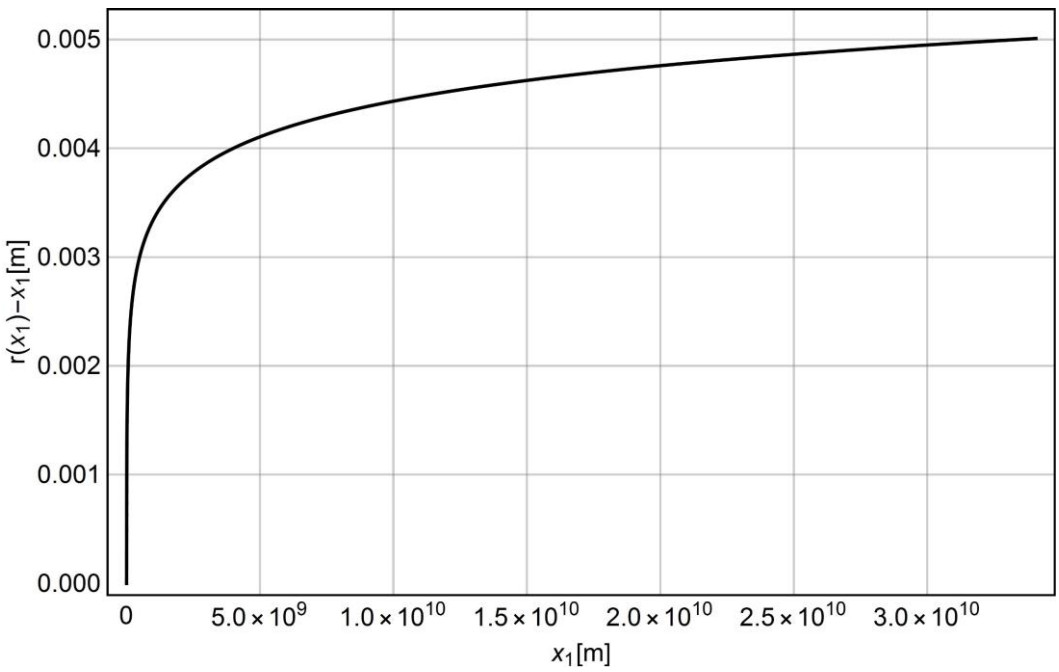

Fig. 46. Dependence diagram $r(x_1) - x_1$ for Mars.

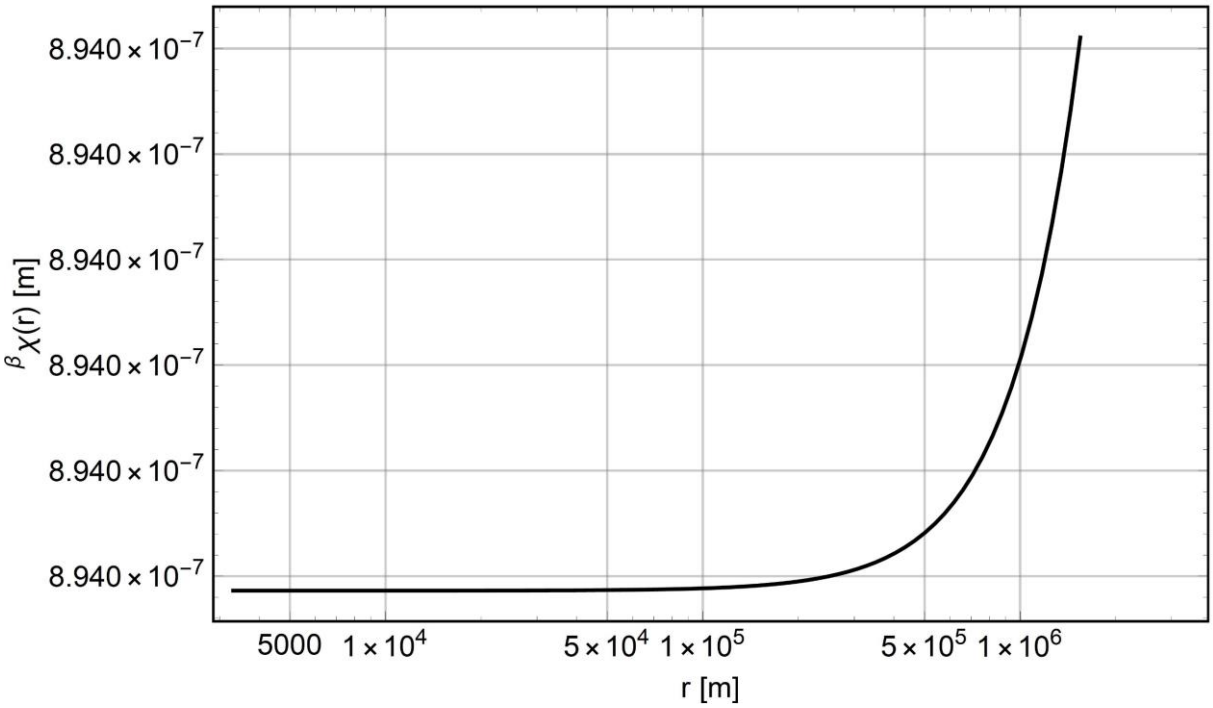

Fig. 47. Dependence diagram ${}^{\beta}\chi(r)$ for $0 \leq r \leq R_E$ for Mars.

JUPITER

$Asymmetry\ vector\ on\ the\ surface$: ${}^{\alpha\beta}\xi(\mathrm{R}) = -5.156802338761135 \times 10^{-22} m$

$Distance\ between\ boundary\ hipersurfaces$: ${}^{\beta}\chi(\mathrm{R}) = 8.939999819741395 \times 10^{-7} m$

$Distance\ between\ boundary\ hipersurfaces$: ${}^{\beta}\chi(0) = 8.939999819741395 \times 10^{-7} m$

$Distance\ decrease\ between\ boundary\ hipersurfaces$: ${}^{\beta}\chi(\mathrm{R}) - {}^{\beta}\chi(0) = 1.802586041525648 \times 10^{-14} m$

$Maximum\ hypersurface\ inclination\ {}^{\alpha}\chi$: $\forall_{i\in\{1,2,3\}} \frac{\partial\, {}^{\alpha}\chi}{\partial x_i}(0) = 2.4594606565857464 \times 10^{-4}\ rad$

$Maximum\ inclination\ of\ hypersurface\ {}^{\alpha}\chi\ on\ the\ surface\ of\ the\ astronomical\ object$: $\forall_{i\in\{1,2,3\}} \frac{\partial\, {}^{\alpha}\chi}{\partial x_i}(x_R)$

$= 2.008141198599821 \times 10^{-4}\ rad$

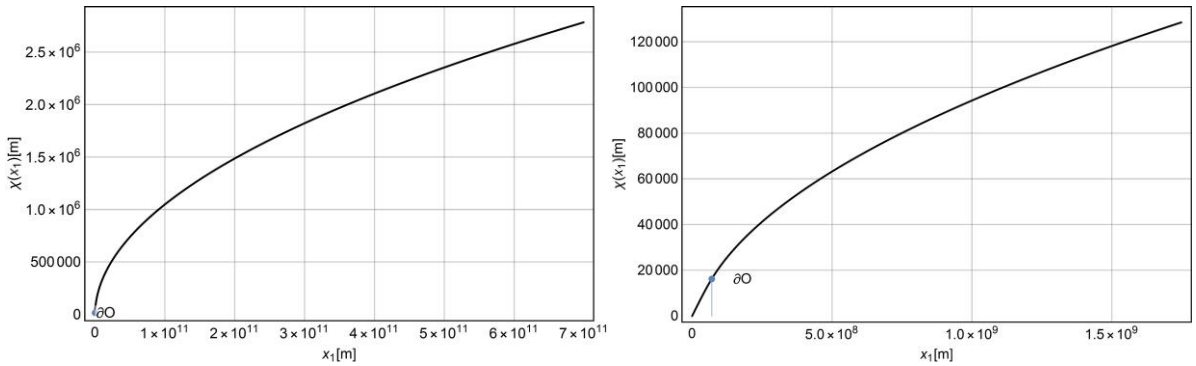

Fig. 48 Deformation of boundary hypersurface ${}^{\alpha}\chi(x_1)$ for Jupiter.

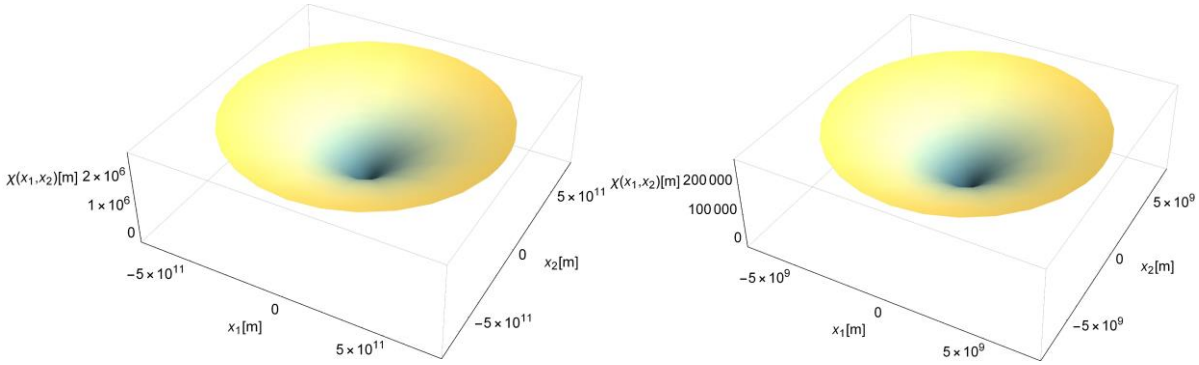

Fig. 49 Deformation of boundary hypersurface ${}^{\alpha}\chi(x_1, x_2)$ for Jupiter.

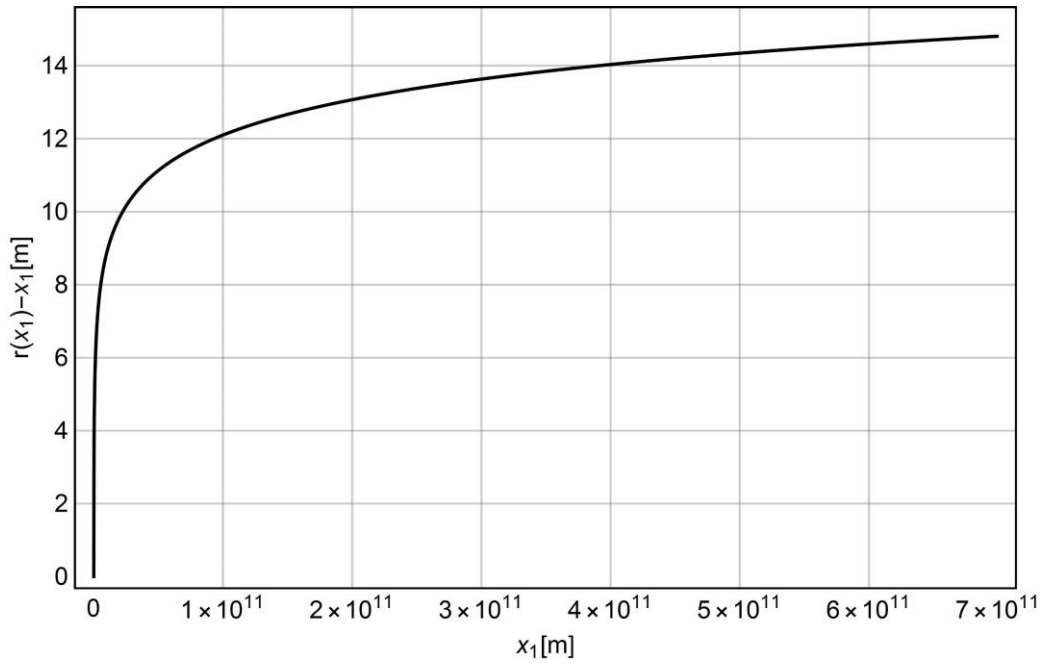

Fig. 50 Dependence diagram $r(x_1) - x_1$ for Jupiter.

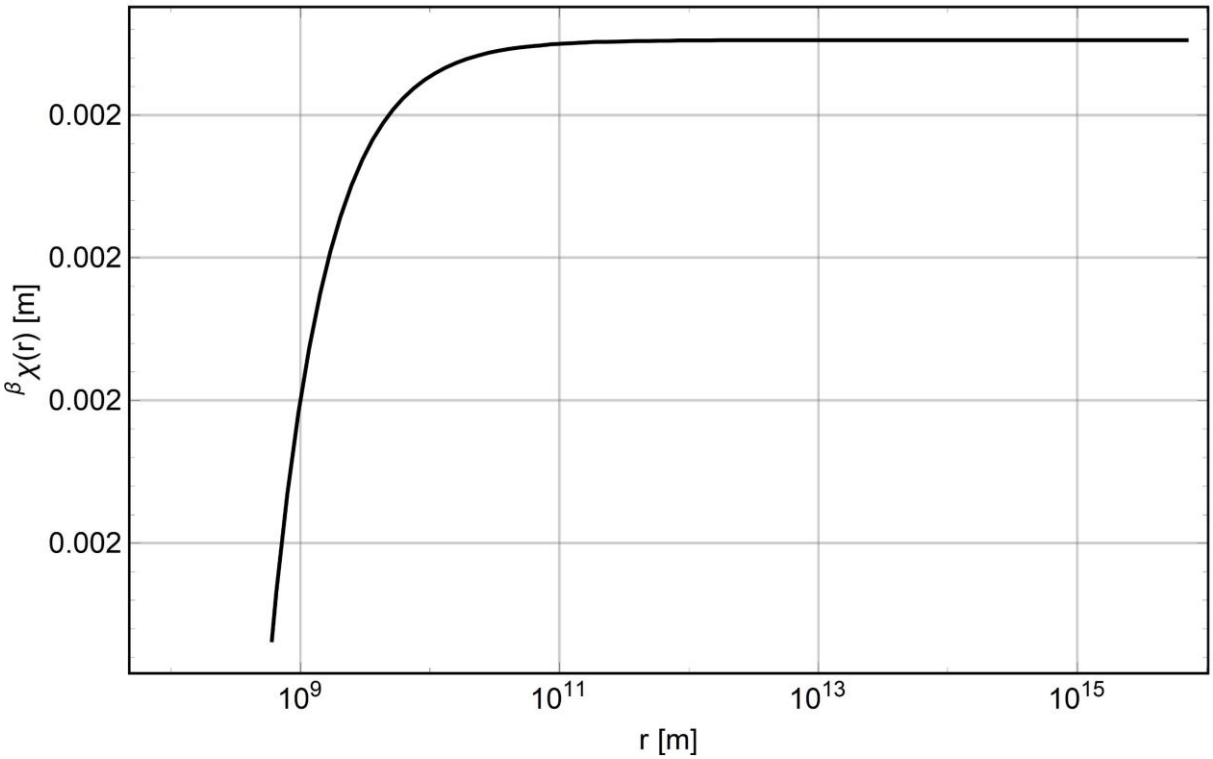

Fig. 51. Dependence diagram $^{\beta}\chi(r)$ for $r \geq R_E$ for Jupiter.

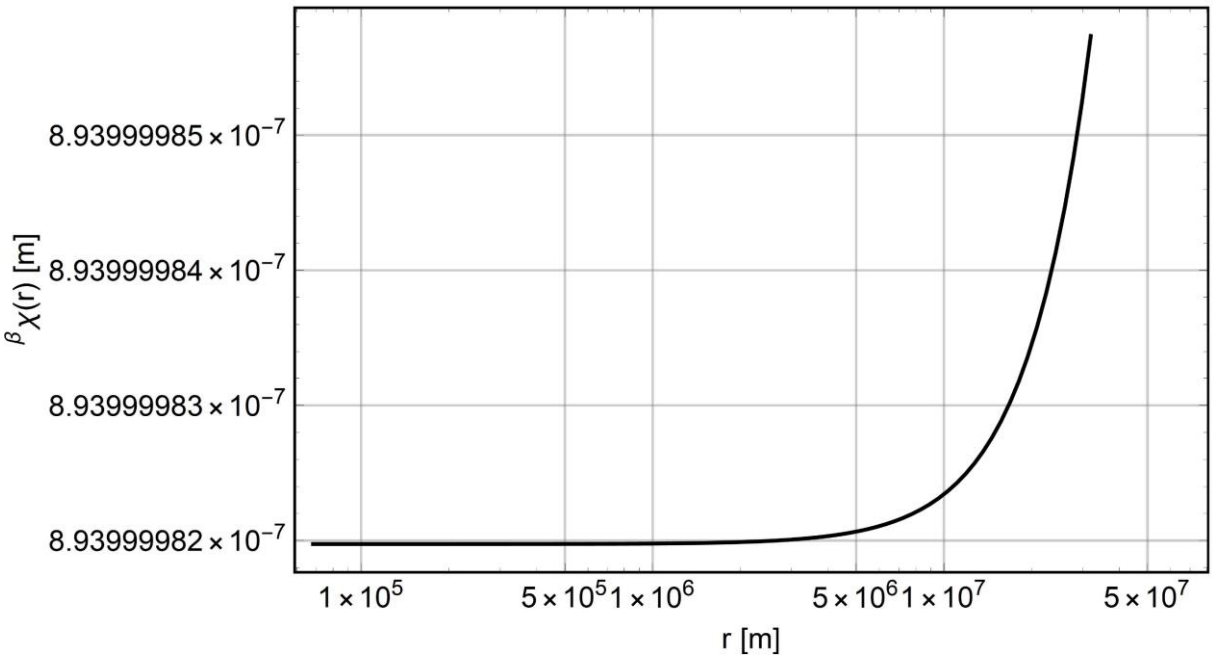

Fig. 52. Dependence diagram $^{\beta}\chi(r)$ for $0 \leq r \leq R_E$ for Jupiter.

SATURN

$Asymmetry\ vector\ on\ the\ surface$: $^{\alpha\beta}\xi(R) = -2.225443858484261 \times 10^{-22} m$

$Distance\ between\ boundary\ hipersurfaces$: $^{\beta}\chi(R) = 8.939999935203977 \times 10^{-7} m$

$Distance\ between\ boundary\ hipersurfaces\colon\ {}^{\beta}\chi(0) = 8.939999935203977 \times 10^{-7} m$

$Distance\ decrease\ between\ boundary\ hipersurfaces\colon\ {}^{\beta}\chi(R) - {}^{\beta}\chi(0) = 6.479602338362773 \times 10^{-15}\mathrm{m}$

$Maximum\ hypersurface\ inclination\ {}^{\alpha}\chi\colon \forall_{i\in\{1,2,3\}} \frac{\partial\, {}^{\alpha}\chi}{\partial x_i}(0) = 1.4745722244132633 \times 10^{-4}\ rad$

$Maximum\ inclination\ of\ hypersurface\ {}^{\alpha}\chi\ on\ the\ surface\ of\ the\ astronomical\ object\ \forall_{i\in\{1,2,3\}} \frac{\partial\, {}^{\alpha}\chi}{\partial x_i}(x_R) = 1.2039831734169209 \times 10^{-4}\ rad$

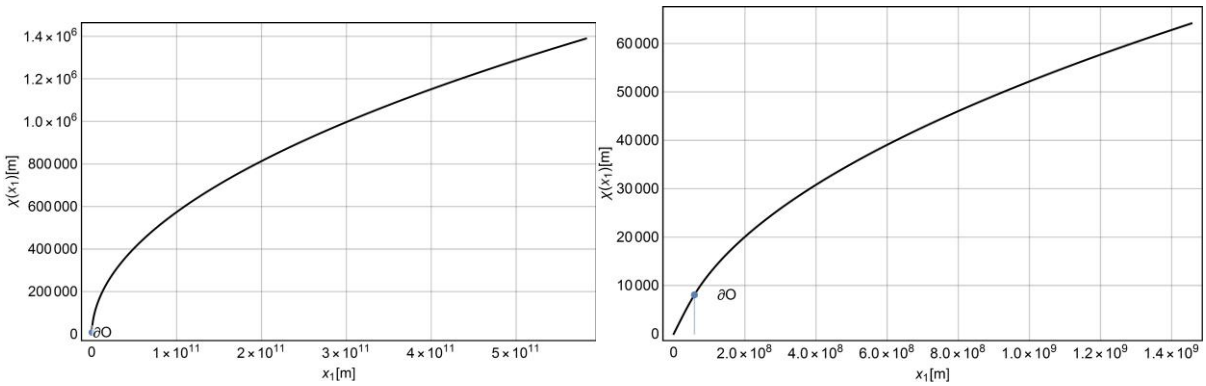

Fig. 53 Deformation of the boundary hypersurface ${}^{\alpha}\chi(x_1)$ for Saturn.

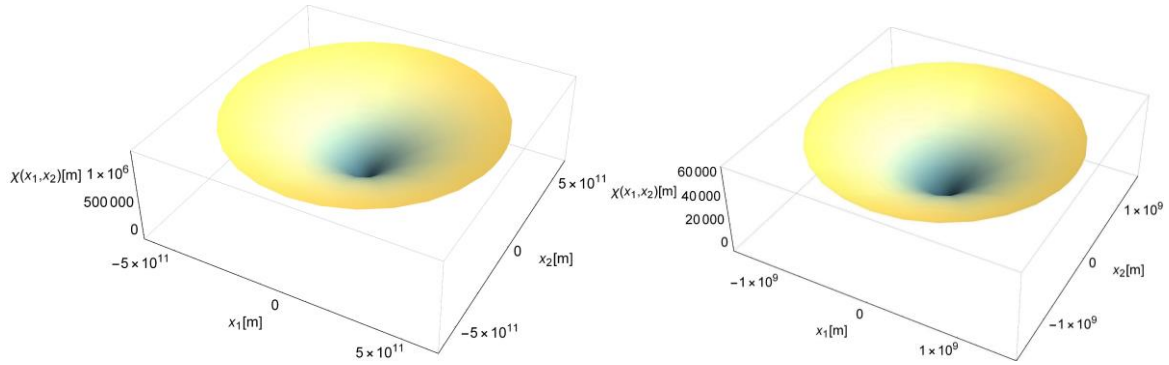

Fig. 54 Deformation of the boundary hypersurface ${}^{\alpha}\chi(x_1, x_2)$ for Saturn.

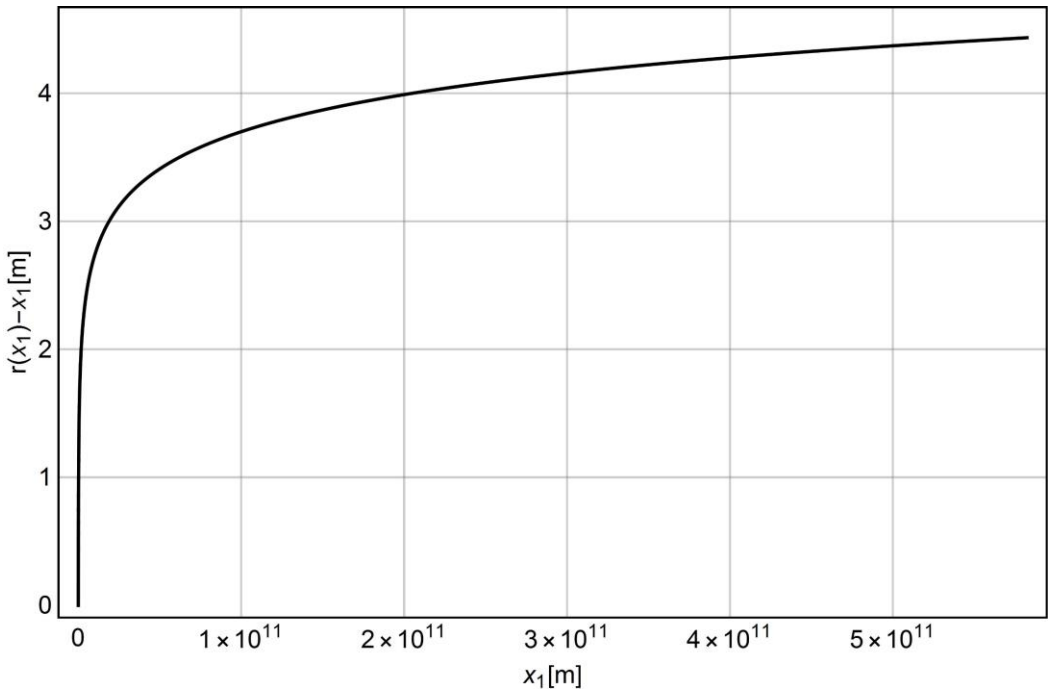

Fig. 55 Dependence diagram $r(x_1) - x_1$ for Saturn.

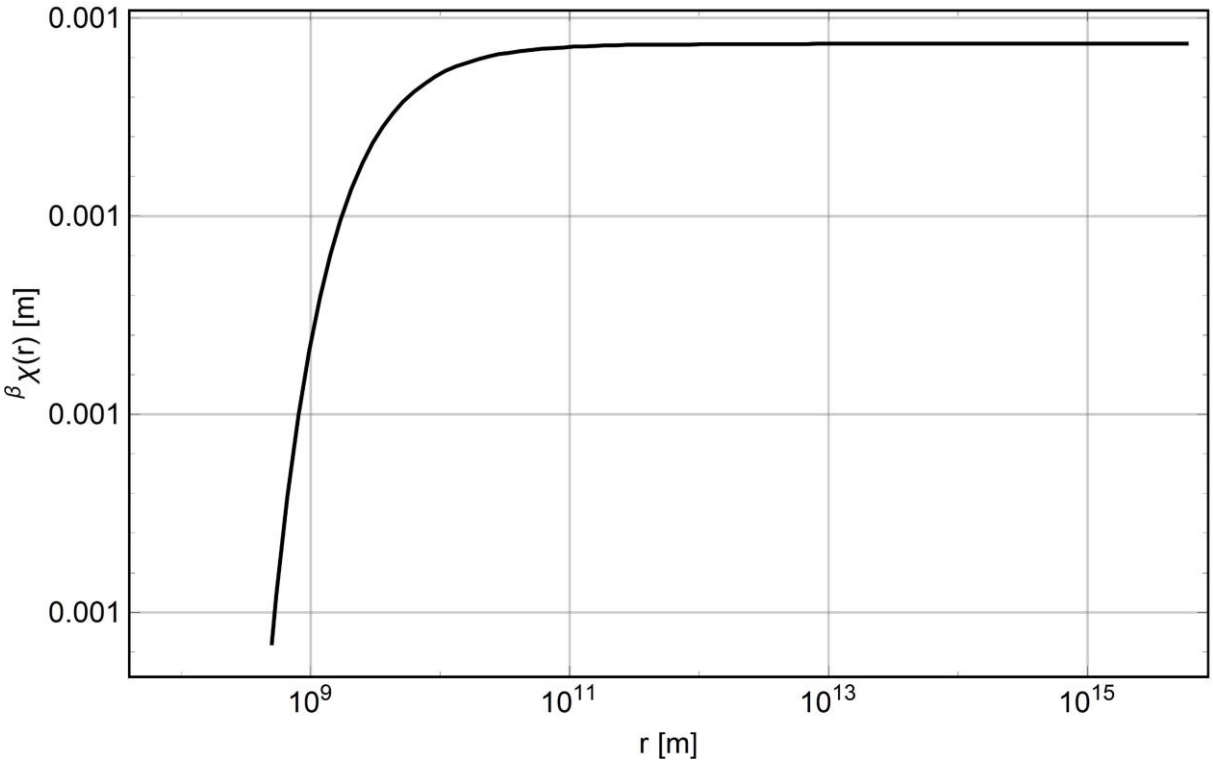

Fig. 56. Dependence diagram ${}^{\beta}\chi(r)$ for $r \geq R_E$ for Saturn.

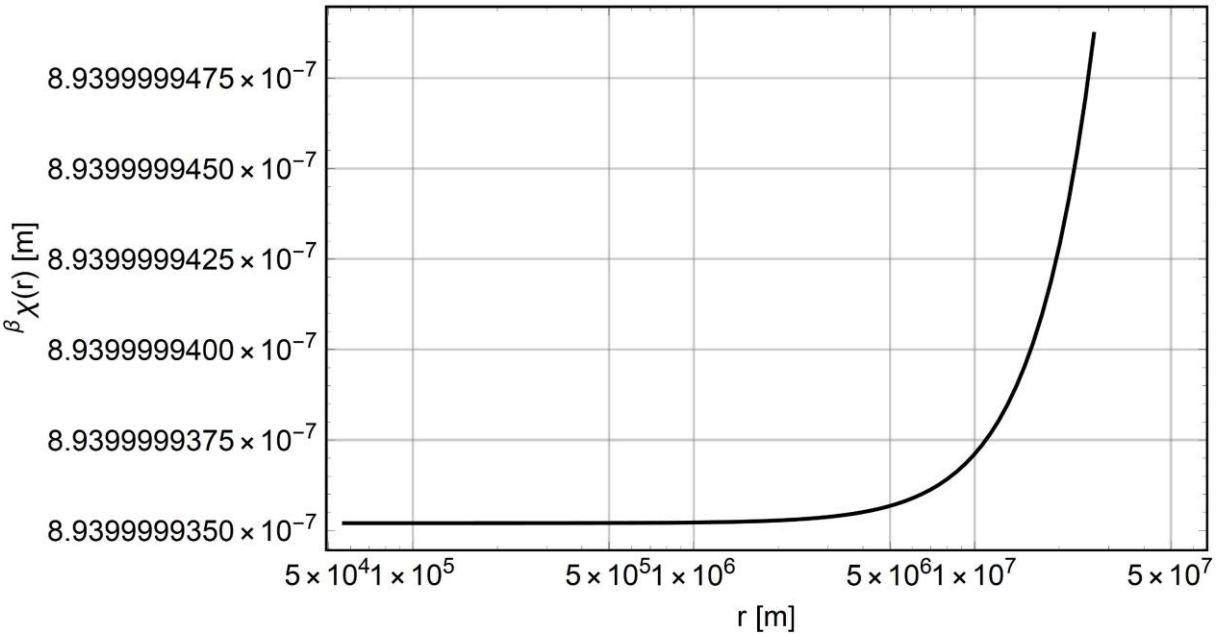

Fig. 57. Dependence diagram ${}^{\beta}\chi(r)$ for $0 \leq r \leq R_E$ for Saturn.

URANUS

Asymmetry vector on the surface: ${}^{\alpha\beta}\xi(\mathrm{R}) = -1.792047845224359 \times 10^{-22}$ m

Distance between boundary hipersurfaces: ${}^{\beta}\chi(\mathrm{R}) = 8.93999997727504 \times 10^{-7}\ m$

Distance between boundary hipersurfaces: ${}^{\beta}\chi(0) = 8.93999997727504 \times 10^{-7}$ m

Distance decrease between boundary hipersurfaces: ${}^{\beta}\chi(\mathrm{R}) - {}^{\beta}\chi(0) = 2.272495872529009 \times 10^{-15}\ m$

Maximum hypersurface inclination ${}^{\alpha}\chi$: $\forall_{i\in\{1,2,3\}} \frac{\partial\, {}^{\alpha}\chi}{\partial x_i}(0) = 8.732596899244125 \times 10^{-5}\ rad$

Maximum inclination of hypersurface ${}^{\alpha}\chi$ *on the surface of the astronomical object*: $\forall_{i\in\{1,2,3\}} \frac{\partial\, {}^{\alpha}\chi}{\partial x_i}(x_R) = 7.130135562755738 \times 10^{-5}\ rad$

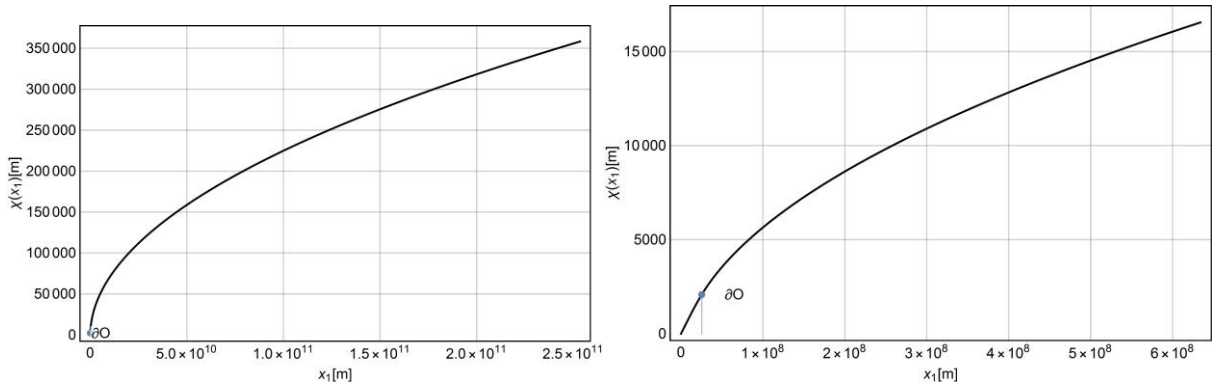

Fig. 58 Deformation of the boundary hypersurface ${}^{\alpha}\chi(x_1)$ for Uranus.

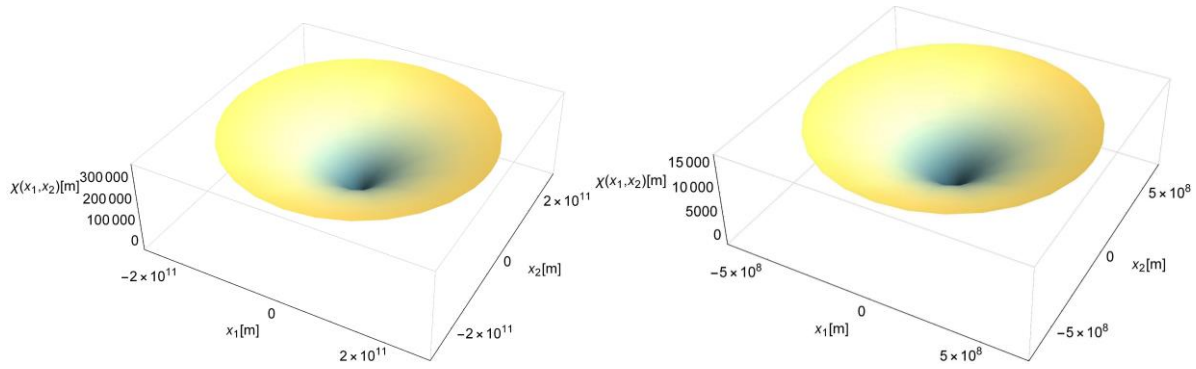

Fig. 59 Deformation of the boundary hypersurface ${}^{\alpha}\chi(x_1, x_2)$ for Uranus.

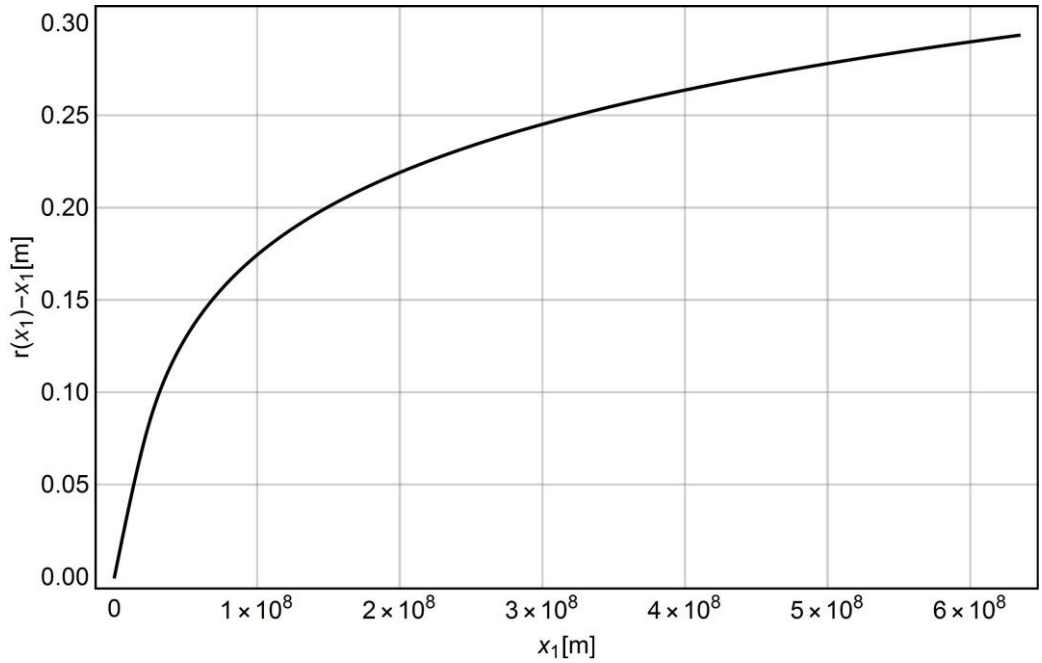

Fig. 60 Dependence diagram $r(x_1) - x_1$ for Uranus.

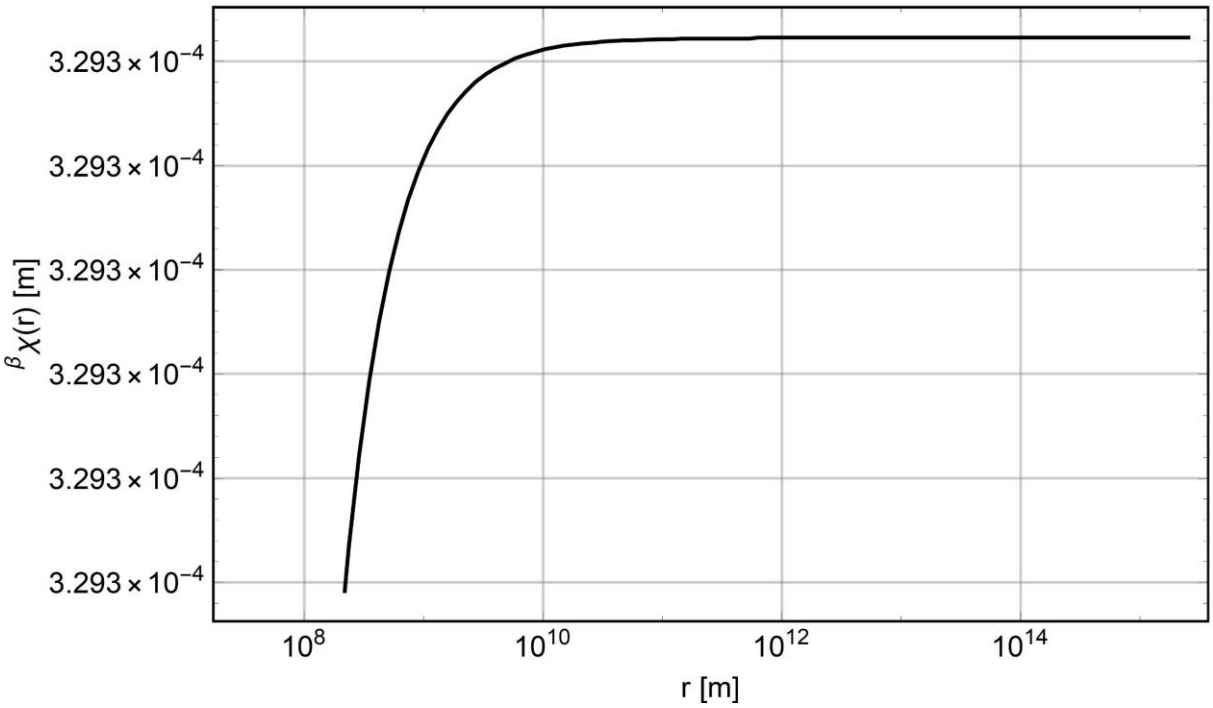

Fig. 61. Dependence diagram ${}^{\beta}\chi(r)$ for $r \geq R_E$ for Uranus.

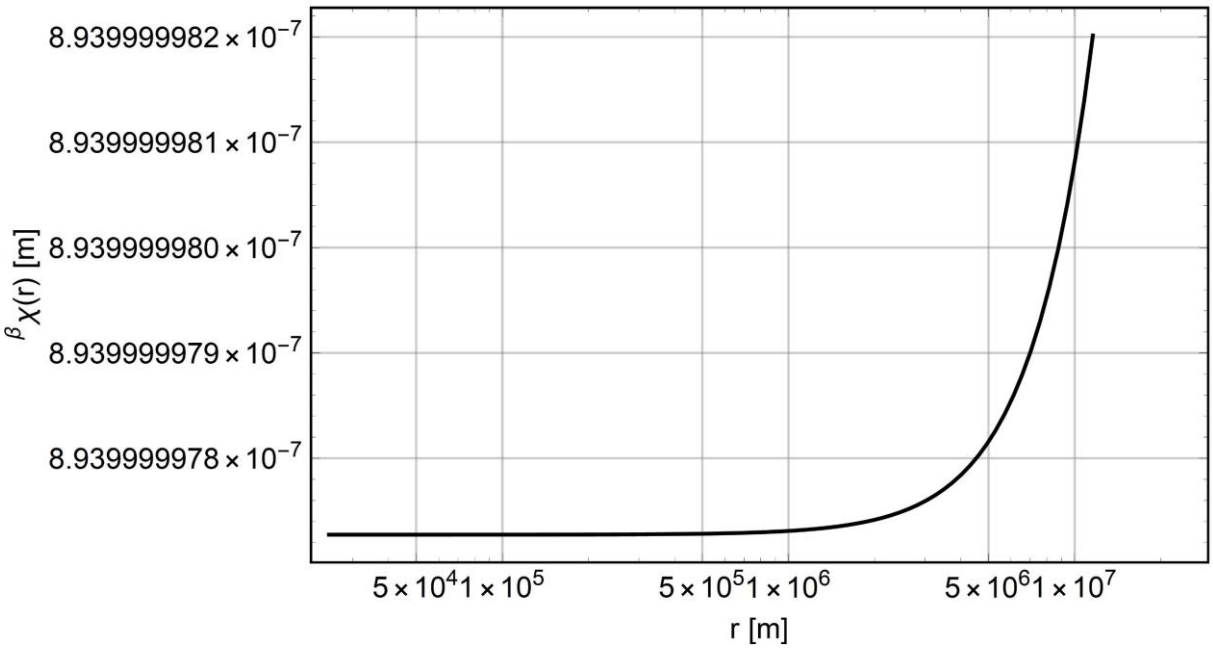

Fig. 62. Dependence diagram ${}^{\beta}\chi(r)$ for $0 \leq r \leq R_E$ for Uranus.

NEPTUNE

Asymmetry vector on the surface: ${}^{\alpha\beta}\xi(R) = -2.21740657045625 \times 10^{-22}$ m

Distance between boundary hipersurfaces: ${}^{\beta}\chi(R) = 8.93999997254407 \times 10^{-7}\ m$

Distance between boundary hipersurfaces: ${}^{\beta}\chi(0) = 8.93999997254407 \times 10^{-7}$m

Distance decrease between boundary hipersurfaces: ${}^{\beta}\chi(R) - {}^{\beta}\chi(0) = 2.745592815538929 \times 10^{-15}$ m

$$Maximum\ hypersurface\ inclination\ {}^{\alpha}\chi\colon \forall_{i\in\{1,2,3\}}\frac{\partial\,{}^{\alpha}\chi}{\partial x_i}(0) = 9.626283917811249\times 10^{-5}\ rad$$

$$Maximum\ inclination\ of\ hypersurface\ {}^{\alpha}\chi\ on\ the\ surface\ of\ the\ astronomical\ object\colon \forall_{i\in\{1,2,3\}}\frac{\partial\,{}^{\alpha}\chi}{\partial x_i}(x_R) = 7.85982790593244\times 10^{-5}\ rad$$

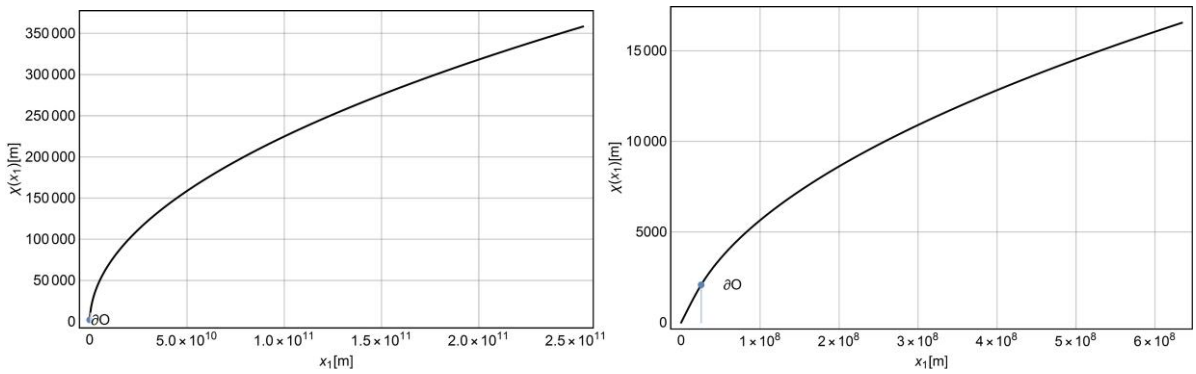

Fig. 63 Deformation of the boundary hypersurface ${}^{\alpha}\chi(x_1)$ for Neptune.

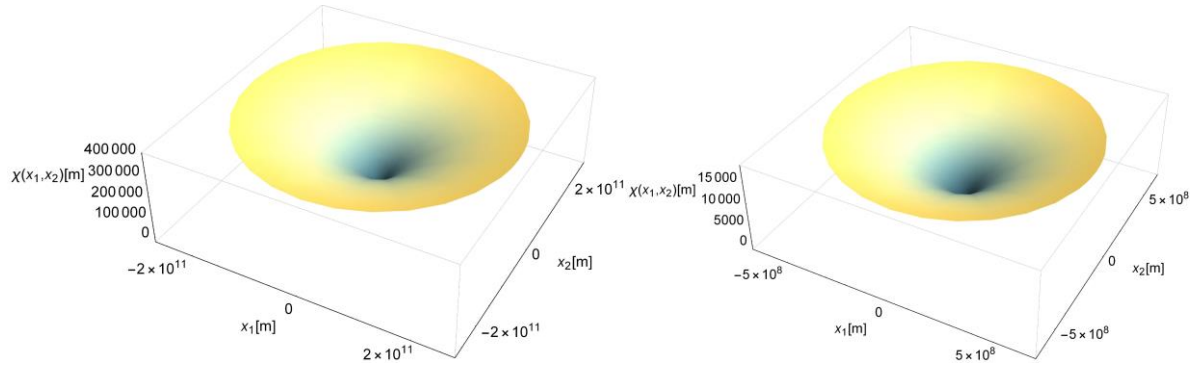

Fig. 64 Deformation of the boundary hypersurface ${}^{\alpha}\chi(x_1, x_2)$ for Neptune.

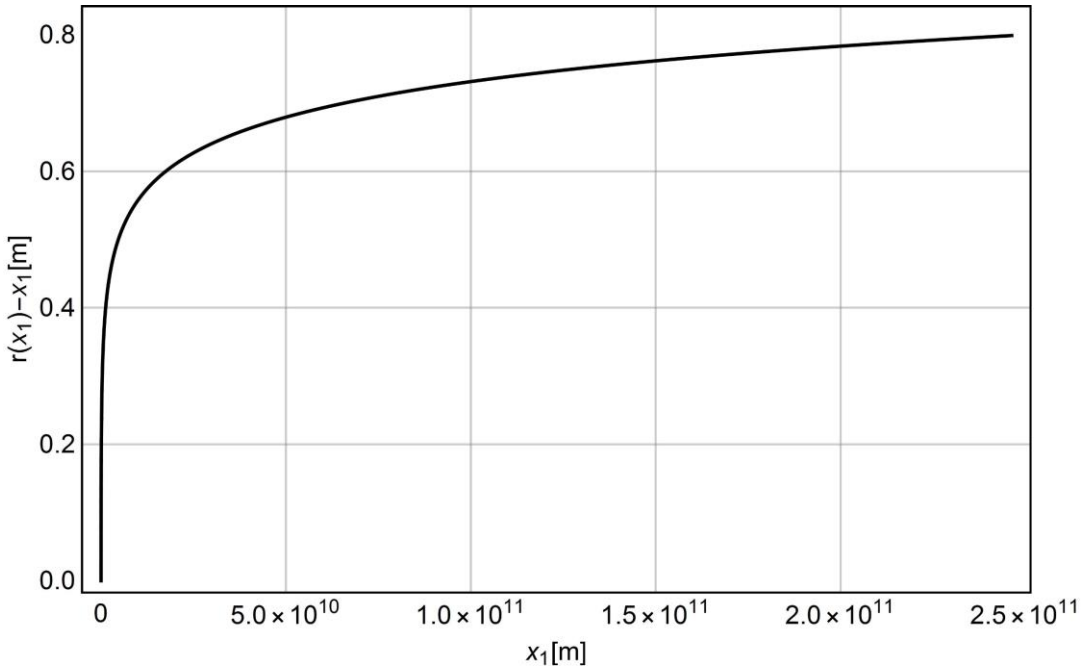

Fig. 65 Dependence diagram $r(x_1) - x_1$ for Neptune.

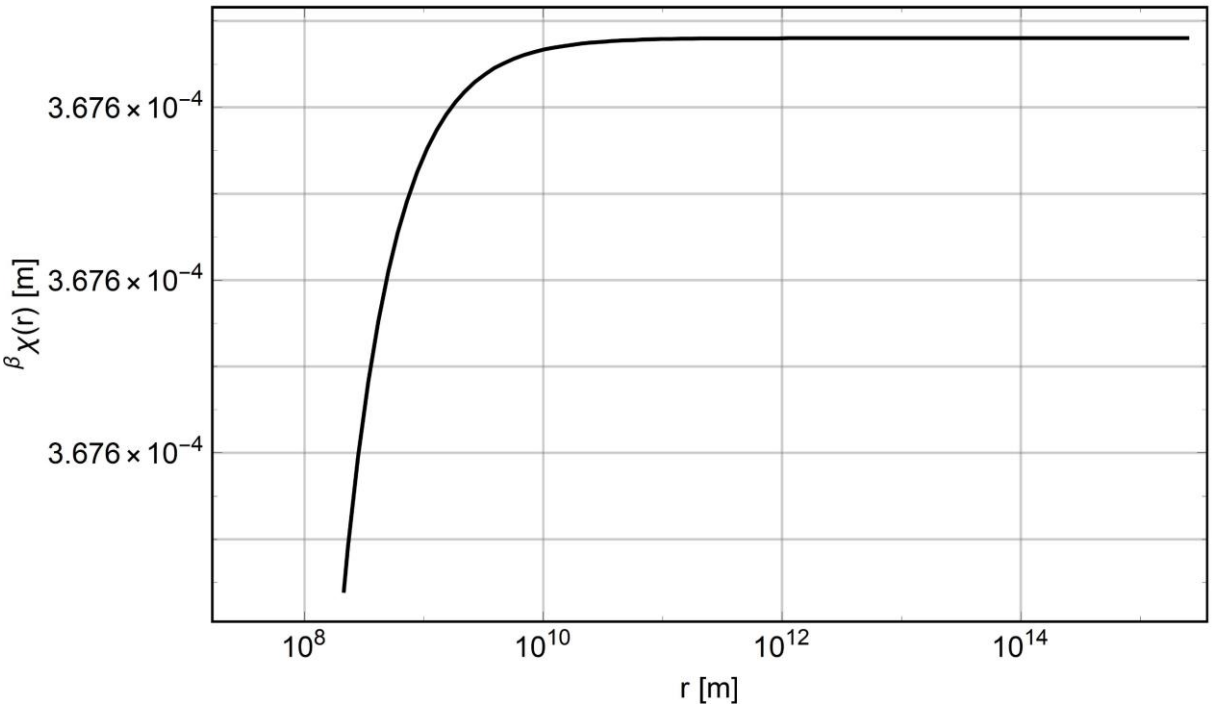

Fig. 66. Dependence diagram ${}^{\beta}\chi(r)$ for $r \geq R_E$ for Neptune.

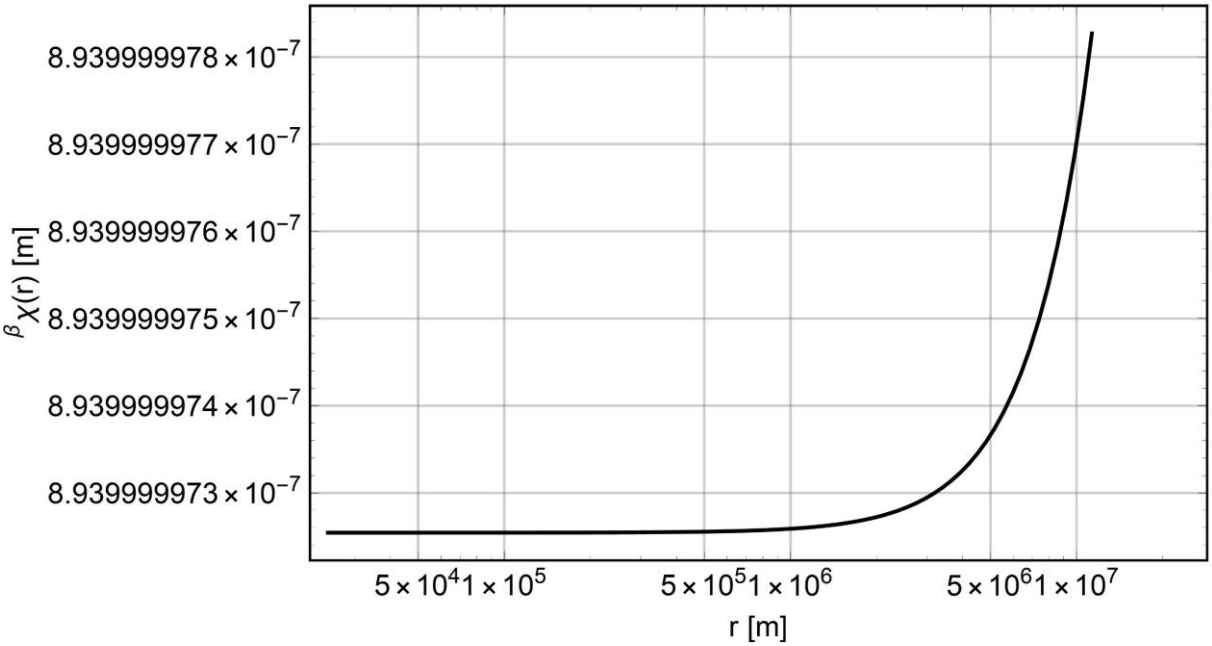

Fig. 67. Dependence diagram ${}^{\beta}\chi(r)$ for $0 \leq r \leq R_E$ for Neptune.

THE SUN

$Asymmetry\ vector\ on\ the\ surface$: ${}^{\alpha\beta}\xi(R) = -5.45496 \times 10^{-21}$ m

$Distance\ between\ boundary\ hipersurfaces$: ${}^{\beta}\chi(R) = 8.939981024921204 \times 10^{-7} m$

$Distance\ between\ boundary\ hipersurfaces$: ${}^{\beta}\chi(0) = 8.939981024921204 \times 10^{-7}$ m

$Distance\ decrease\ between\ boundary\ hipersurfaces$: ${}^{\beta}\chi(R) - {}^{\beta}\chi(0) = 1.897507879532646 \times 10^{-12}$ m

$Maximum\ hypersurface\ inclination\ {}^{\alpha}\chi$: $\forall_{i\in\{1,2,3\}} \frac{\partial\, {}^{\alpha}\chi}{\partial x_i}(0) = 0.0025233918661764134$

$Maximum\ inclination\ of\ hypersurface\ {}^{\alpha}\chi\ on\ the\ surface$: $\forall_{i\in\{1,2,3\}} \frac{\partial\, {}^{\alpha}\chi}{\partial x_i}(x_R) = 0.002060339191250505$

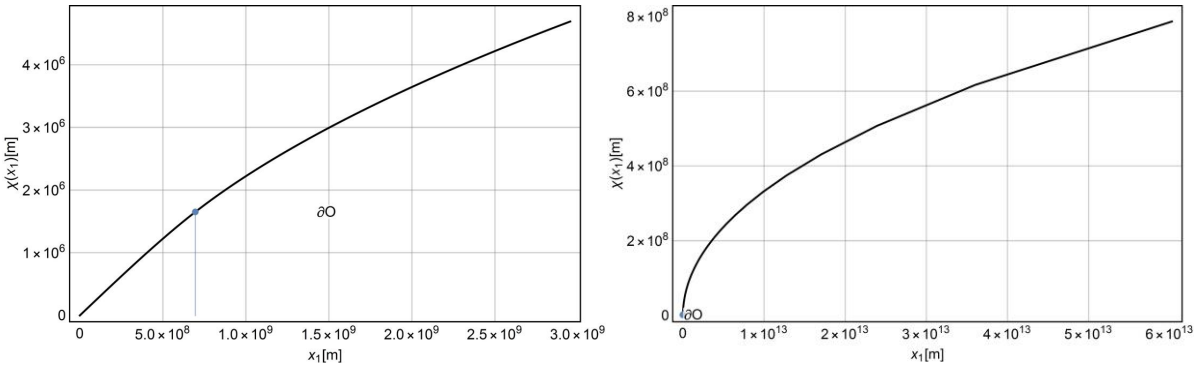

Fig. 68 Deformation of the boundary hypersurface ${}^{\alpha}\chi(x_1)$ for Sun.

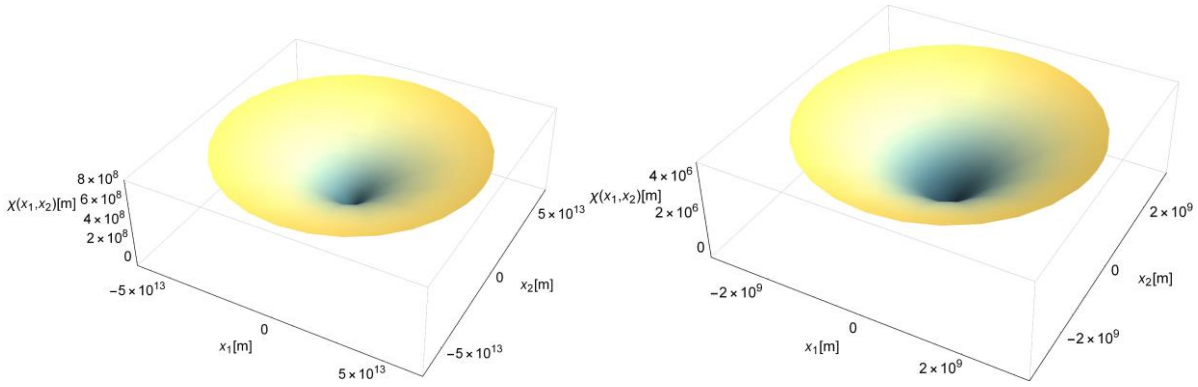

Fig. 69 Deformation of the boundary hypersurface ${}^{\alpha}\chi(x_1, x_2)$ for Sun.

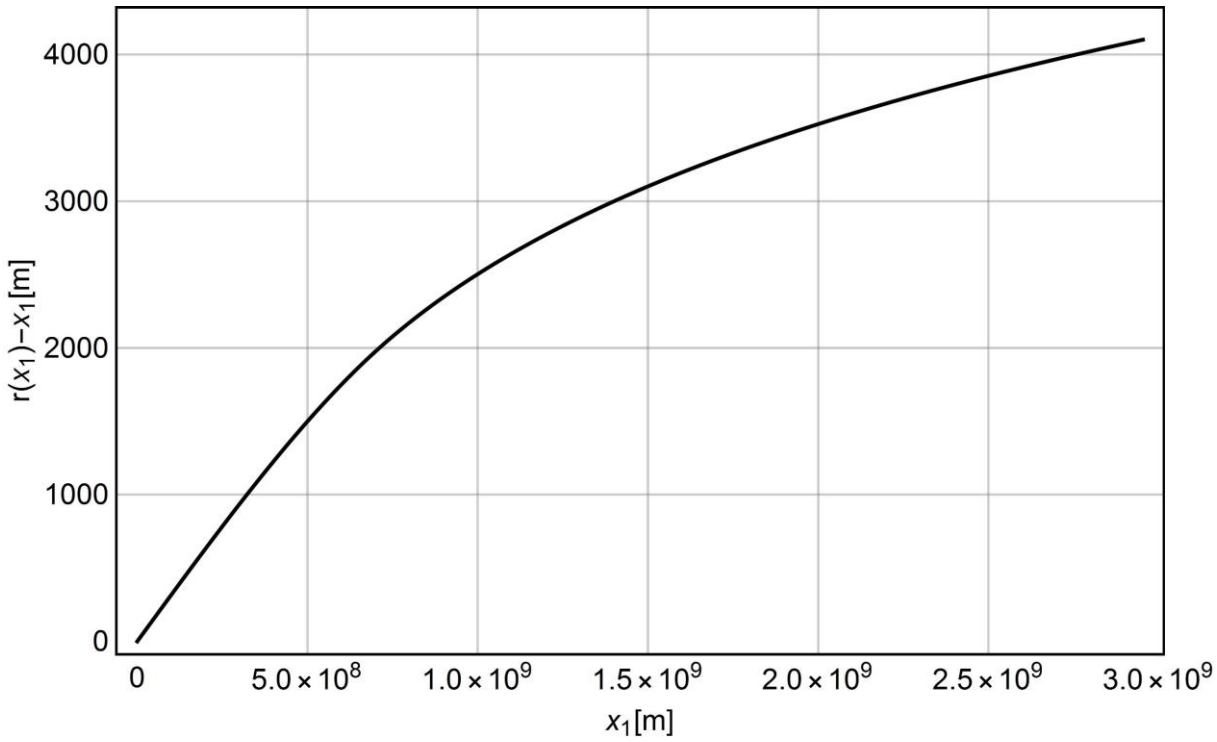

Fig. 70 Dependence diagram $r(x_1) - x_1$ for Sun.

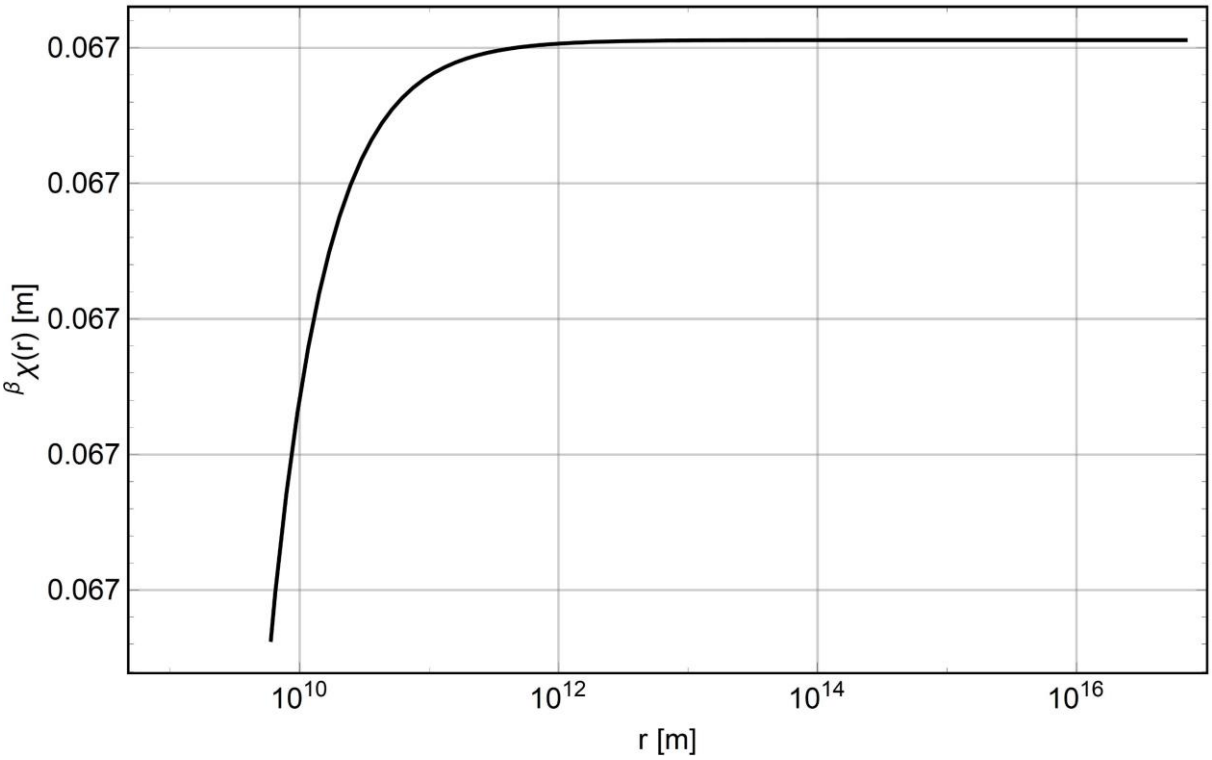

Fig. 71. Dependence diagram ${}^{\beta}\chi(r)$ for $r \geq R_E$ for Sun.

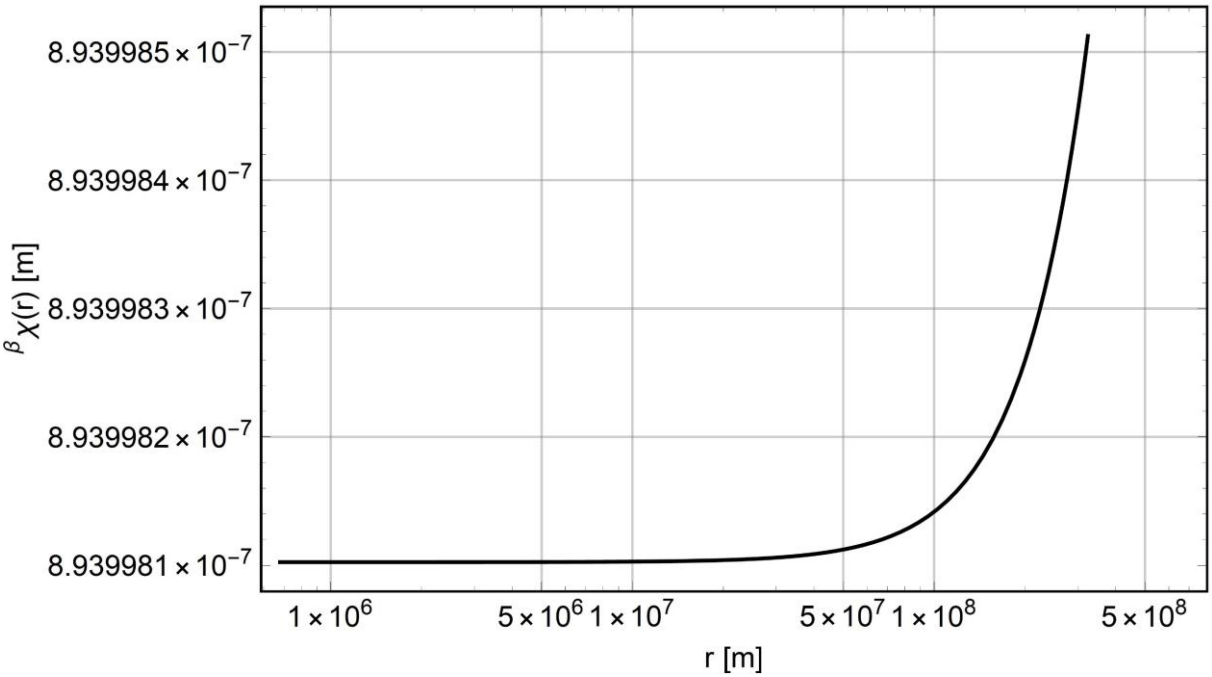

Fig. 72. Dependence diagram ${}^{\beta}\chi(r)$ for $0 \leq r \leq R_E$ for Sun.

INTERPRETATION OF THE RADIUS OF THE UNIVERSE

The volume of a sphere in four-dimensional space of radius R_w is:

$$V = 2\pi^2 {R_w}^3 \quad (54)$$

Therefore, substituting for V the volume of a sphere in three-dimensional space and comparing the two volumes we have:

$$2\pi^2 {R_w}^3 = \frac{4}{3}\pi R_{3D}^3 \quad (55)$$

$$\pi {R_w}^3 = \frac{2}{3} R_{3D}^3 \quad (56)$$

$$R_{3D} = \sqrt[3]{\frac{3}{2}\pi {R_w}^3} = R_w \sqrt[3]{\frac{3}{2}\pi} = 1.2468 \times 10^{26} m \times 1.68 = 2.09 \times 10^{26} m \quad (57)$$

The apparent radius of the universe R_v is half the circumference of a four-dimensional sphere, i.e. magnitude πR_w:

$$R_v = \pi R_w = \pi\, 1.2468 \times 10^{26} m = 3.92 \times 10^{26} m \quad (58)$$

The apparent diameter of the universe S_v is equal to $2R_v$, that is:

$$S_v = 2R_v = 2 \times 3.92 \times 10^{26} m = 7.83 \times 10^{26} m \quad (59)$$

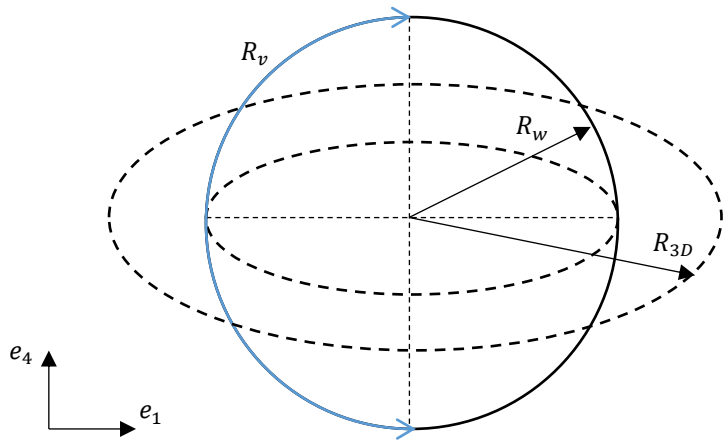

Fig. 73. Universe of radius R_w with the apparent radius marked R_v and the radius of a three-dimensional sphere R_{3D} with a volume equal to the 3D surface of a four-dimensional sphere.

Conclusions

The article presents the results of the next stage of research of the scientific and research unit HTS High Technology Solutions, which is part of a project aimed at creating a basis for simulating electromagnetic, strong, weak and gravitational interactions of elementary particles.

This means that the revealed results, including curvature of the space with a layered structure immersed in Euclidean space E^4 space will be the basis for the determination of the space properties, including its boundary hypersurfaces ${}^{\alpha}\aleph^{\alpha}$ and ${}^{\beta}\aleph^{\beta}$, the understanding of which is necessary to explain the stability of space turbulence and the formation of tubes shown in Fig. 1 and formulation of boundary conditions in finite element simulations.

In view of the objectives thus set, the co-authors of this paper could not abstract from the reference system, that is, from the geometrical aspects of space, which is essentially a differential manifold immersed in E^4.

The co-authors of this paper were surprised by the results obtained concerning the deformation of space by astronomical objects, since they have important implications for cosmological issues. In connection with this fact, cosmological consequences are also presented in this paper, which are astonishing, because thanks to the presented results it is possible to analyse not only the possibility of creating space tunnels by astronomical objects, but also to predict the effects of interacting universes, if any.

Furthermore, the paper presents the theoretical possibilities of using the Earth's gravitational field to pre-configure the orientation of the rocket's space channels prior to launch with its passengers and describes the anticipated effects that would be experienced by the passengers during such a process. This step was taken because the subject was covered in a previous publication entitled "New Generations of Rocket Engines". (Sobolewski D. S., Sobolewski, Sobolewski, Sobolewska, & Sobolewska, 2020) (Sobolewska, Sobolewska, Sobolewski, Sobolewski, & Sobolewski, 2021).

References

1. Sobolewska, N. J., Sobolewska, J. P., Sobolewski, M. J., Sobolewski, M. A., & Sobolewski, D. S. (2021). *New Generations of Rocket Engines.* Berlin: LAP LAMBERT Academic Publishing.
2. Sobolewski, D. S. (2016). *Theory of Space.* Cambridge International Science Publishing Ltd. and Viva Books Private Limited.
3. Sobolewski, D. S. (2017). *Theory of Space.* HTS High Technology Solutions.
4. Sobolewski, D. S. (2022 - new unpublished edition). *Theory of Space.* Poznań: HTS High Technology Solutions.

5. Sobolewski, D. S., Sobolewski, M. A., Sobolewski, M. J., Sobolewska, J. P., & Sobolewska, N. J. (2020, May 22). New Generations of Rocket Engines. *JOURNAL OF ADVANCES IN PHYSICS*, pp. 322-346.
6. Sobolewski, M. J., Sobolewski, M. A., & Sobolewski, D. S. (2017, July). Geometry of the Dark Matter and Preliminary Analysis of Alpha and Beta Photons' Properties Based on Theory of Space. *International Journal of Innovative Research in Science*.